

Crystal Growth: Physics, Technology and Modeling

Stanisław Krukowski & Michał Leszczyński
Institute of High Pressure Physics PAS
01-142 Warsaw, Sokołowska 29/37
e-mail: stach@unipress.waw.pl, mike@unipress.waw.pl

Sławomir Kret
Institute of Physics PAS
02-668 Warsaw, Al. Lotników 32/46
E-mail: kret@ifpan.edu.pl

Lecture 10. **Selected methods of transmission electron microscopy**
26 April 2022

<http://w3.unipress.waw.pl/~stach/cg-2021-22/>

Transmission Electron Microscopy

Direct information from inside of material on :

- type and density of defects
 - elemental and phase composition
 - strain field distribution (3D)
 - local electric and magnetic fields (up to 1 nm)
 - interfaces atomic structure
 - crystallography
-
- resolution depending on the operating mode but below 35 pm is possible in some cases
-
- Thin sample
 - Local info
 - Destructive

The Genesis of TEM

In 1923, Prince Louis de Broglie postulated the wave nature of matter.

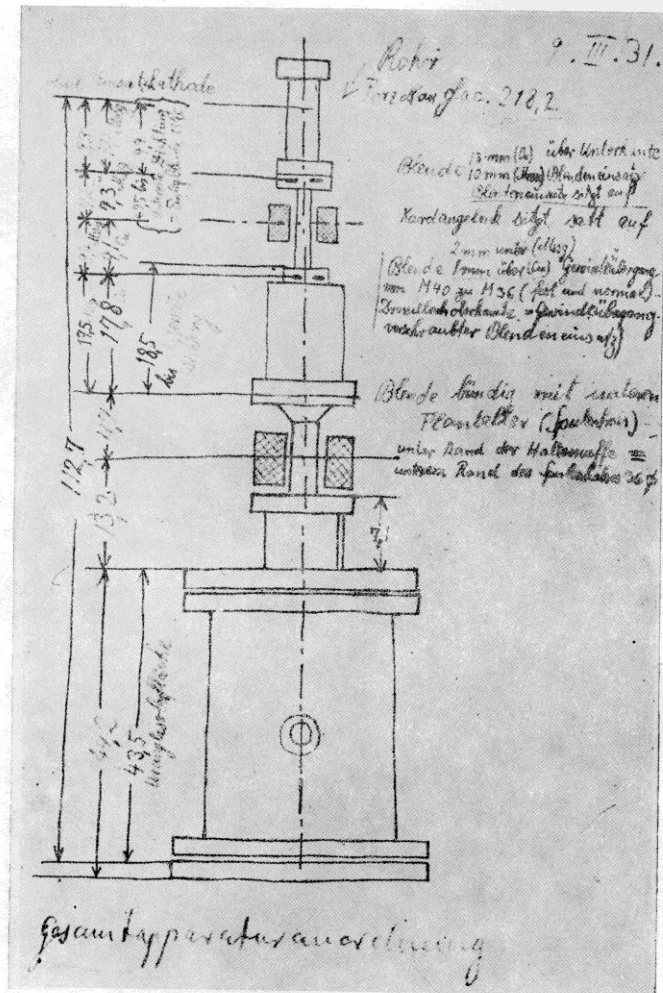
In 1927, Hans Bush showed that magnetic coils can focus an electron beam in the same way as glass lenses to light.

In 1927 C.J. Davisson and L.H Germer and G. P. Thompson and A. Reid independently demonstrated electron diffraction => the wave nature of electrons confirmed.

On April 7, 1931, Ernst Ruska and Max Knoll obtained the first TEM image using two magnetic lenses.

1936 - the first commercial TEM- Metropolitan-Vickers EM1.

First experimental TEM

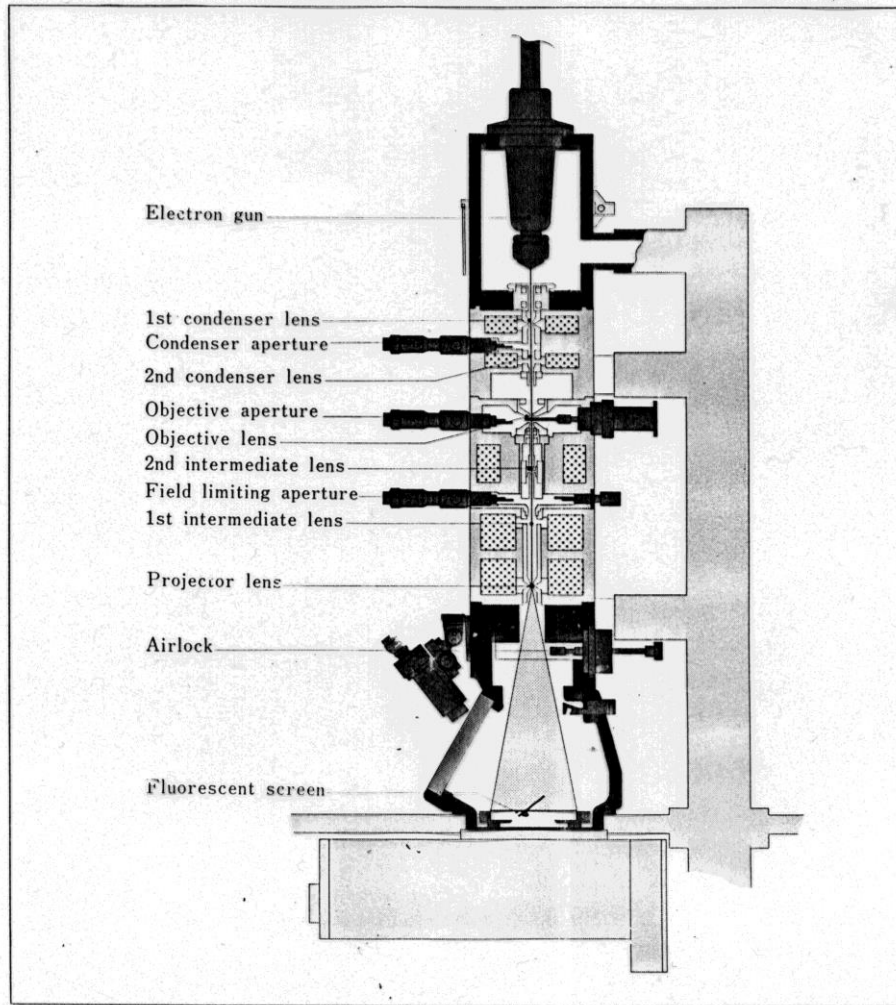


Rys. 2. Szkic Autora (9 marca 1931), przedstawiający lampę promieni katodowych do testowania jedno- i dwustopniowego odwzorowania elektronowo-optycznego za pośrednictwem dwóch magnetycznych soczewek elektronowych (mikroskop elektronowy) [8].



**Ernst Ruska and Max Knoll built
the first electron microscope in 1931**
(Nobel Prize to Ruska in 1986)

Convectional TEM like biological light microscope

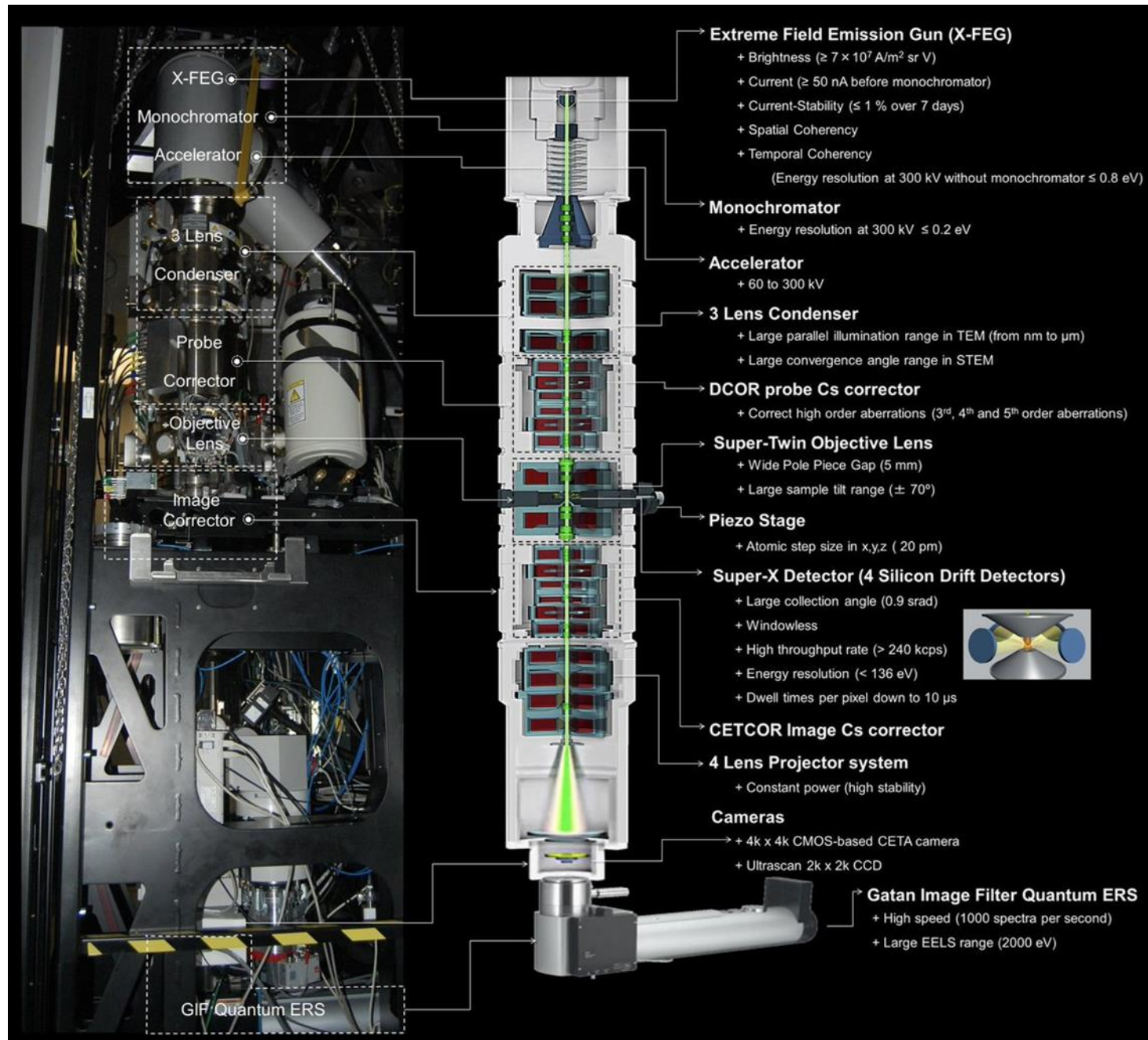


Cross section of electron microscope column



Jeol 2000EX IFAPN from 1989
200KV 0.27 nm Lab6 catode

Modern aberration corrected TEM/STEM





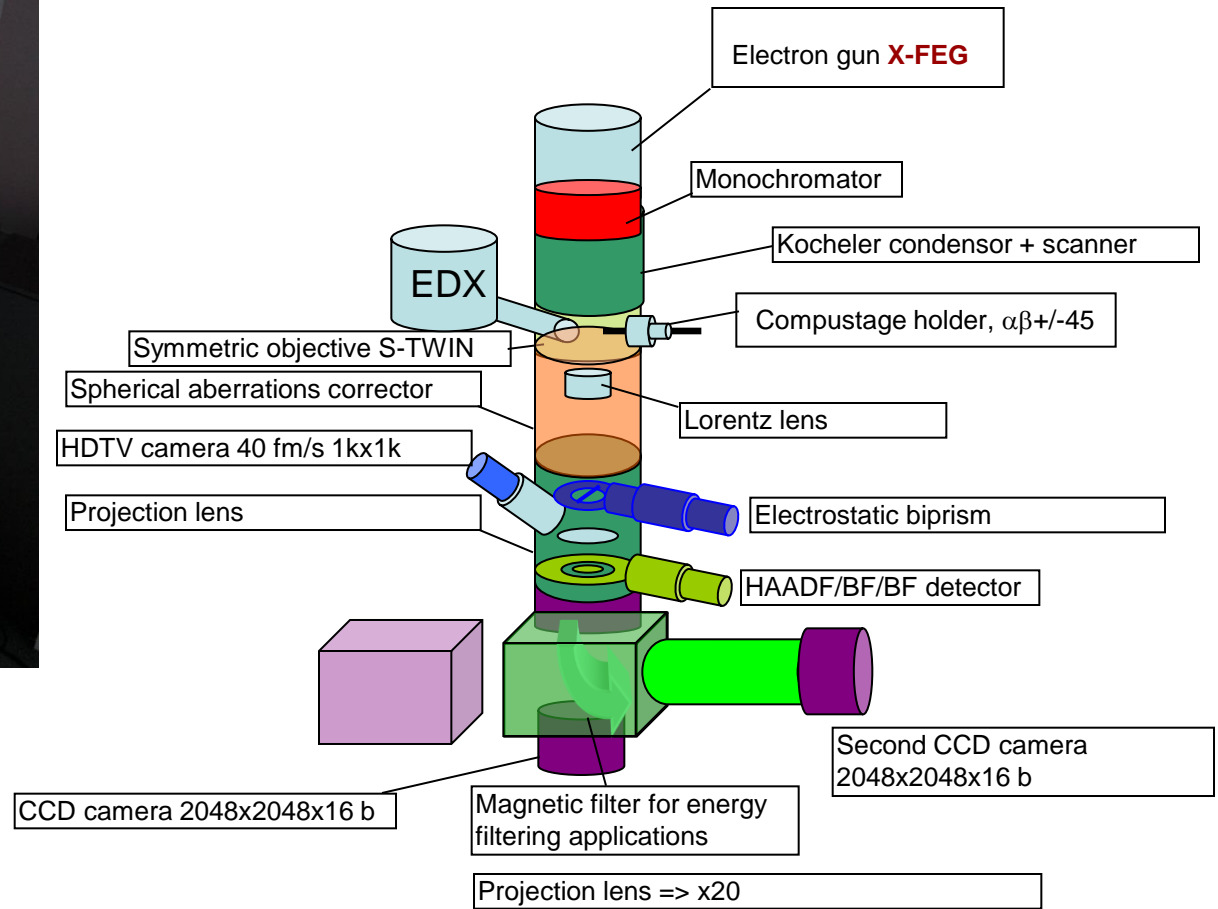
IFPAN from September 2010

TITAN³ CUBED 80-300 KV

Resolution in TEM → 0.07 nm

Energy resolution EELS → 0.2 eV

Electron Holography, EDX, STEM, HADAF, Lorentz



Young's double-slit experiment performed with electrons .

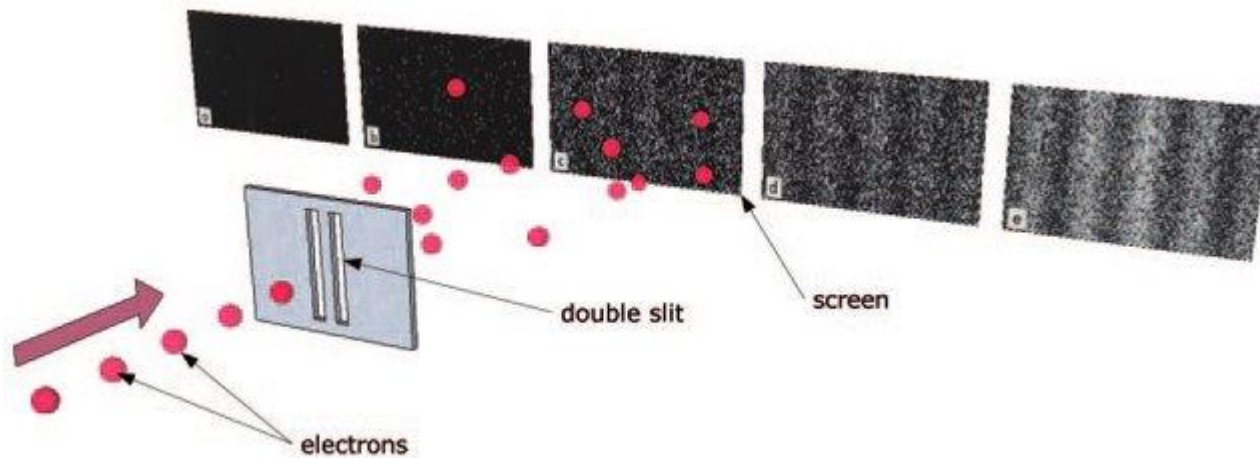
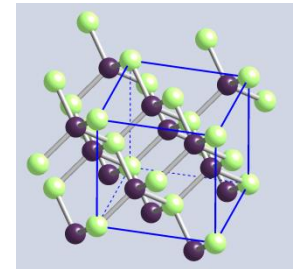
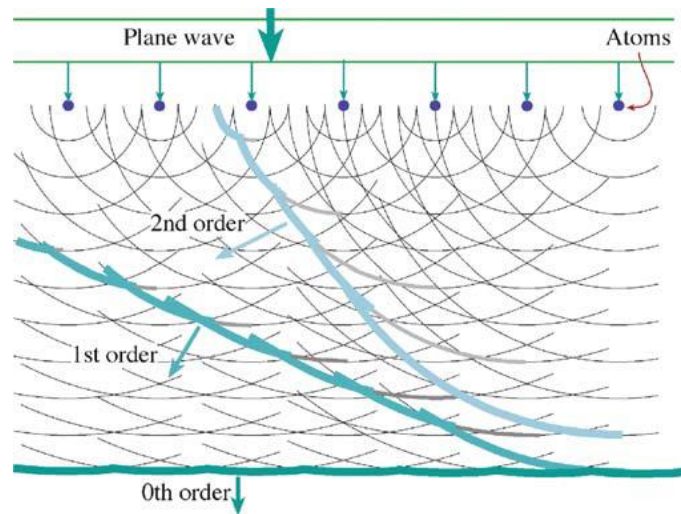
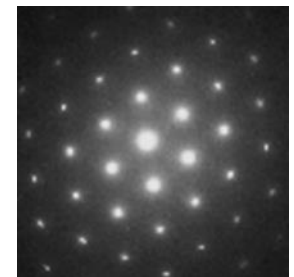


Image by Mehul Malik



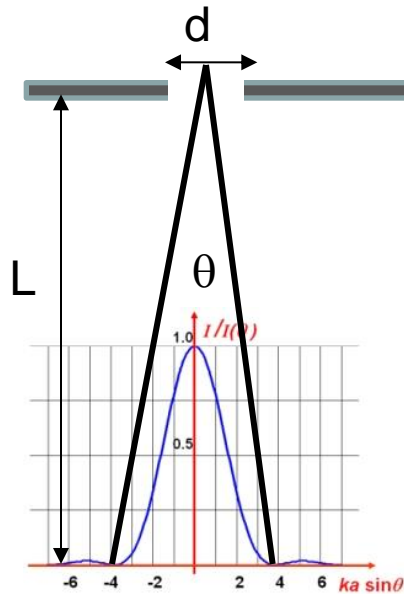
3D crystal



Electron diffractogram

A plane, coherent electron wave generates secondary wavelets from a row of scattering centers (atoms)
The secondary wavelets interfere, resulting in a strong direct (zero order) beam and several (higher order) beams scattered (diffracted) at specific angles.

Circular aperture Diffraction of fotons or electrons- Difrraction limit

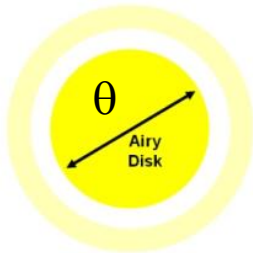


Airy Disk

These rings are produced by Fraunhofer Diffraction by the circular aperture.

$L \gg \lambda$

Using the small angle approximation
Airy disk diameter θ in radians



$$d \sin \theta = 1.22 \lambda$$

$$\theta \cong 1.22 \frac{\lambda}{d}$$

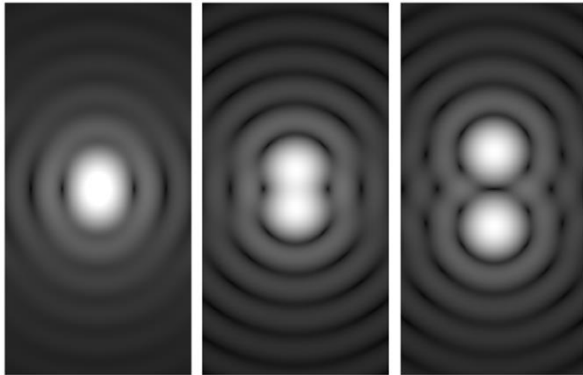
According to the Rayleigh Criterion, two point sources cannot be resolved if their separation is less than the radius of the Airy disk. The Airy disk is named for the English astronomer Sir George Biddell Airy, who served as the seventh Astronomer Royal from 1835-1881

Abbe Resolution = $2\lambda/NA$ 1873

$$d_0 = \frac{\lambda}{NA} = \frac{\lambda}{2n \sin \theta}$$

refined by Lord Rayleigh in 1896

$$d_0 = \frac{0.61\lambda}{n \sin \theta} \approx \frac{0.61\lambda}{\sin \theta}$$



For electrons $n=1$, and small angles

So for better resolution $\theta \uparrow$ and $\theta \downarrow$

wavelength of electrons

L. De Broglie 1924

Phil. Mag., 47 446

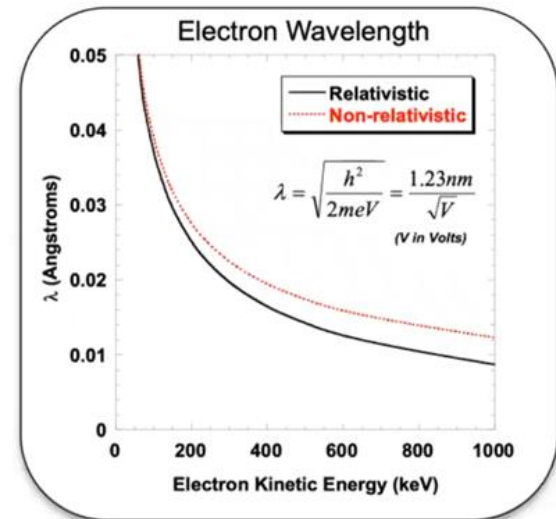
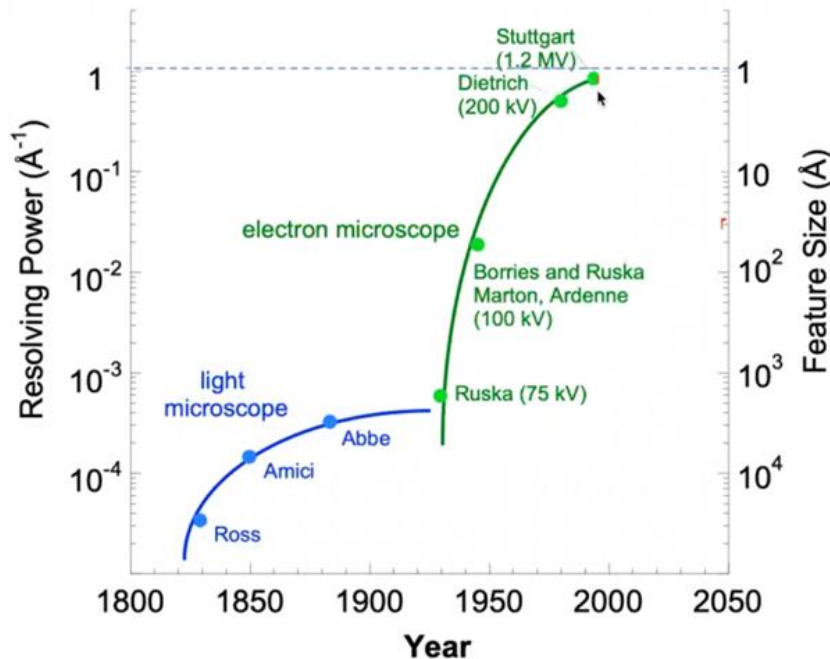
$$\lambda = h/p = h/mv$$

h Planck constant

p the momentum of the particle

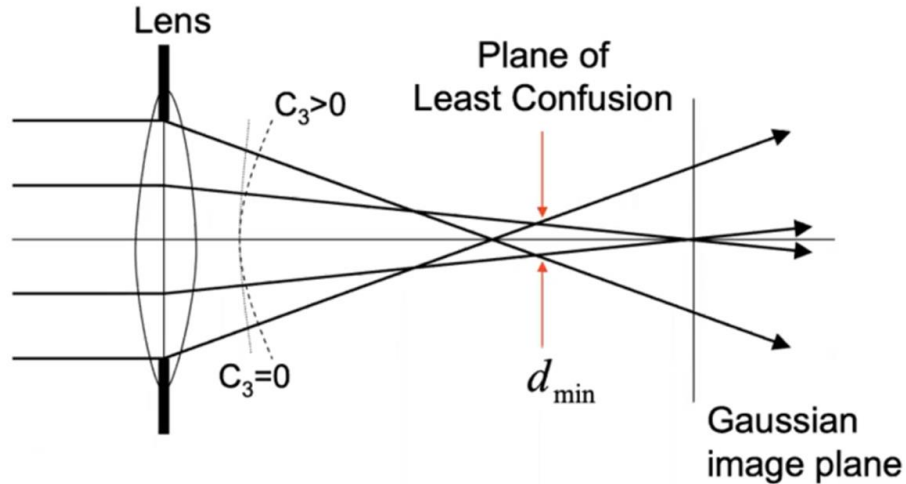
$$\lambda_B = \frac{h}{mv} = \frac{h}{\frac{m_0}{\sqrt{1-\frac{v^2}{c^2}}}v} = \frac{h\sqrt{1-\frac{v^2}{c^2}}}{m_0v}$$

Acceleration voltage	λ [nm]	λ (nm) relativistic	% of c
100	0.00386	0.00370	0.54%
200	0.00273	0.00251	0.69%
300	0.00223	0.00197	0.77%



Resolution limit due to spherical aberration

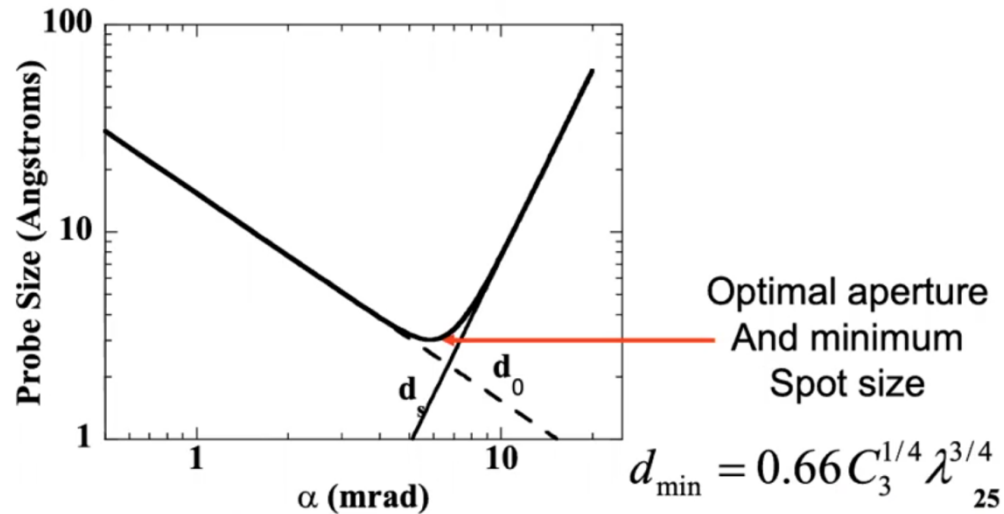
C_3 spherical aberration coefficient of objective lens



For a lens with aperture angle α , the minimum blur is $d_{\min} = \frac{1}{2} C_3 \alpha^3$

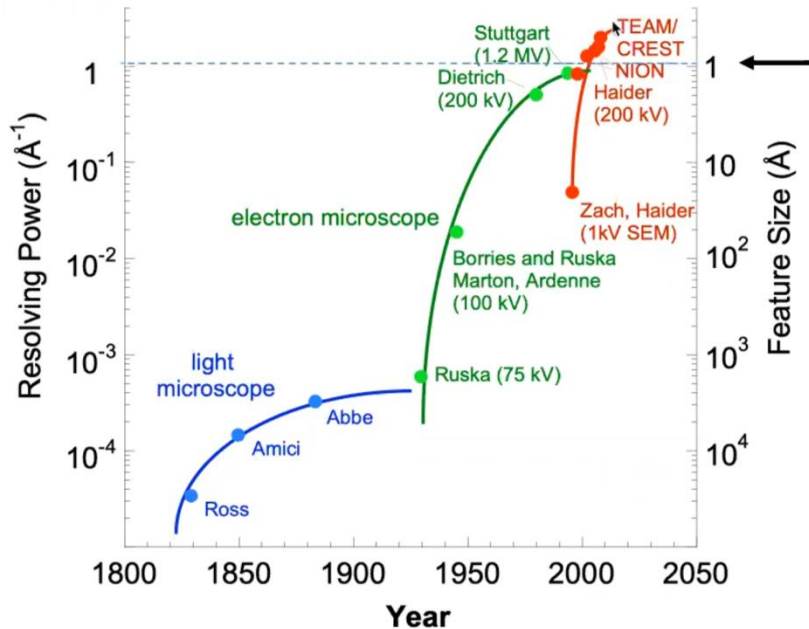
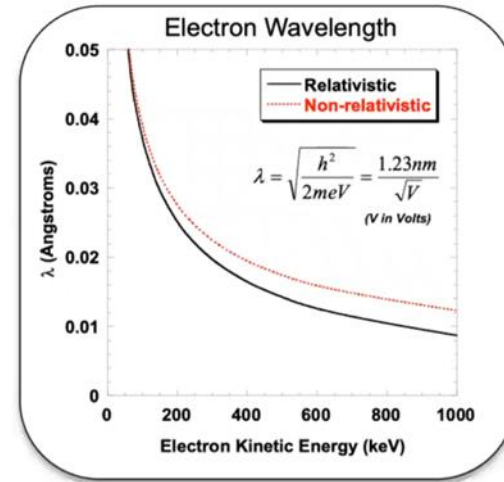
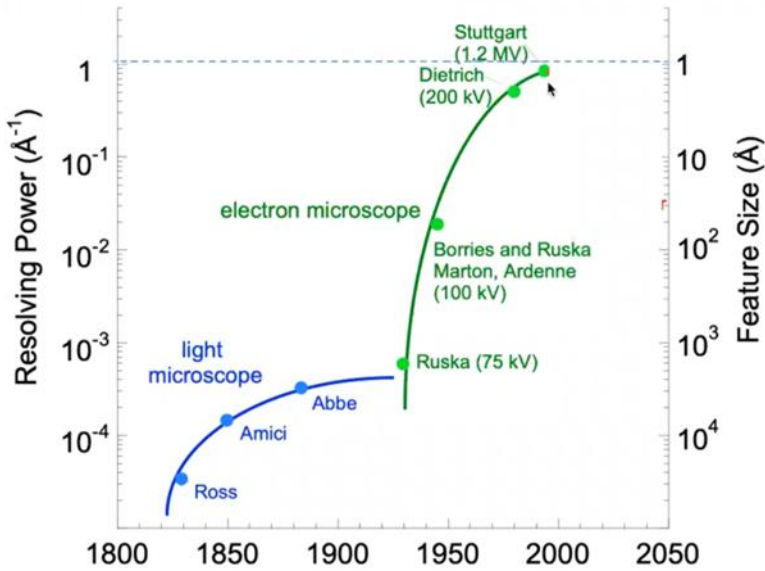
Typical TEM numbers: $C_3 = 1 \text{ mm}$, $\alpha = 10 \text{ mrad}$ $\rightarrow d_{\min} = 0.5 \text{ nm}$

Resolution limit due to spherical aberration minimum beam spot in STEM



For a rough estimate of the optimum aperture size, convolve blurring terms
-If the point spreads were gaussian, we could add in quadrature:

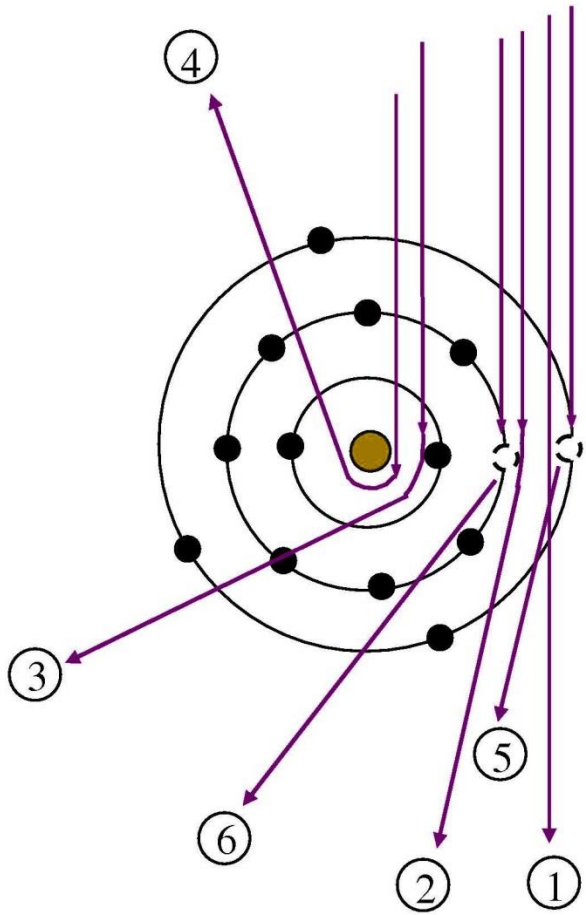
$$d_{tot}^2 \approx d_0^2 + d_s^2 = \left(\frac{0.61\lambda}{\alpha_0} \right)^2 + \left(\frac{1}{2} C_3 \alpha_0^3 \right)^2$$



Aberation corection technology
Sub angstrom microscopy
Resolution in pm

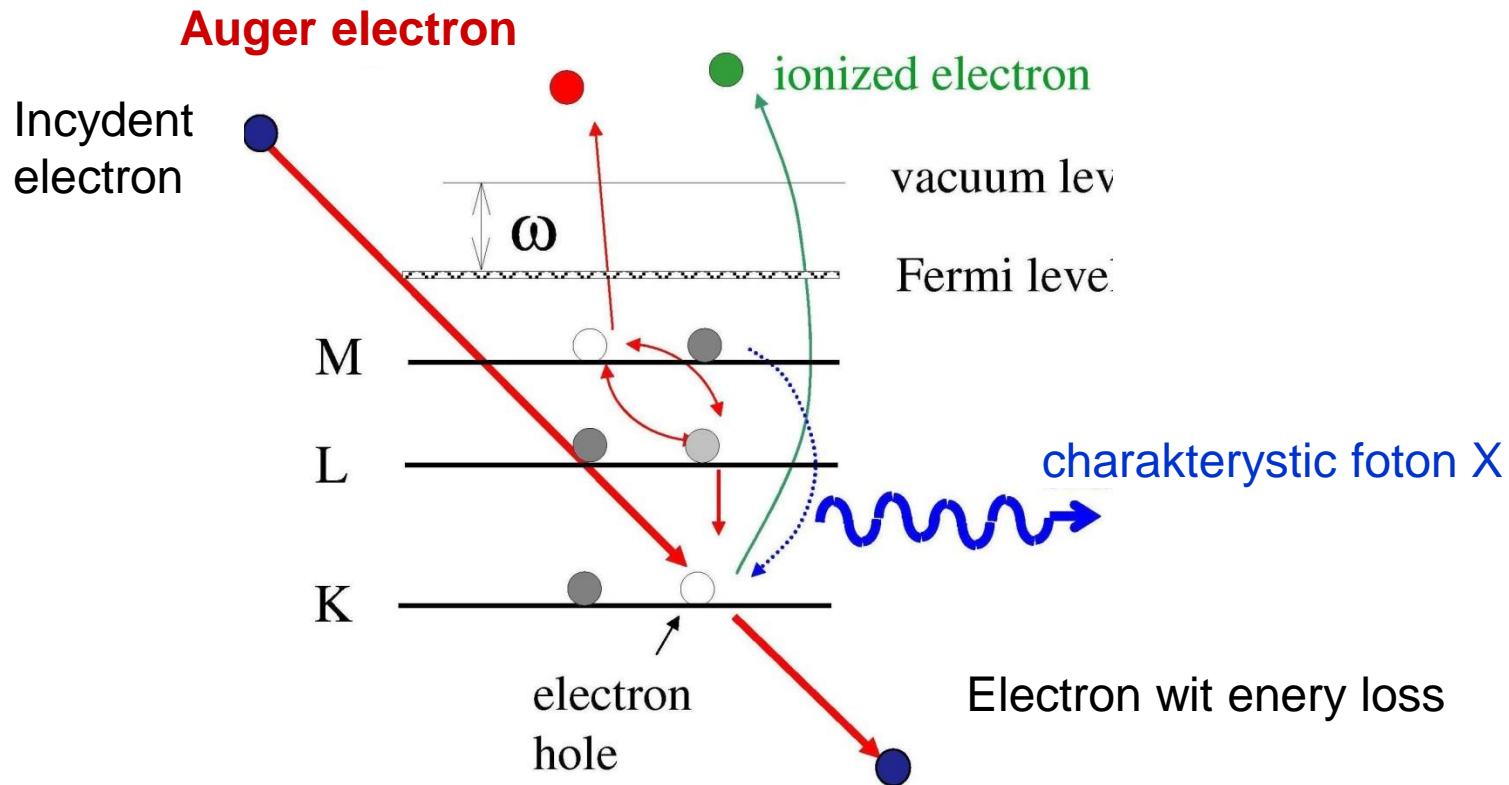
The interaction of high-energy electrons with an atom

- energy 30-1000 KeV

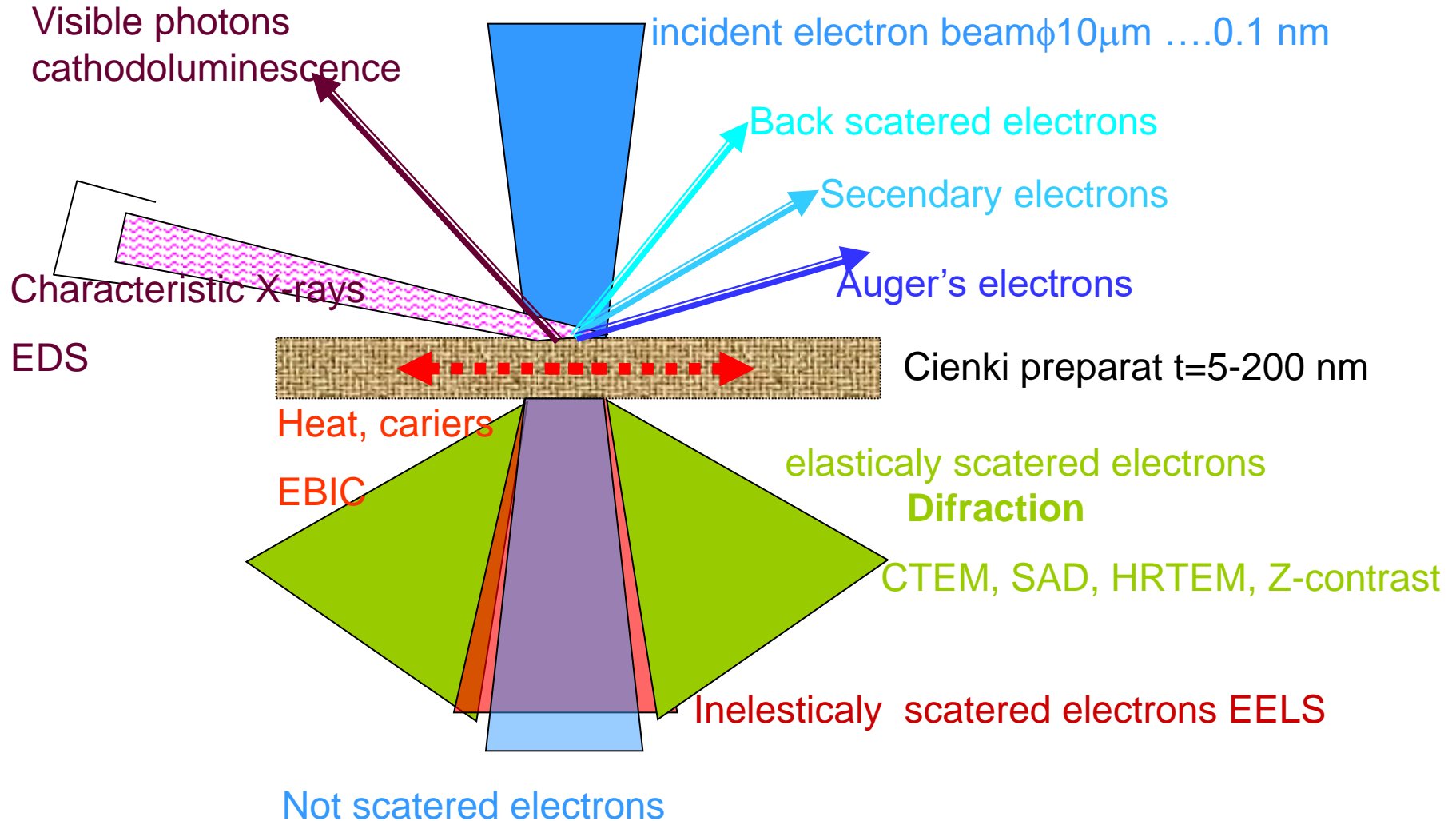


1. Not scattered electron
2. Low angle elastic scattering
3. High angle elastic scattering
4. Backward scatter
5. Inelastic scattering on outer shell
6. Inelastic scattering on inner shell

The interaction of high-energy electrons with a solid - inelastic scattering



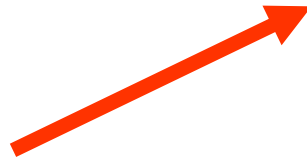
The signals produced by an electron probe in a thin crystal used for imaging and / or spectroscopy



Why are electrons so interesting?

	Scattered on :	Mean free path [nm]	Absorption length [nm]
Neutrons	nucleus	10^7	10^8
X-rays	electrons	10^3	10^5
electrons	potential	10	10^2

Very strong interaction with matter



The signal from 1 atom in the sample for electrons is **10^4** bigger than for X-rays !!

Thin electron transparent sample : 10-50 nm grubości

- Ion milling

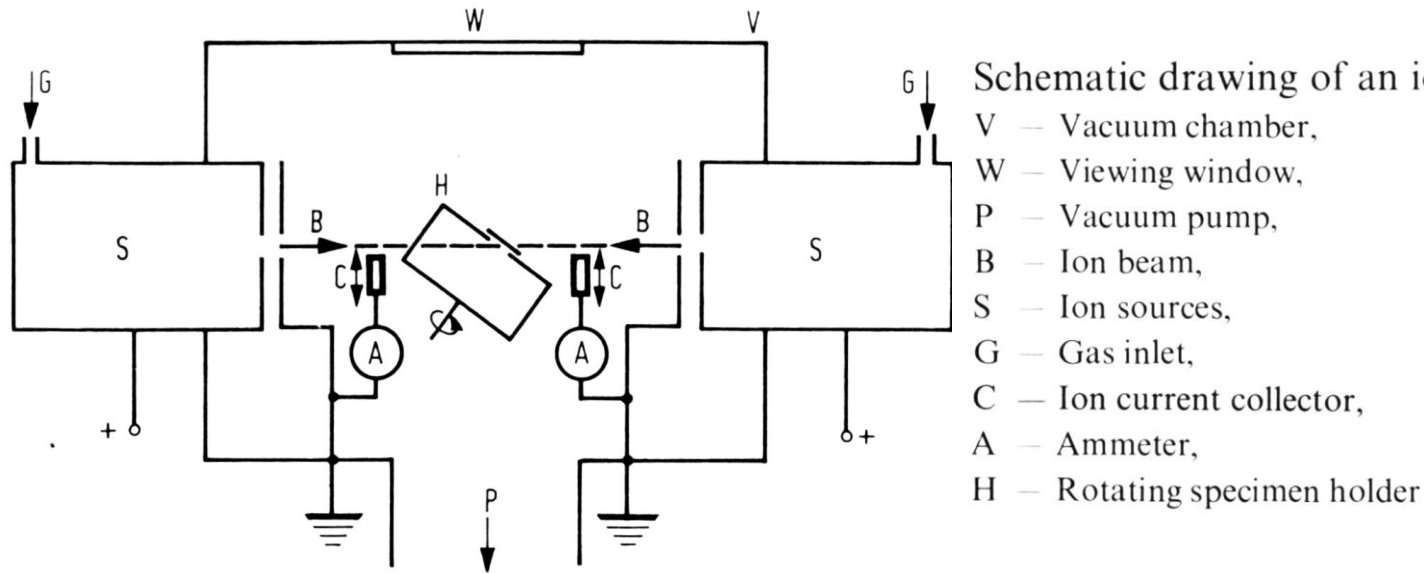


Image from: Electron Microscopy in Solid State Physics H. Bethge and J. Heydenreich, Elsevier 1987

Ion beam incidence angle 1-25 ° but <5 ° avoids selective etching

Accelerating voltage 4-9kV (200V- 8kV) time 1-48h

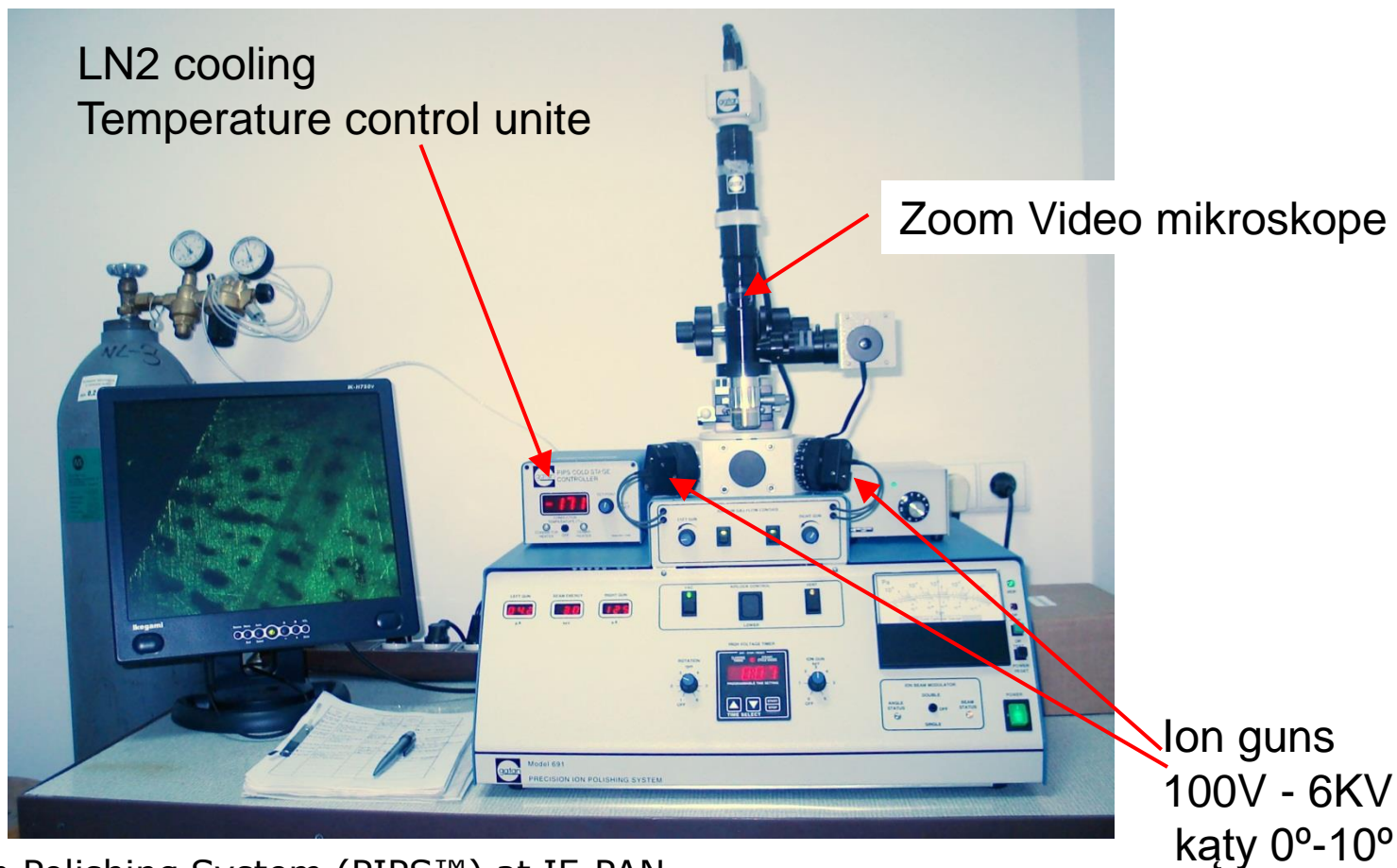
Argon ions, cooling with liquid nitrogen indirectly, (with a stream of inert gas)

vacuum 10⁻⁵ Torr (10⁻³ Torr when etching)

Ion milling

Radiation damage , surface amorphization

Damage limitation by: lower voltage, reducing the angle of incidence of the ion beam, cooling of sample





IFPAN from Jun 2010

Electron resolution

→ 0.9 nm @ 15 kV

→ 1.4 nm @ 1 kV

Ion resolution

→ 5.0 nm @ 30kV

Ion energy 500V-30kV

EDX

Omiprobe

GIS- Pt

GIS-W

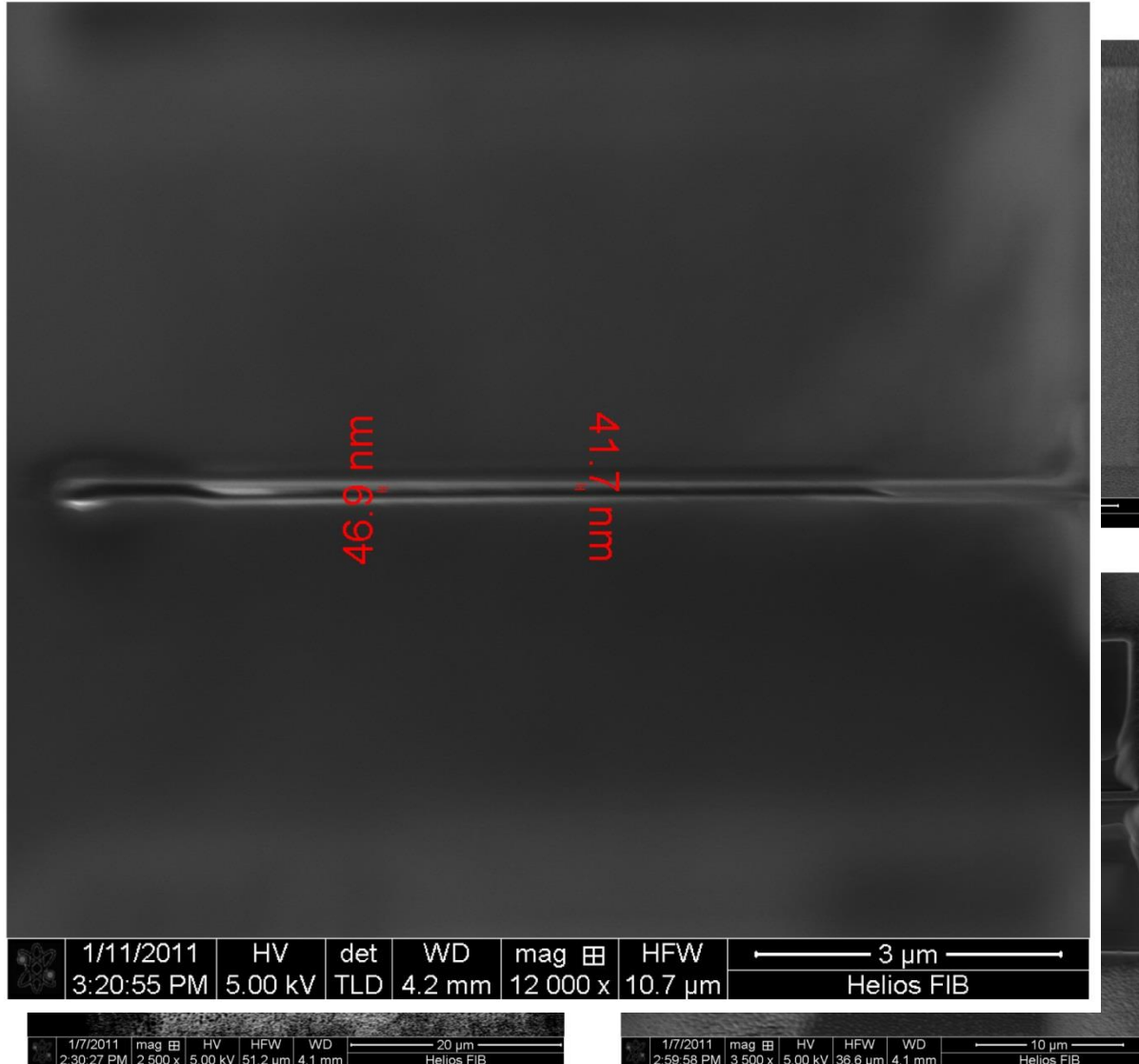
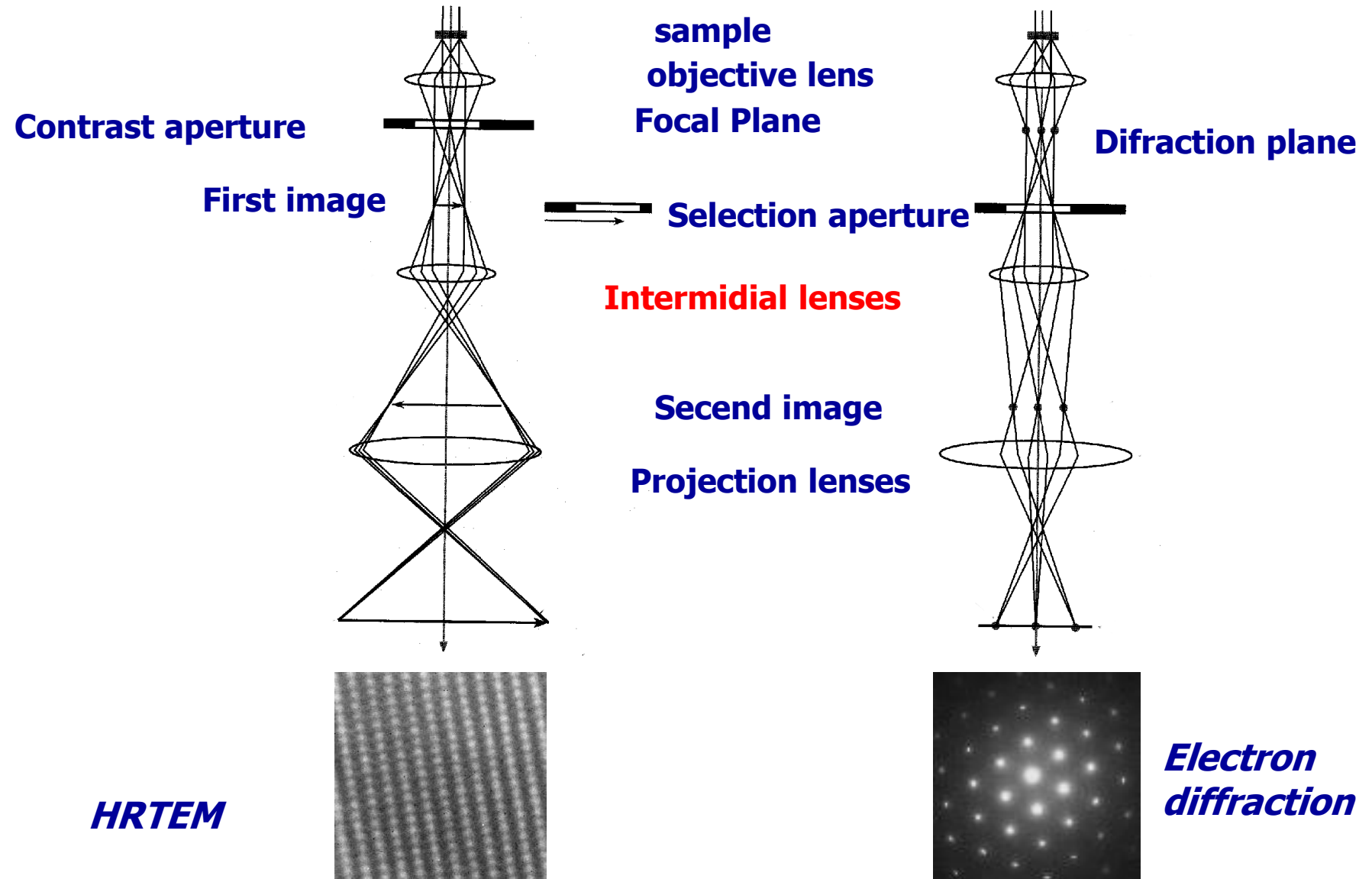


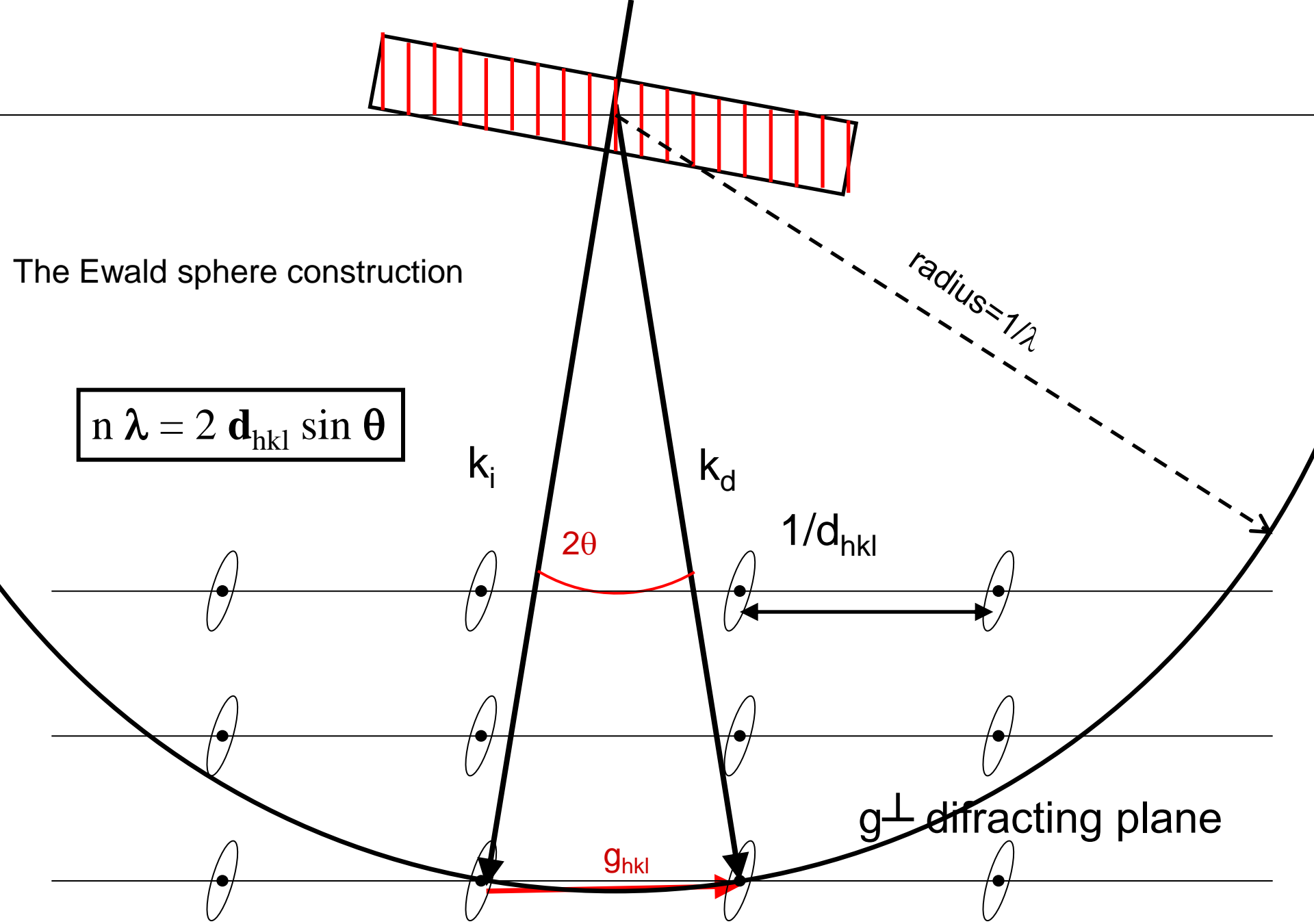
*Photo B.Kurowska
M.Klepka*

Basic Modes of Operation of the TEM microscope



The Ewald sphere construction

$$n \lambda = 2 d_{hkl} \sin \theta$$

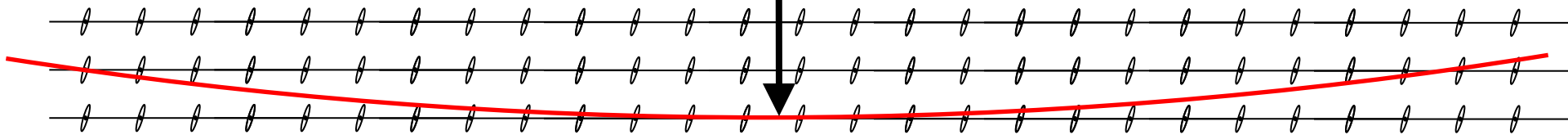
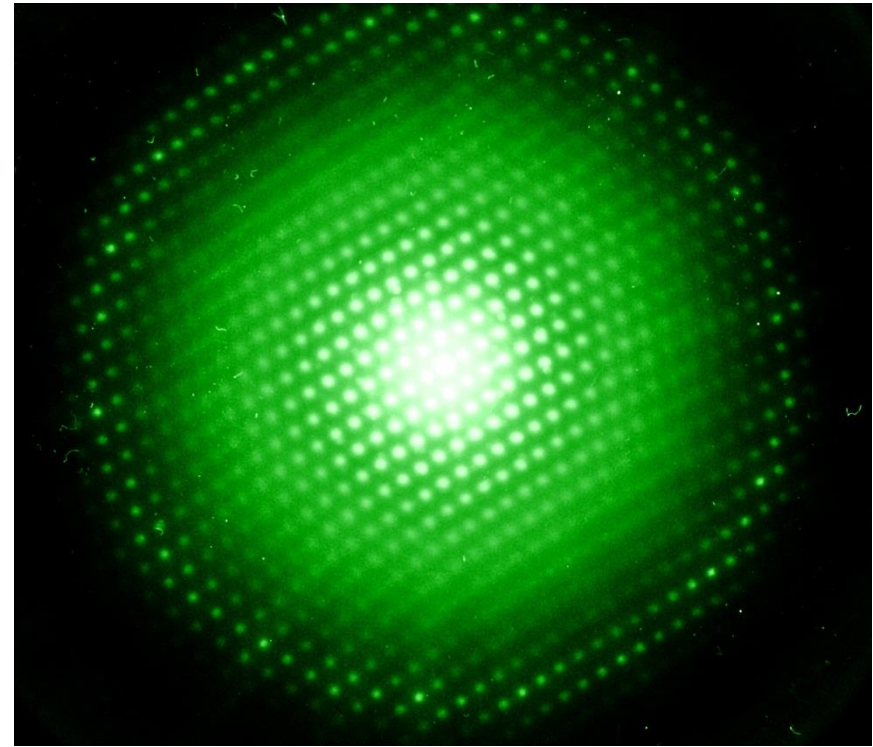


The Ewald sphere for high energy electrons

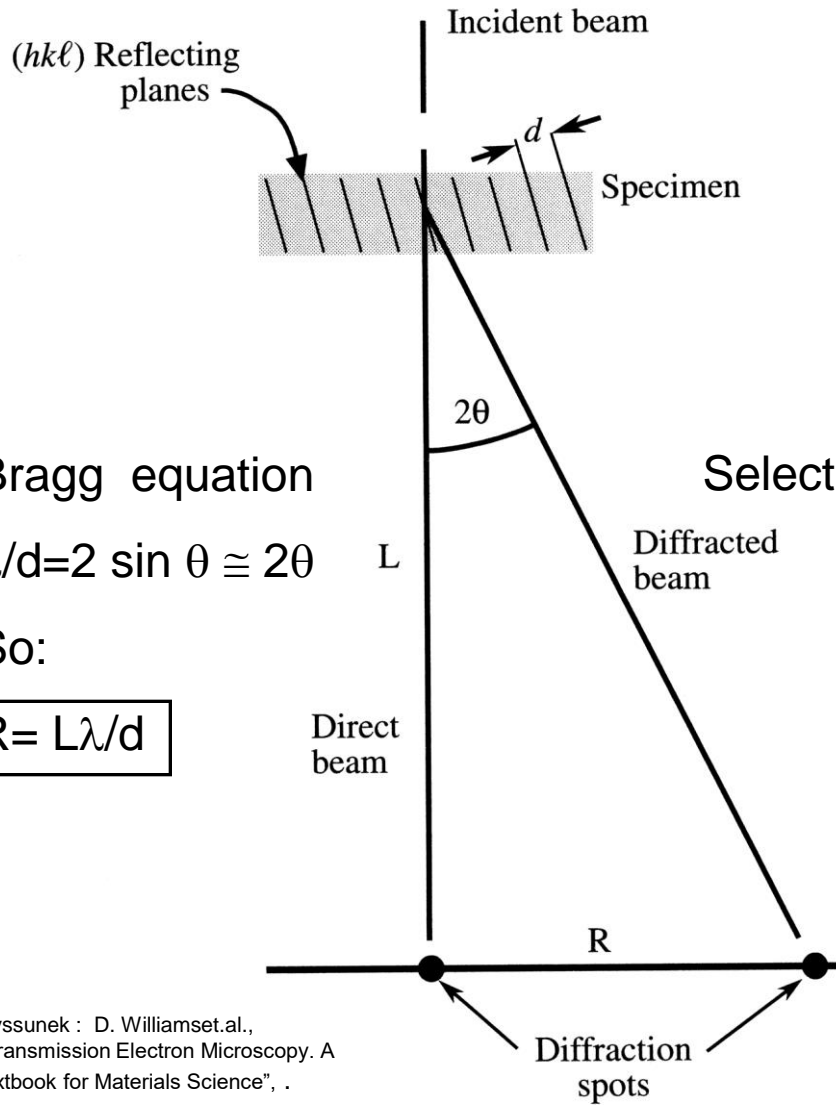
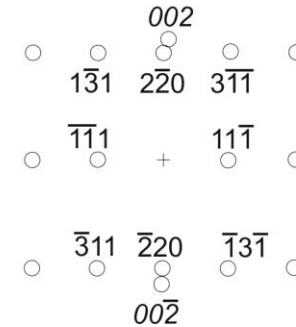
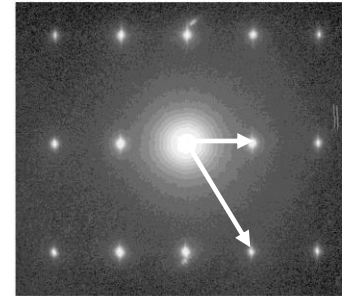
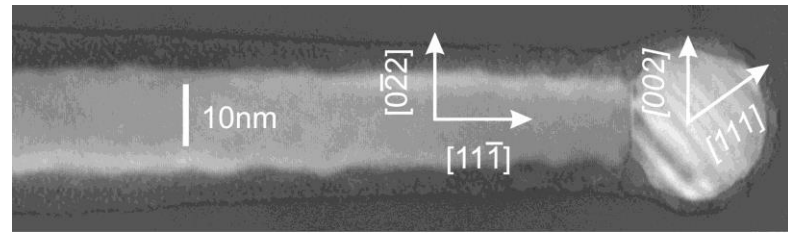
Diffraction occurs when the Ewald sphere intersects a reciprocal lattice node

$$1/\lambda$$

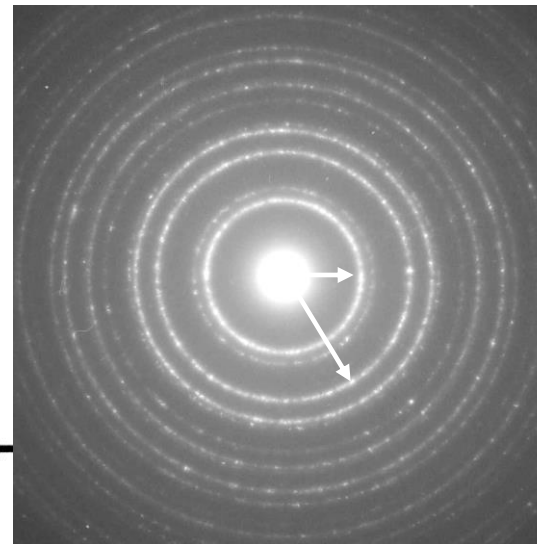
For 200 kV electrons,
 $1/\lambda = 1/0.00273 \text{ nm} =$
366 nm⁻¹



Electron diffraction



Selected area diffraction SAD from ZnTe nanowire

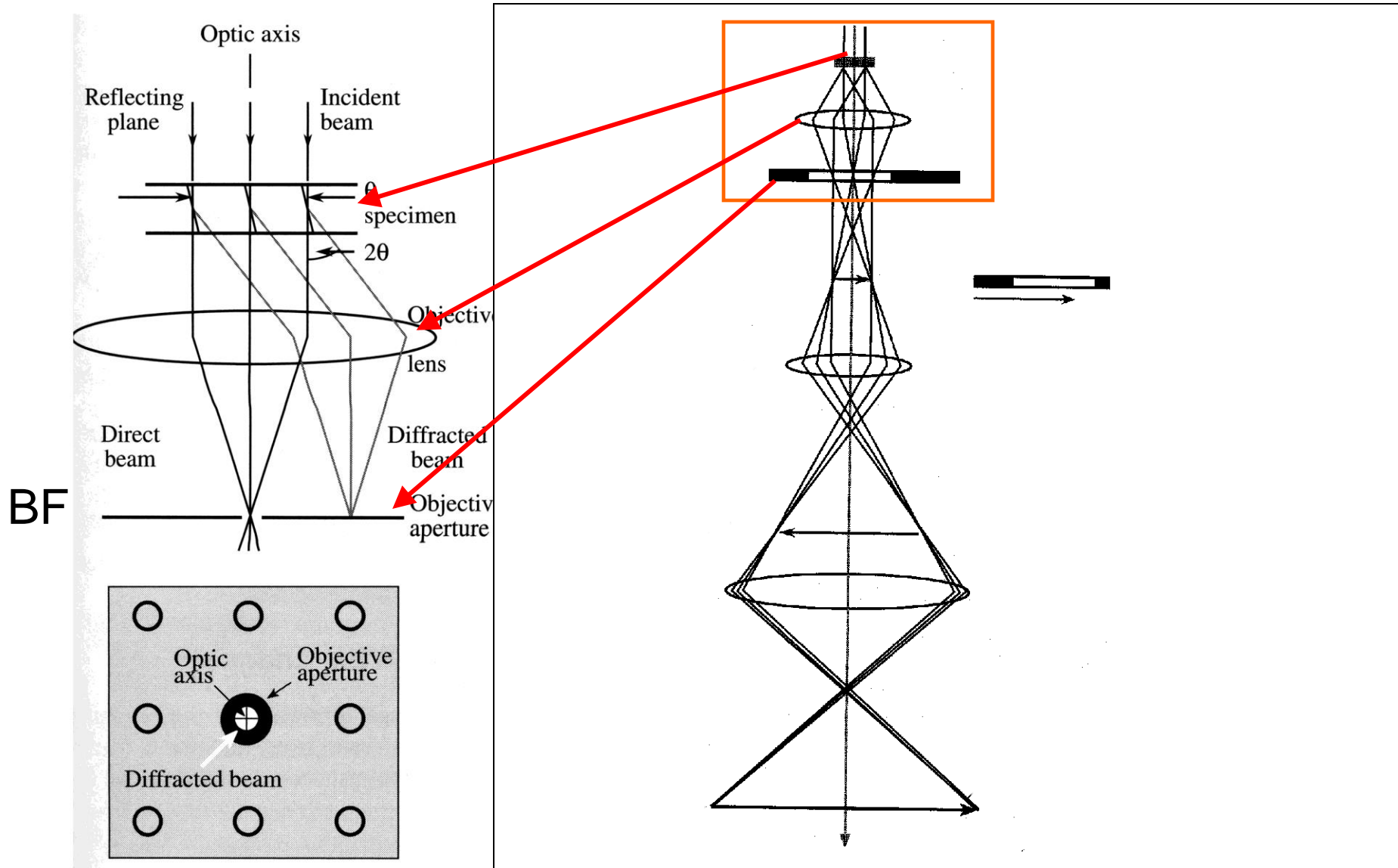


Difraction from many nanowires as X-ray powder diffraction

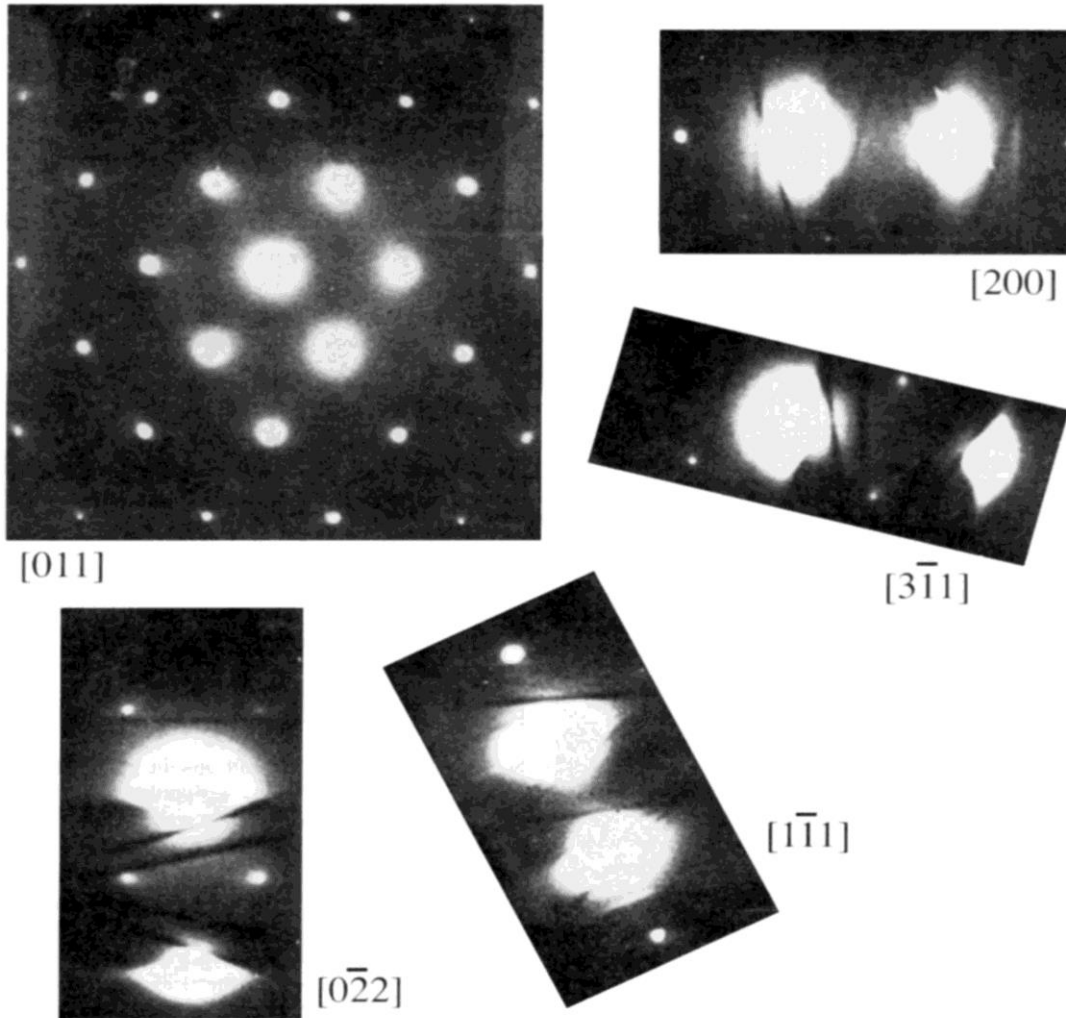
Fot. P.Dluzewski, S.Kret IF-PAN

Ryssunek : D. Williamset.al.,
"Transmission Electron Microscopy. A
textbook for Materials Science", .

Diffraction contrast: bright and dark field

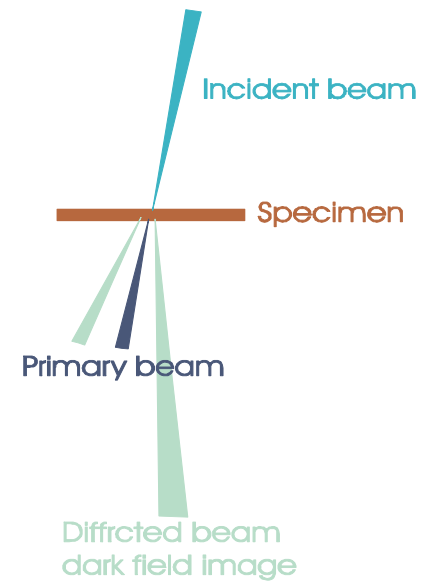
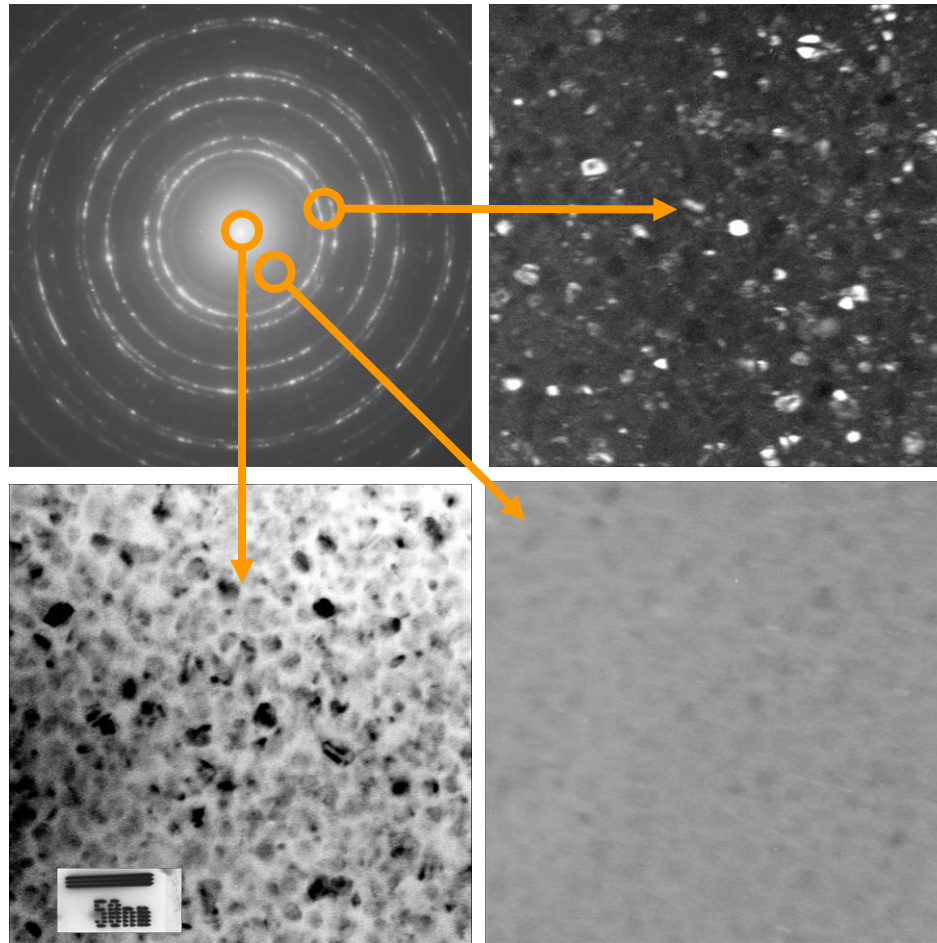
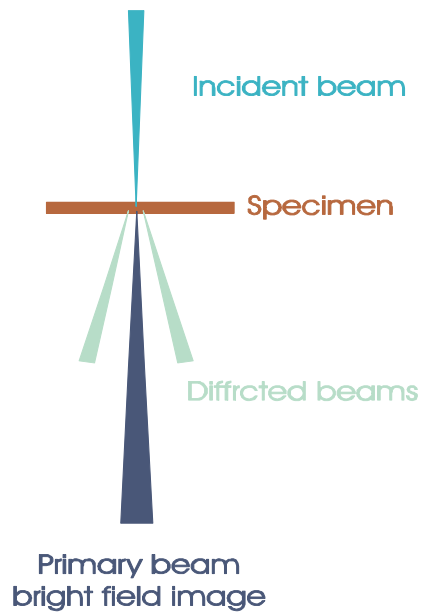


Two-beam conditions for Si near 001 zone axis



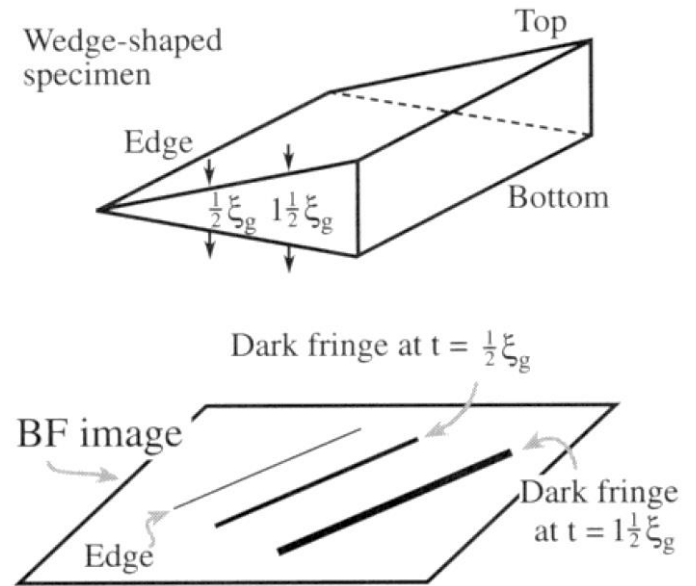
Diffraction contrast: bright and dark field

Pd crystallites 5-15 nm



PERFECT CRYSTALS → Thickness contours

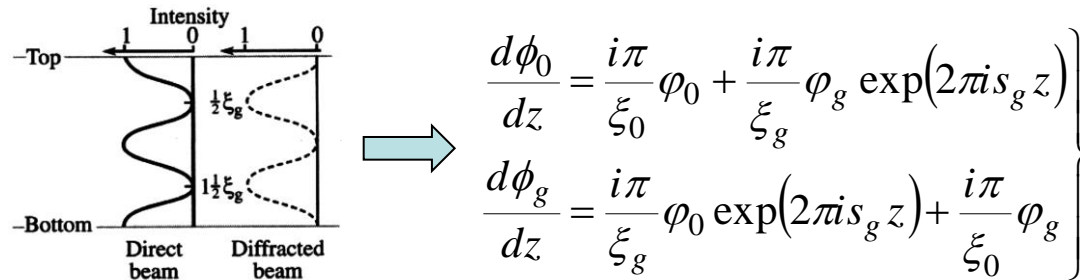
InGaN/GaN 11-20 zone axis DF image



For a wedge specimen, the separation of the fringes in the image is determined by the angle of the wedge and the extinction distance, ξ_g .

The Howie-Whelan equations for two beams and perfect crystal

Description of the amplitude of diffracted ϕ_0 and ϕ_g as a function of z is given by :



The diagram on the left shows the intensity profiles of the direct and diffracted beams as a function of position z from the top to the bottom of a crystal. The direct beam intensity (solid line) starts at 1 at the top and decreases sinusoidally. The diffracted beam intensity (dashed line) starts at 0 at the top and increases sinusoidally. The vertical axis is labeled z with markers for 0 , $\frac{1}{2}\xi_g$, and $1\frac{1}{2}\xi_g$. The horizontal axis is labeled 'Intensity' with markers for 0 and 1. The regions are labeled 'Direct beam' and 'Diffracted beam'. A blue arrow points from the diagram to the equations on the right.

$$\left. \begin{aligned} \frac{d\phi_0}{dz} &= \frac{i\pi}{\xi_0} \phi_0 + \frac{i\pi}{\xi_g} \phi_g \exp(2\pi i s_g z) \\ \frac{d\phi_g}{dz} &= \frac{i\pi}{\xi_g} \phi_0 \exp(2\pi i s_g z) + \frac{i\pi}{\xi_0} \phi_g \end{aligned} \right\}$$

Integration over the entire thickness gives the ϕ_0 and ϕ_g at exit surface of the specimen

The bright-field intensity is then given by $\phi_0 \phi_0^*$

The dark-field intensity is then given by $\phi_g \phi_g^*$

The extinction distance is given by:

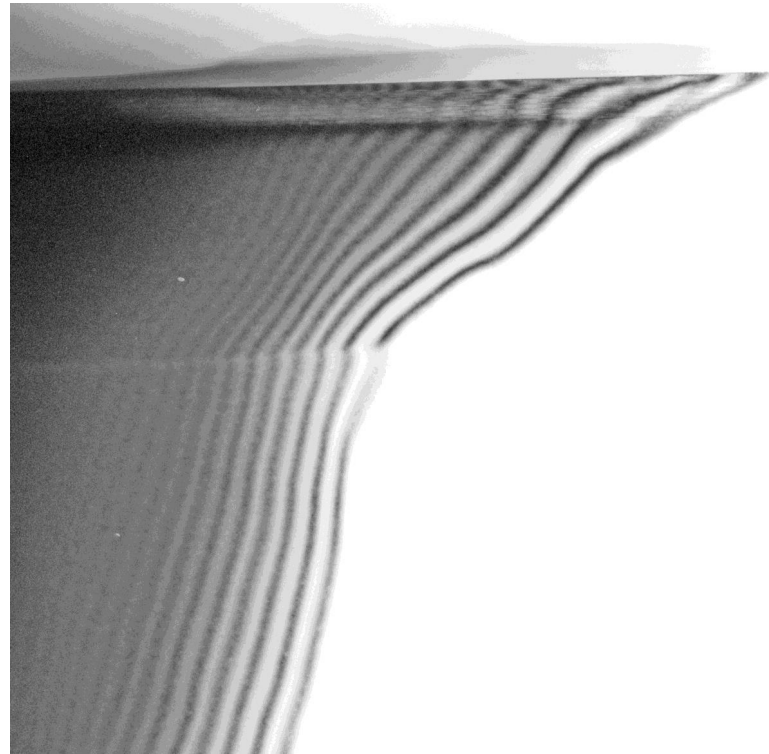
$$\xi_g = \frac{\pi V_c \cos \theta_B}{\lambda F_g}$$

Analytical solution of the Howie-Whelan equations

$$Ig = |\phi_g|^2 = \phi_g \phi_g^* = \frac{\pi^2}{\xi_g^2} \frac{\sin^2 \pi t S_{eff}}{(\pi S_{eff})^2}$$

where

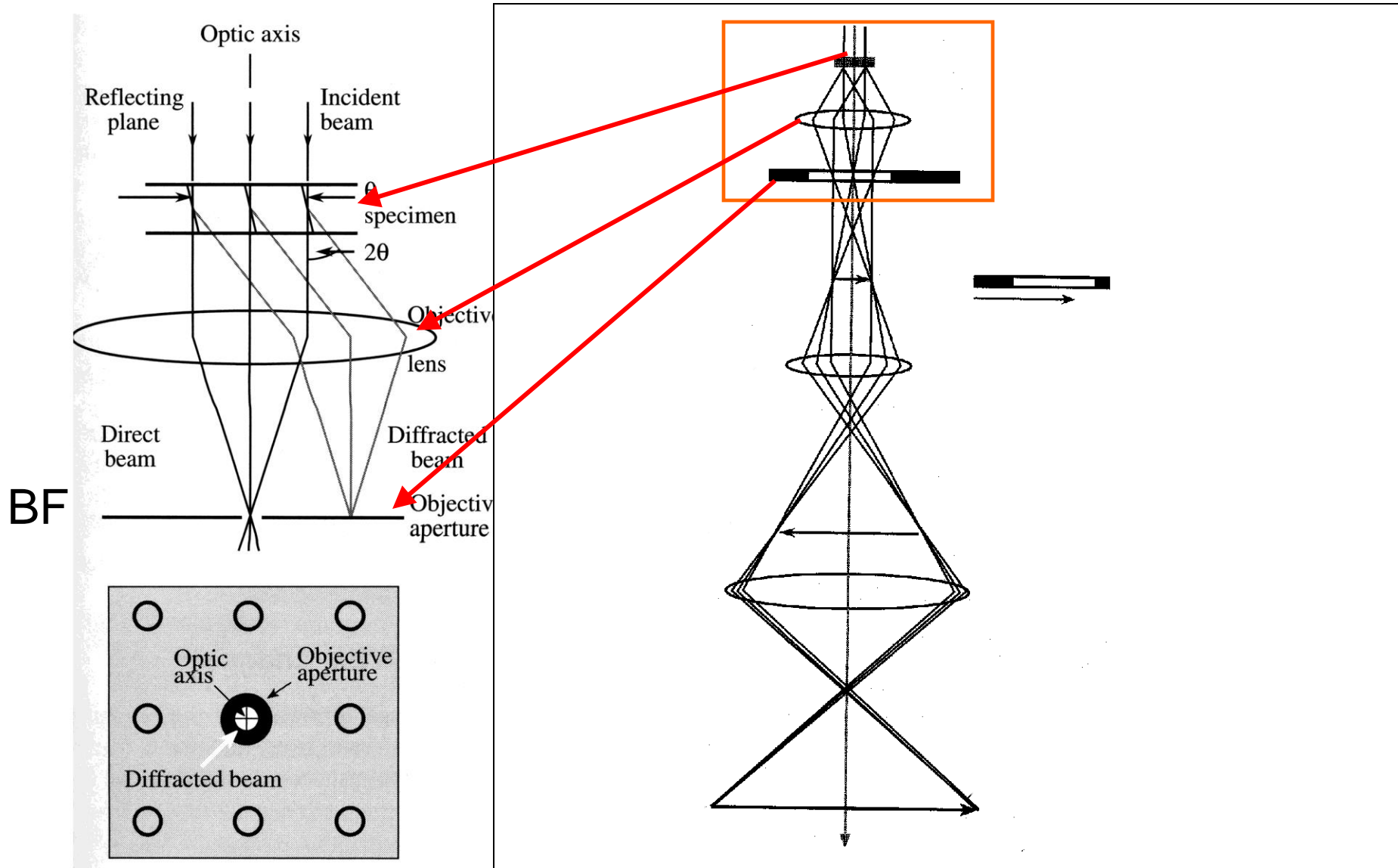
$$S_{eff} = \sqrt{s^2 + \frac{1}{\xi_g^2}}$$



„Absorption” high-angle scattering (elastic and/or inelastic)
can be accounted for by replacing $1/\xi$ by $1/\xi + i/\xi'$

’” a parameter ξ' which is usually about 0.1ξ is really a fudge factor that modifies H-W equations to fit the experimental observations ,,

Diffraction contrast: bright and dark field

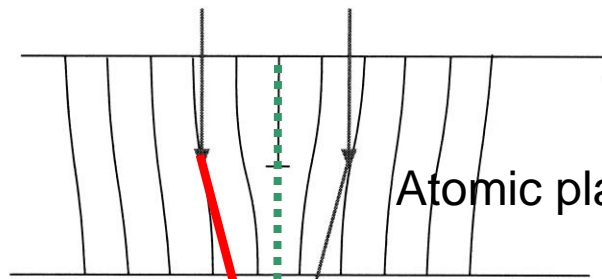


CRYSTAL WITH DEFECTS

Intuitive description of diffraction contrast of dislocation

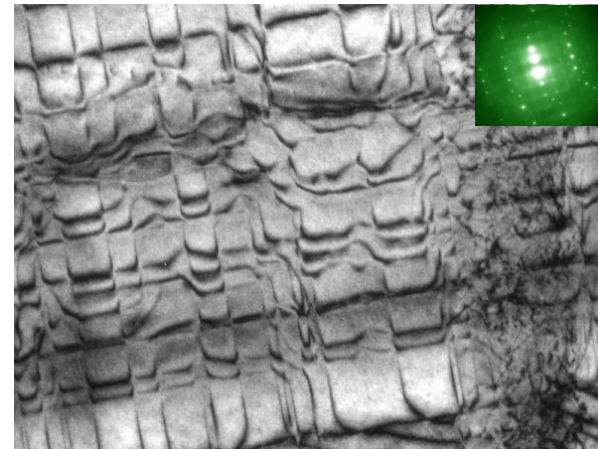
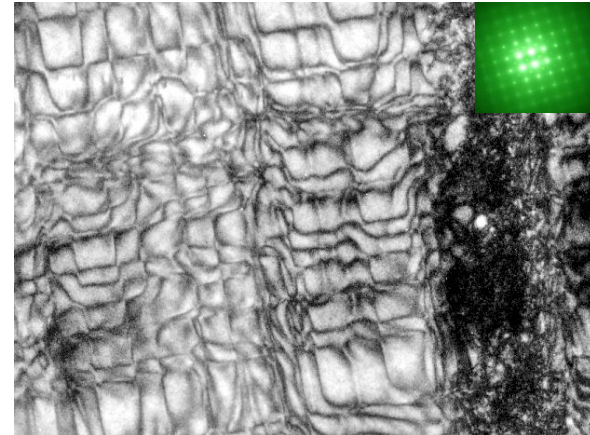
Bragg conditions locally satisfied

A



Axial BF

Atomic plane bending



TB-DF

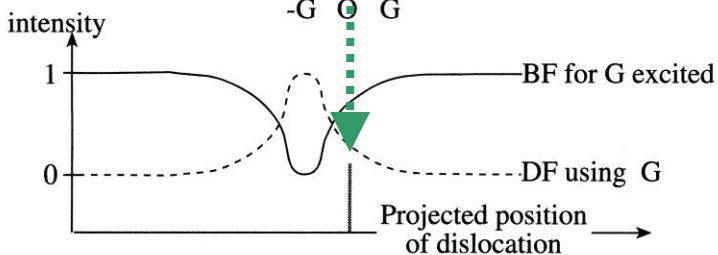
Photo :P.Dłużewski IF-PAN
Sample f. GELCZUK et.al. WEMiF ,Wrocław

Misfit dislocations $\text{GaAs}/\text{In}_{0.07}\text{Ga}_{0.93}\text{As}$

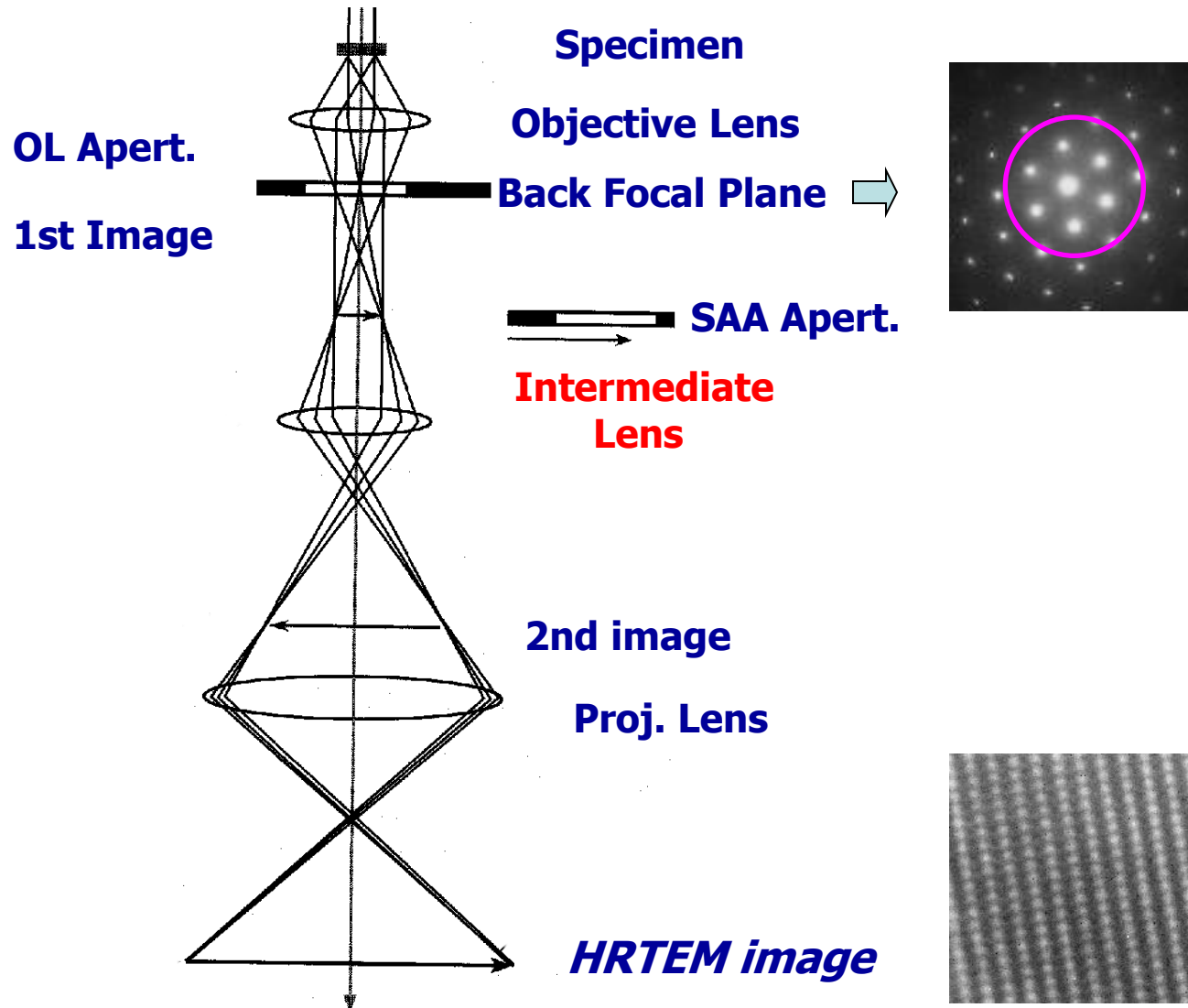
$(\bar{h}\bar{k}\bar{\ell})$ planes diffract $(hk\ell)$ planes diffract



B

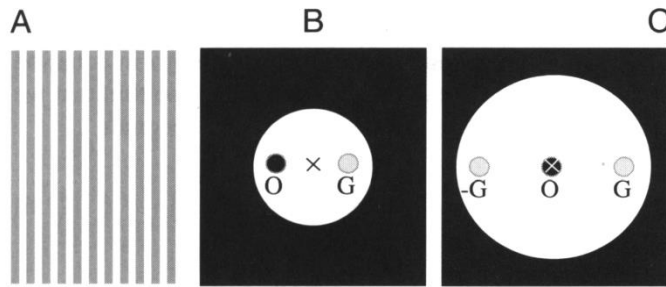


HRTEM image formation

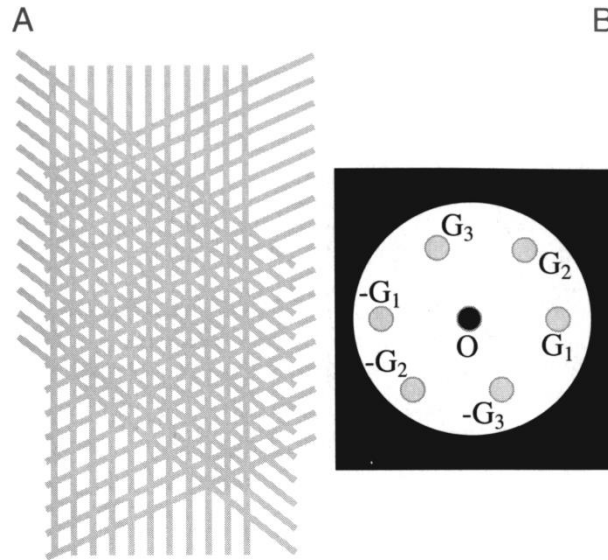


HRTEM image formation

beams selection of on the diffraction pattern



2 beams interference

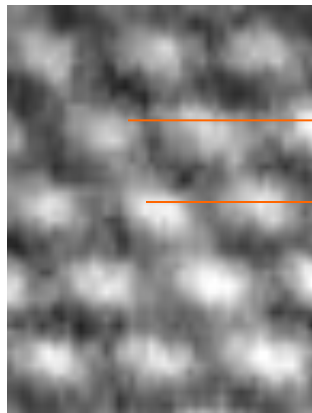
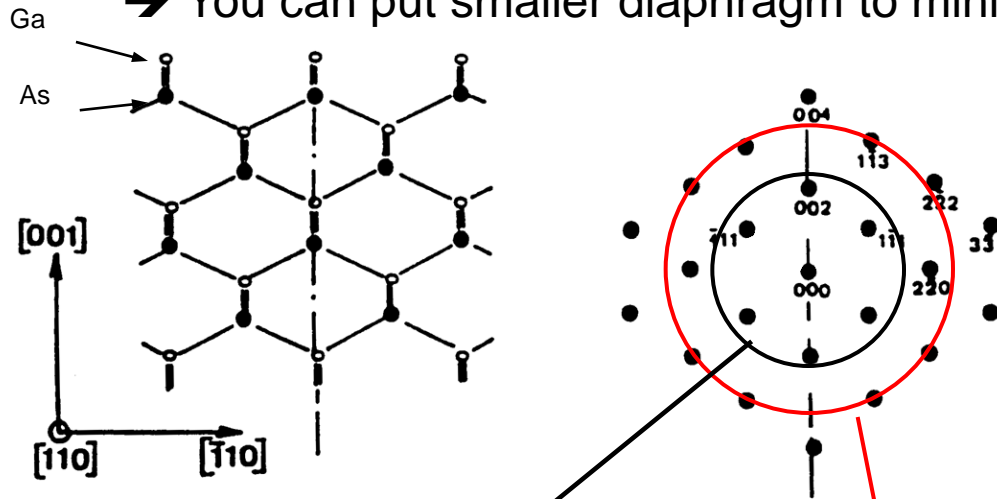


7 beams interference

HRTEM GaAs <110>

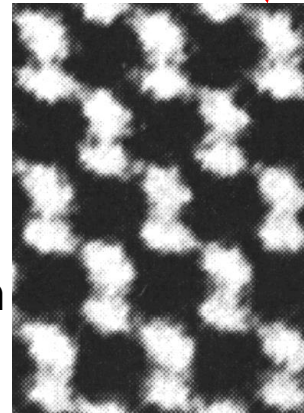
Don't forget about aberration of the lenses and MTF of the microscope

➔ You can put smaller diaphragm to minimize the aberrations



7 beams
Resolution:
0.27 nm

0.3 nm



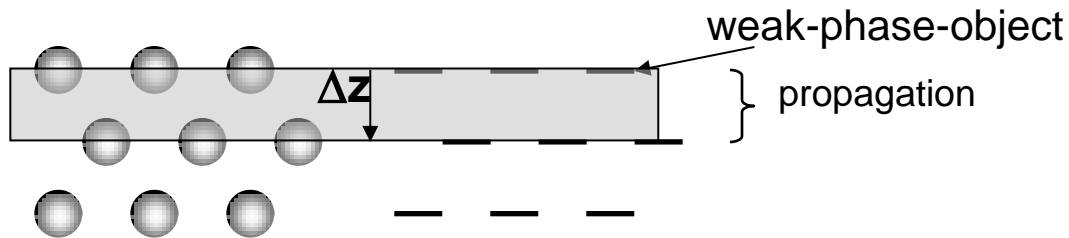
monolayer

13 beams
Resolution 0.16
nm

HRTEM Simulation:

Stage 1 → high-energy electrons in a crystal

metoda " multislice " : dividing a thick crystal into slices
"weak-phase-object aproximation"
Cowley and Moodie (1957)



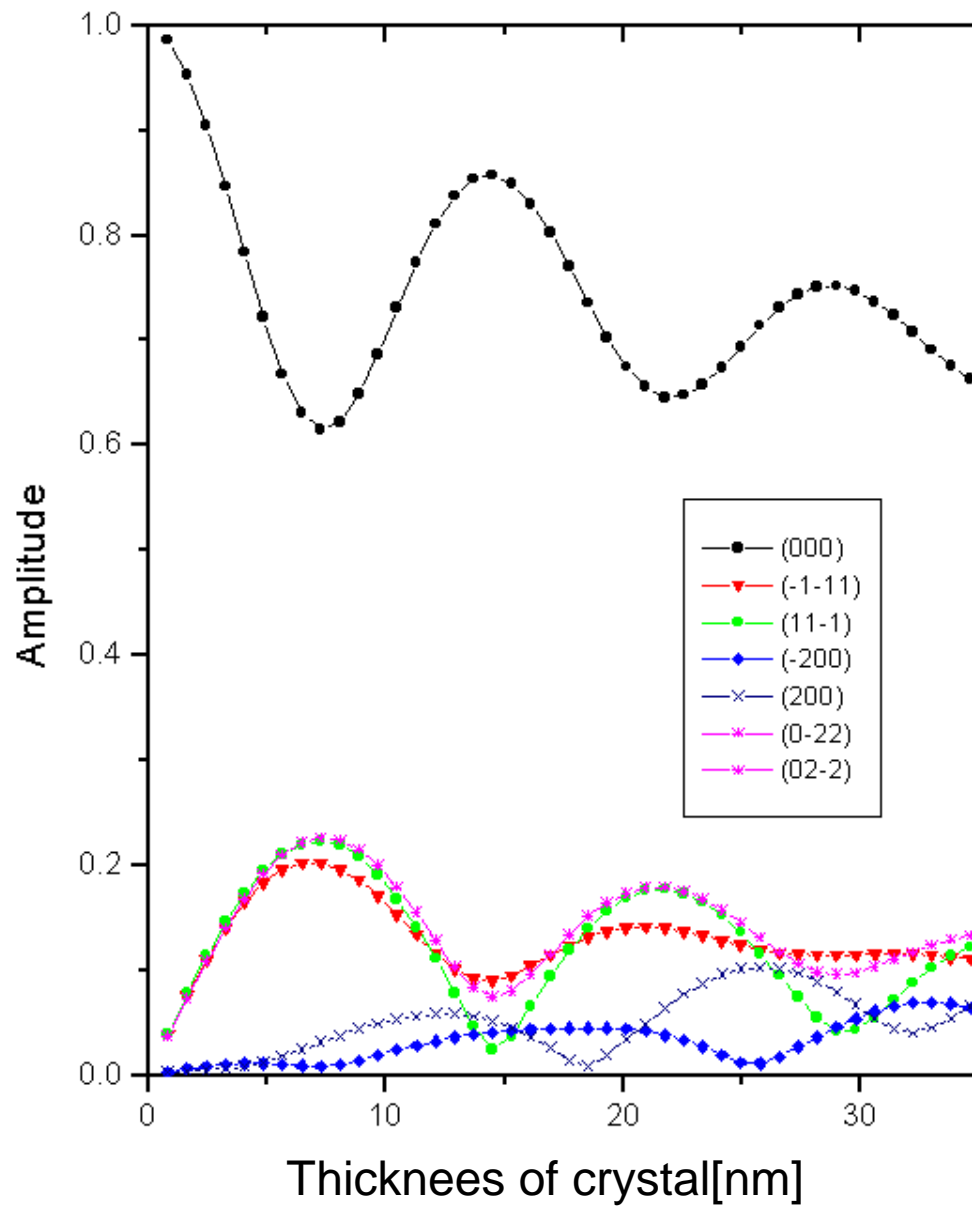
$$\Psi_{n+1}(\vec{r}) = [\Psi_n(\vec{r})q_{n+1}(\vec{r})] * p_{n+1}(\vec{r})$$

$$q_{n+1}(\vec{r}) = \exp\left[i \frac{\pi e}{\lambda E} \int_0^{\Delta z} V(x, y, z) dz\right]$$

Slice "transparency" function (n+1)

$$p_{n+1}(\vec{r}) = \exp\left(-i \frac{k_z (x^2 + y^2)}{2\Delta z}\right)$$

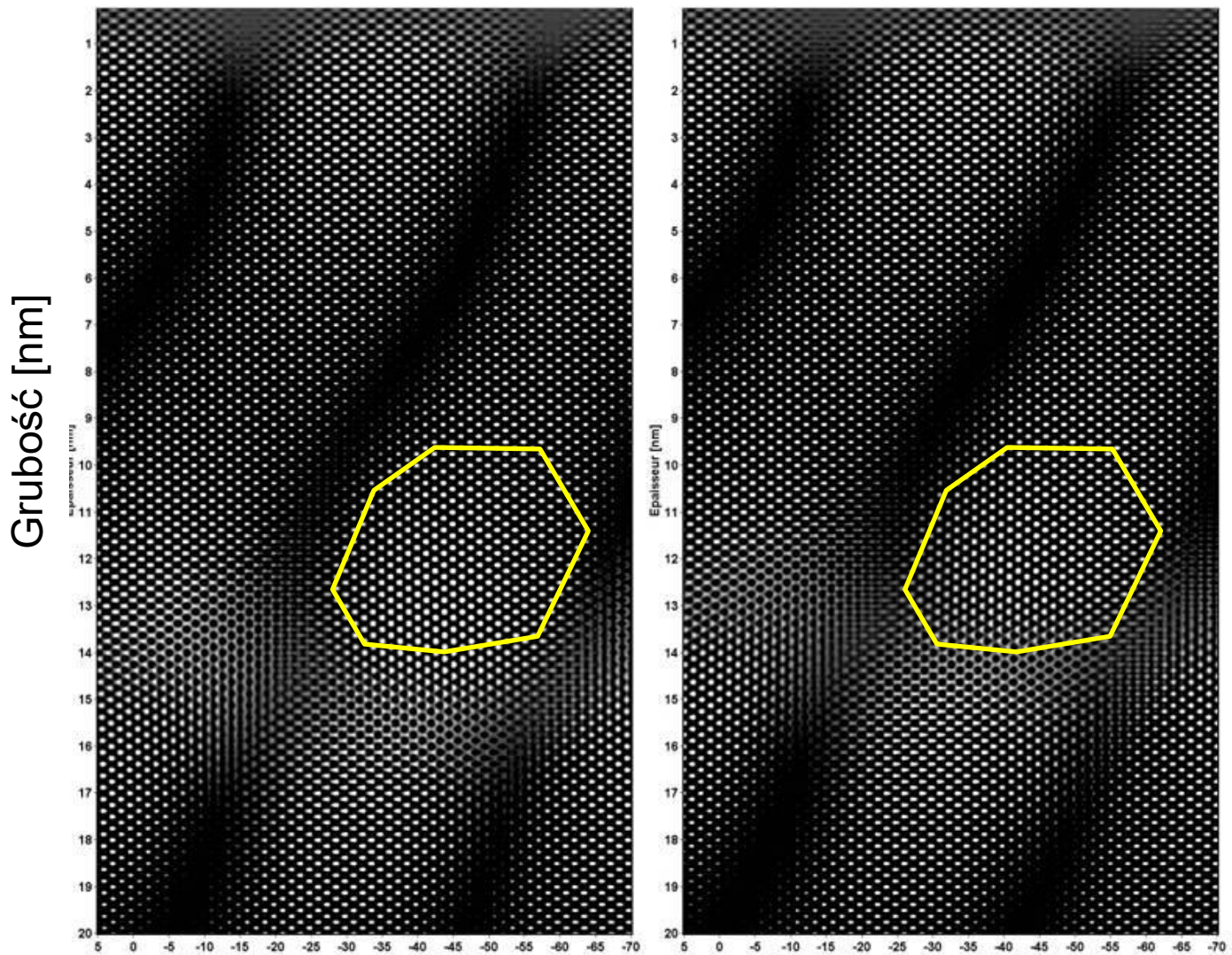
Propagator



Primary beam amplitudes and the main beams are deflected (no absorption)

GaAs incident beam direction $\langle 110 \rangle$

Simulated HRTEMcontrast at 200 kV LaB_6



defocus [nm]

$\text{In}_{0.5}\text{Ga}_{0.5}\text{As}$ <110> Zone axis

GaAs <110> Zone axis

HRTEM SIMULATION: STAGE II

➔ electrons in the optical system of the microscope

nonlinear image formation approximation
in **partially** coherent illumination K. Ishizuk 1980

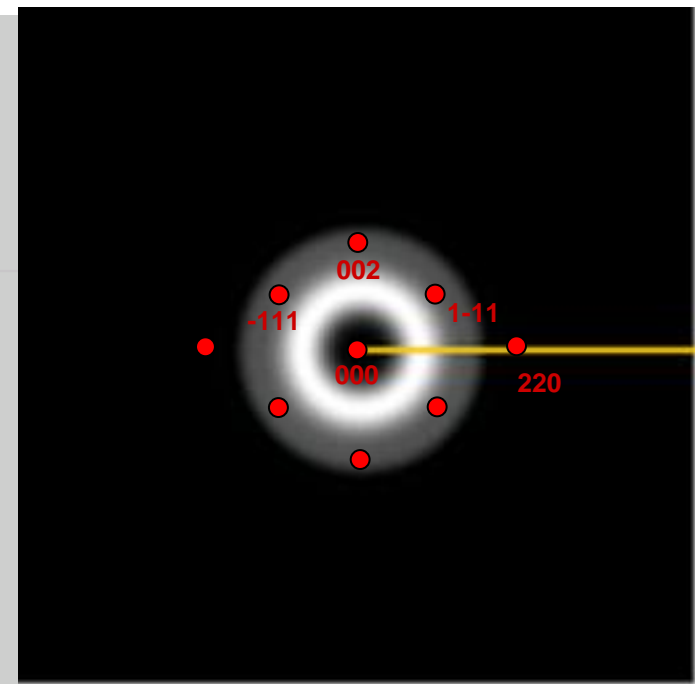
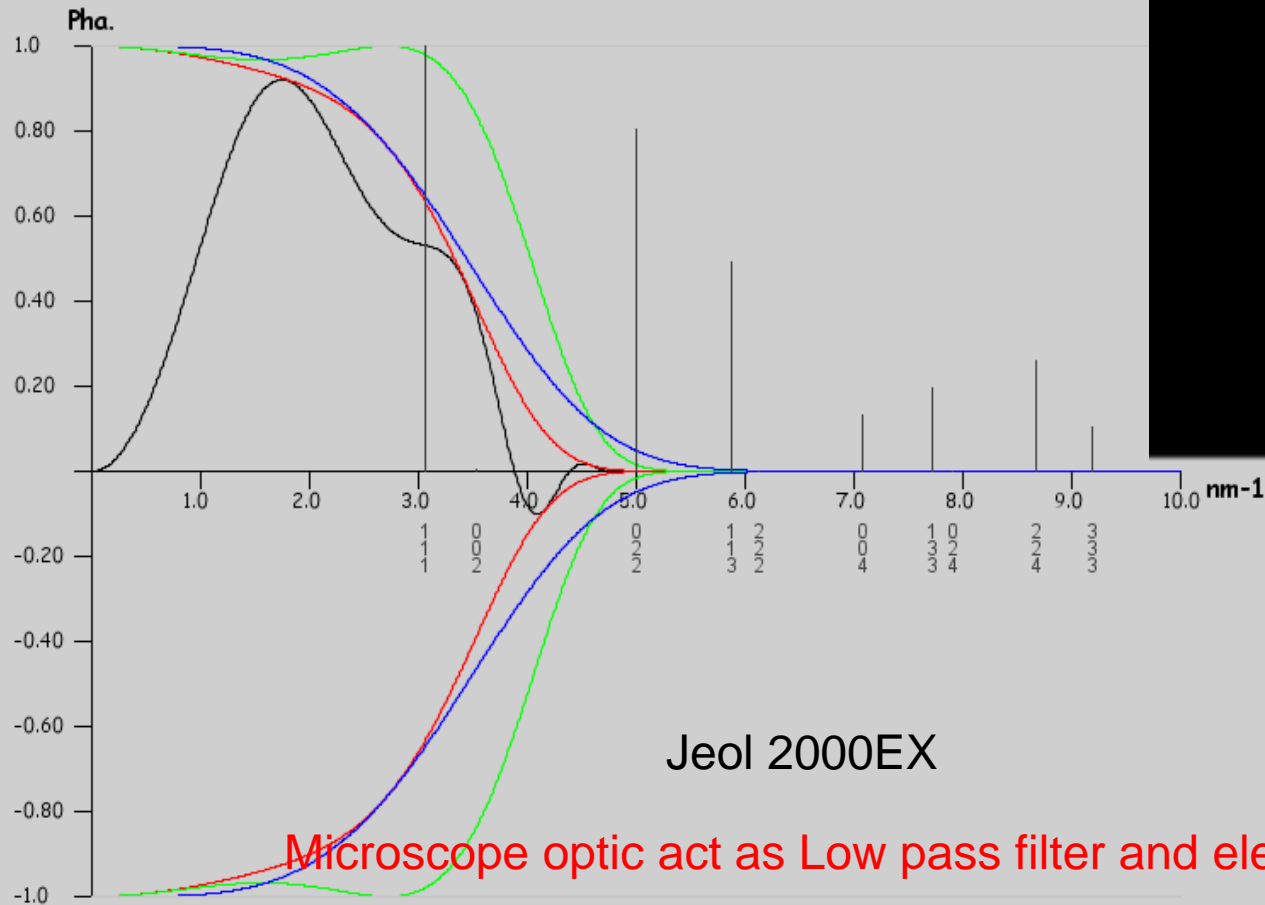
It takes into account the aberrations of the microscope optical system



Contrast Transfer Function (CTF) , Contrast transfer function

Transfer function - imaginary part
Partial spatial and temporal envelopes included
Crystal : GaAs

Acc. Voltage / kV : 200.0 | Defocus / nm : 79.0 | Cs / mm : 1.70
Defocus spread / nm : 18.00 | Beam half conv / mrad : 0.70
Vibration amplitude / nm : 0.00 | Specimen drift / nm/s : 0.00

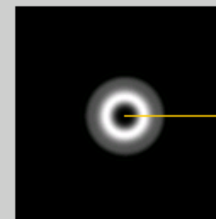


Spatial frequency for
GaAs crystal 1/nm
=>Bragg spots

Product of envelopes

Spatial envelope

Temporal envelope



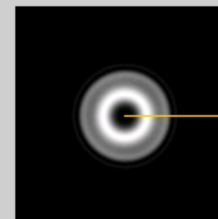
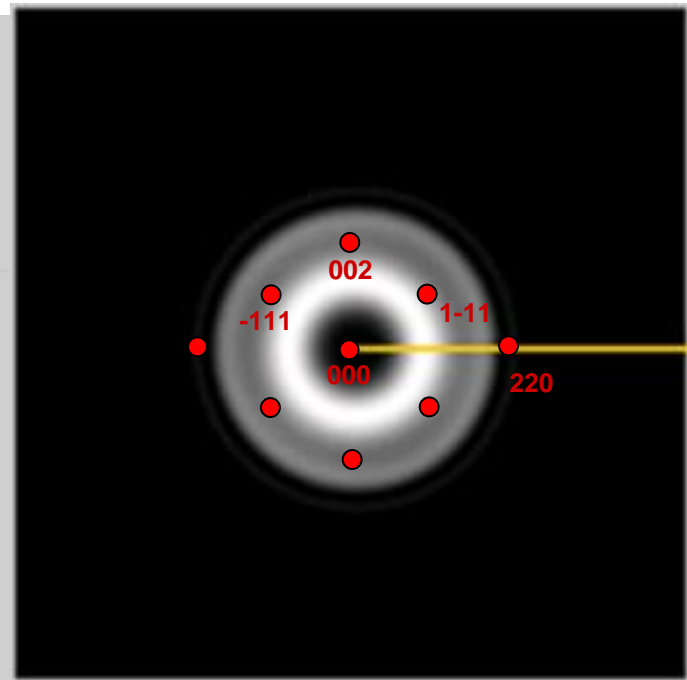
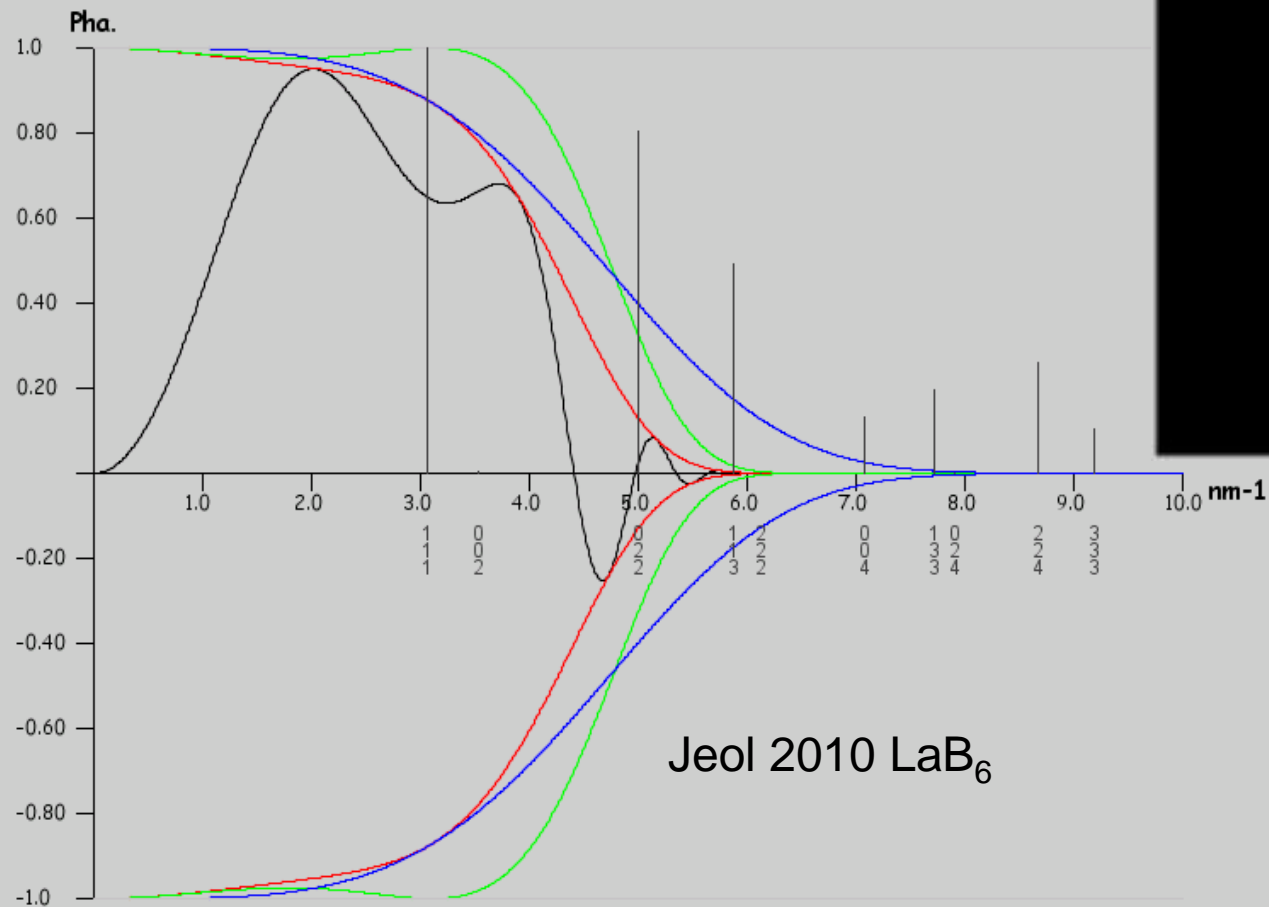
Transfer function - imaginary part
Partial spatial and temporal envelopes included

Crystal : GaAs

Acc. Voltage / kV : 200.0 | Defocus / nm : 61.0 | Cs / mm: 1.00

Defocus spread / nm : 9.80 | Beam half conv / mrad : 0.70

Vibration amplitude / nm: 0.00 | Specimen drift / nm/s: 0.00



Product of envelopes

Spatial envelope

Temporal envelope

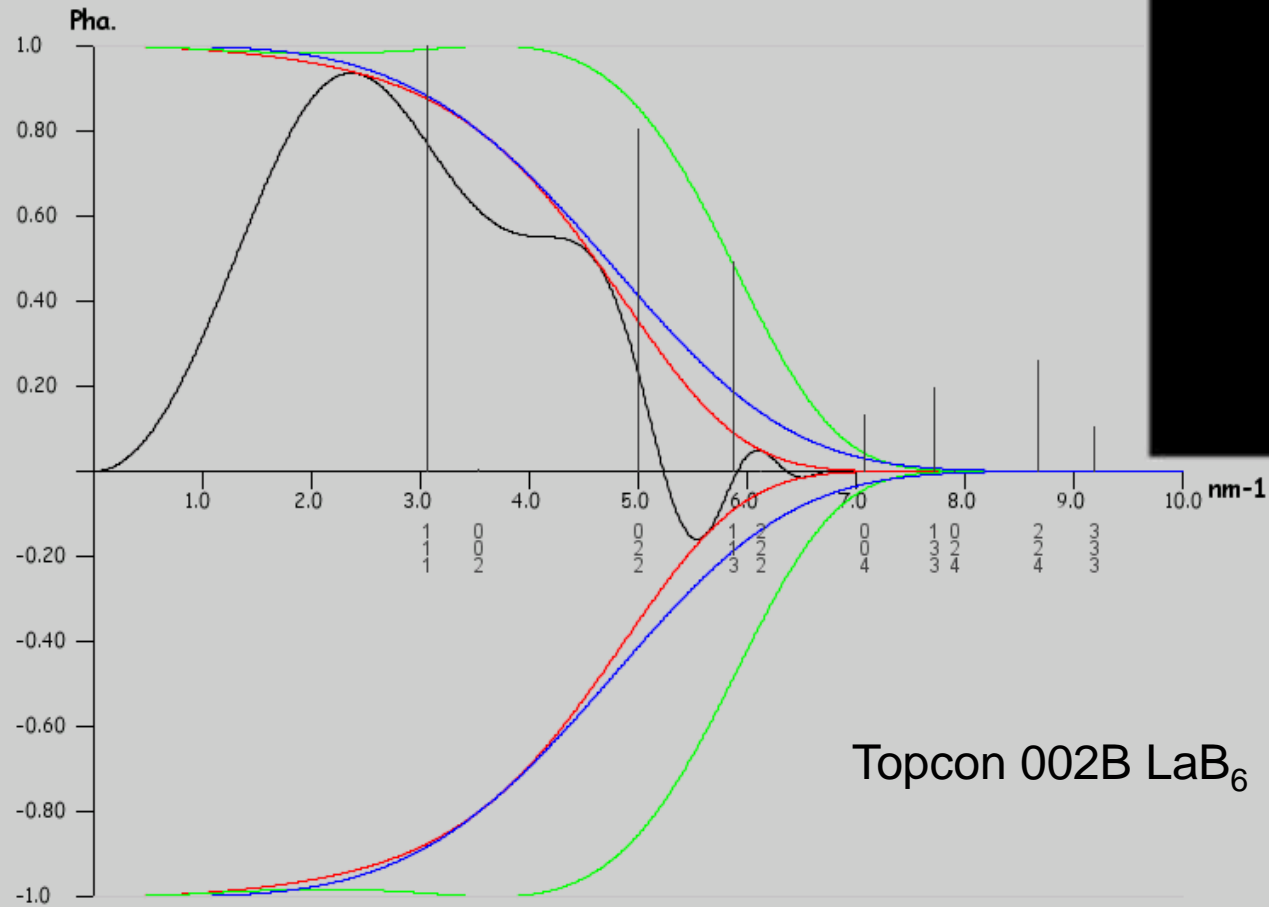
Transfer function - imaginary part
Partial spatial and temporal envelopes included

Crystal : GaAs

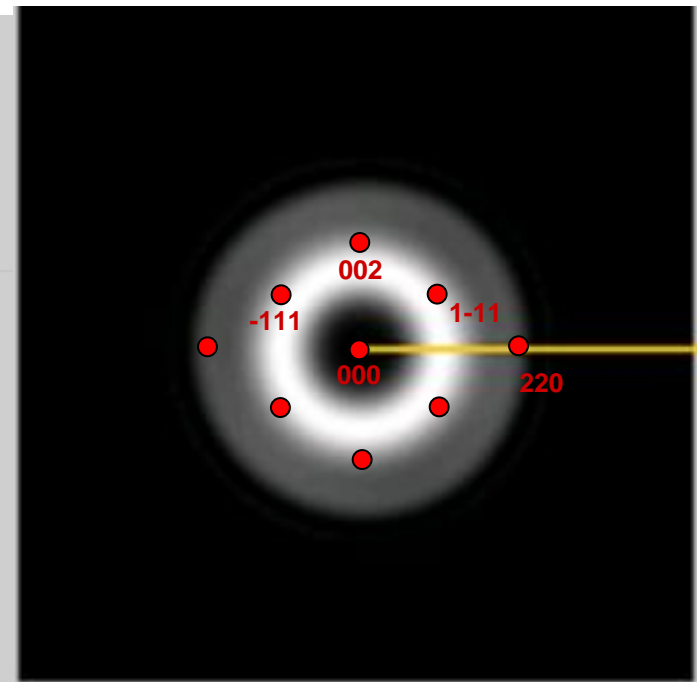
Acc. Voltage / kV : 200.0 | Defocus / nm : 43.0 | Cs / mm: 0.50

Defocus spread / nm : 9.60 | Beam half conv / mrad : 0.70

Vibration amplitude / nm: 0.00 | Specimen drift / nm/s: 0.00



Topcon 002B LaB₆

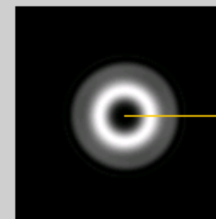


Smaller C3(Cs)

Product of envelopes

Spatial envelope

Temporal envelope



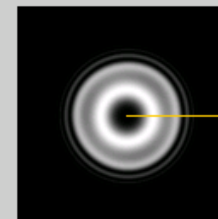
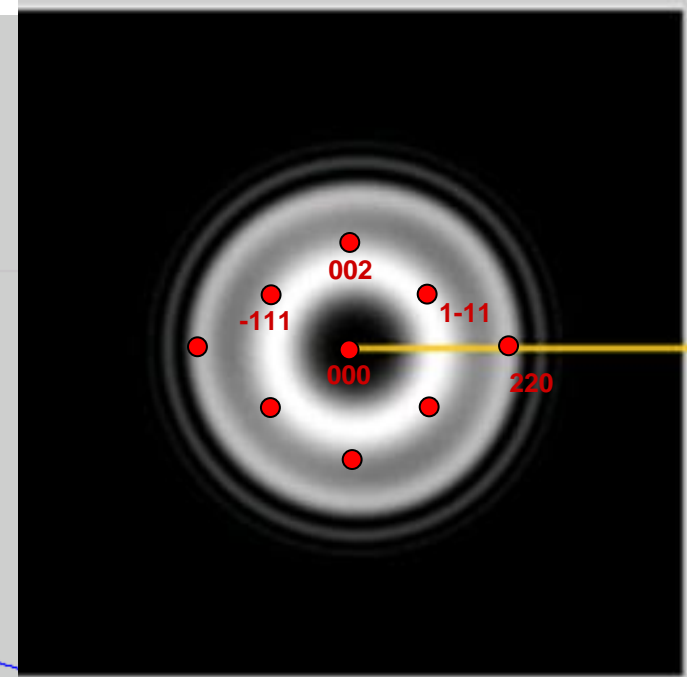
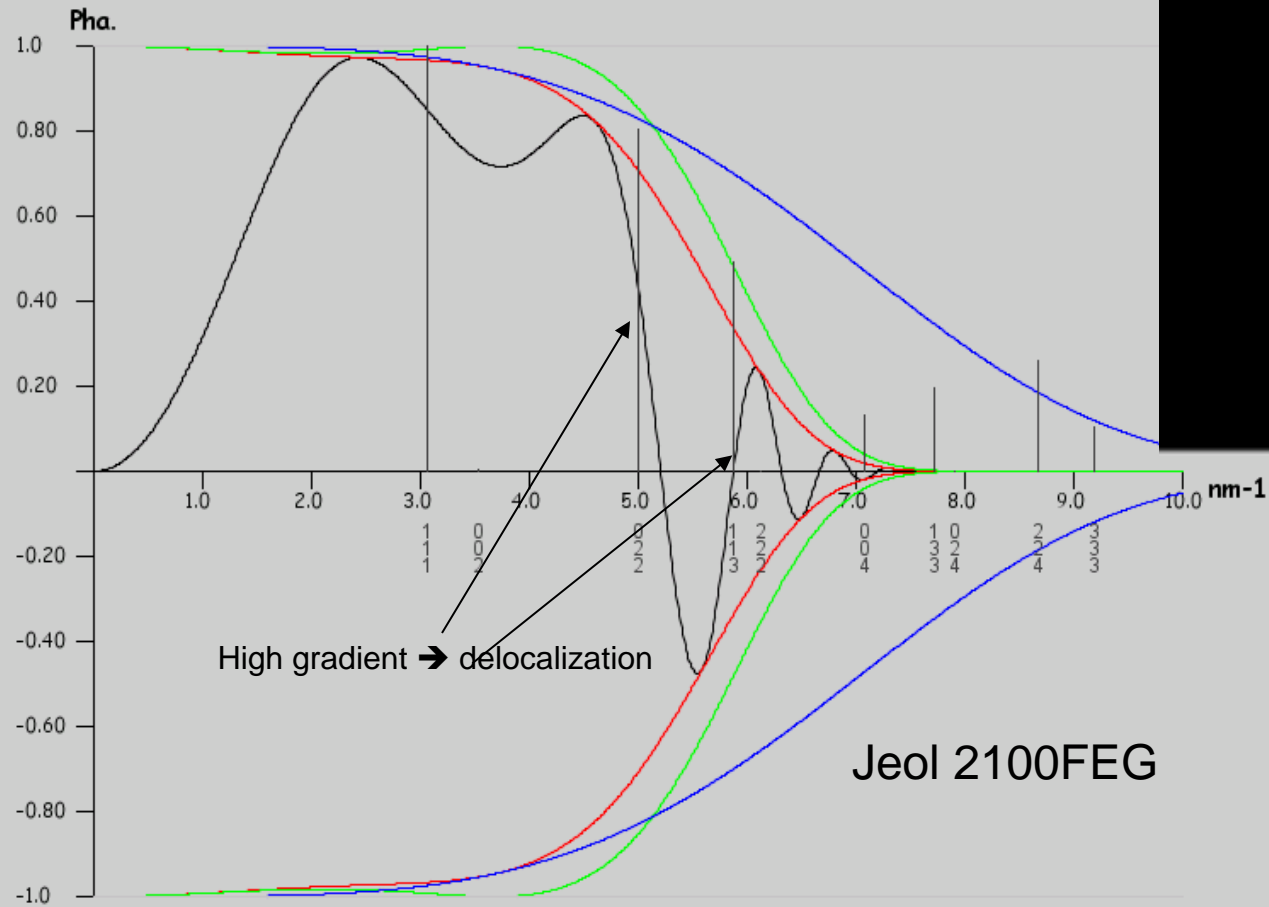
Transfer function - imaginary part Partial spatial and temporal envelopes included

Crystal : GaAs

Acc. Voltage / kV : 200.0 | Defocus / nm : 43.0 | Cs / mm : 0.50

Defocus spread / nm : 4.40 | Beam half conv / mrad : 0.70

Vibration amplitude / nm : 0.00 | Specimen drift / nm/s : 0.00



Product of envelopes

Spatial envelope

Temporal envelope

Transfer function - imaginary part

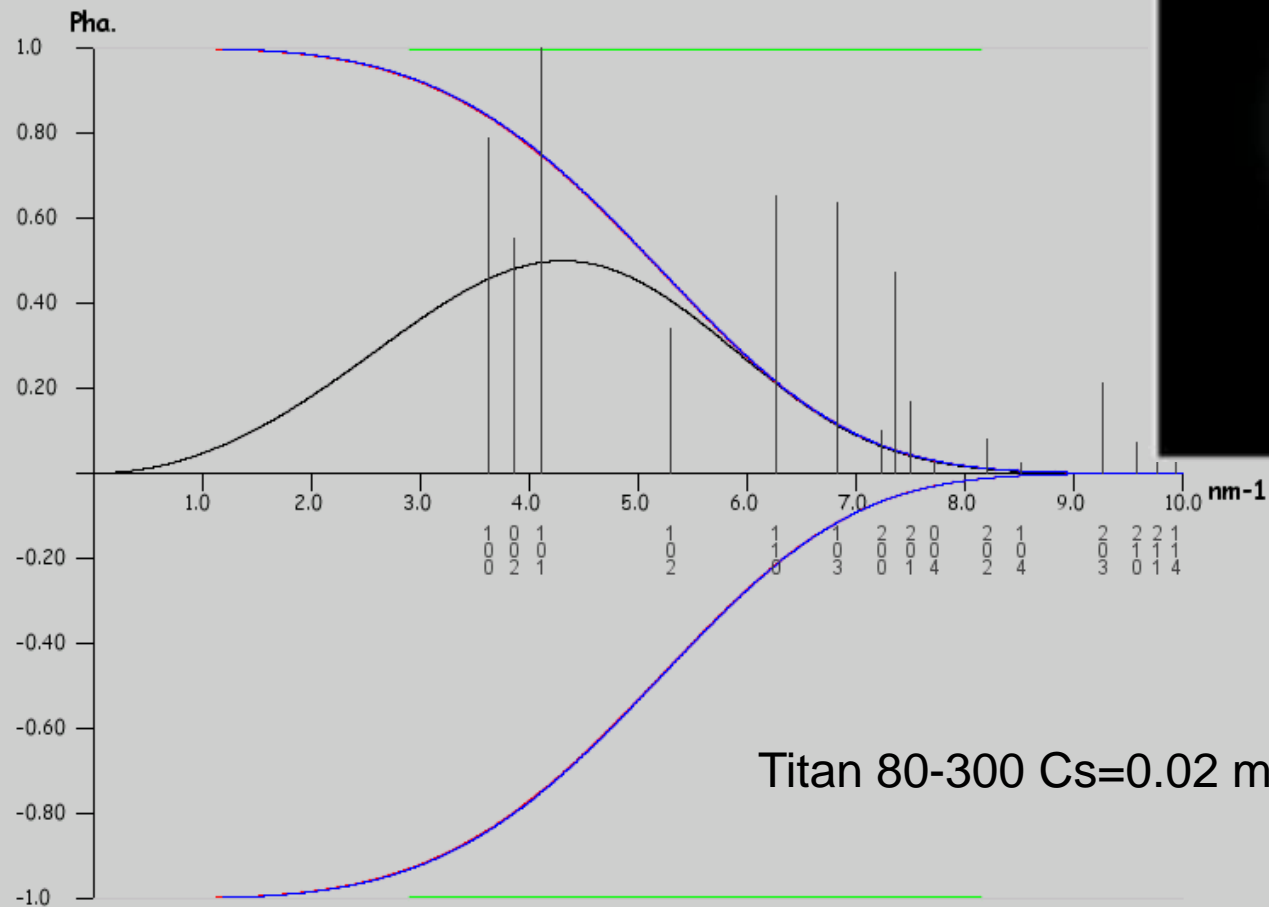
Partial spatial and temporal envelopes included

Crystal : GaN

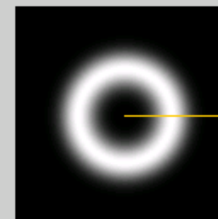
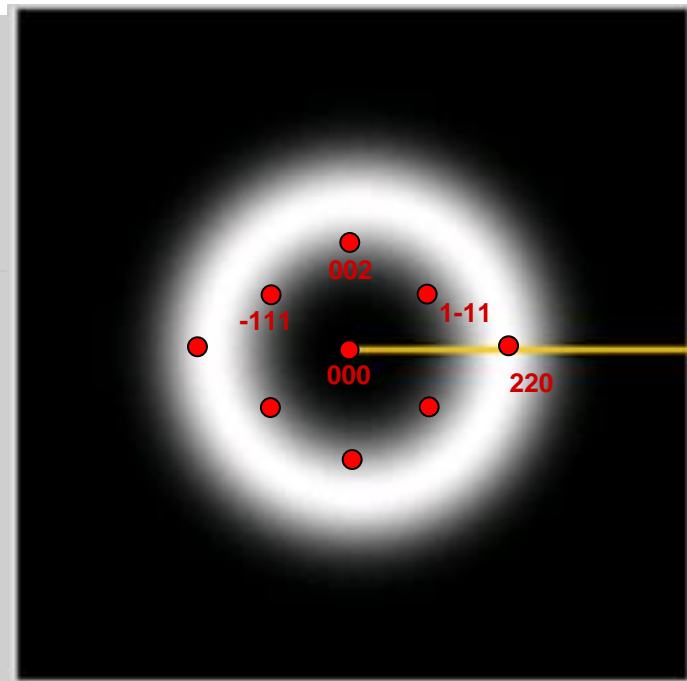
Acc. Voltage / kV : 300.0 | Defocus / nm : 7.7 | Cs / mm: 0.02

Defocus spread / nm : 10.31 | Beam half conv / mrad : 0.70

Vibration amplitude / nm: 0.00 | Specimen drift / nm/s: 0.00



Titan 80-300 Cs=0.02 mm



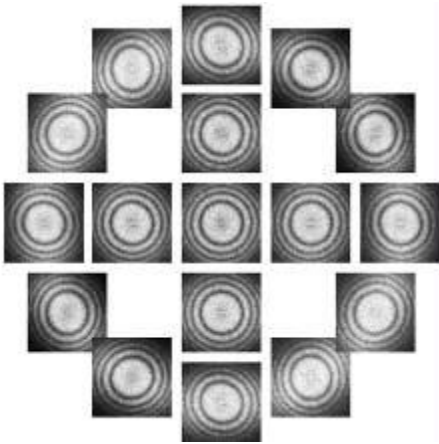
Product of envelopes

Spatial envelope

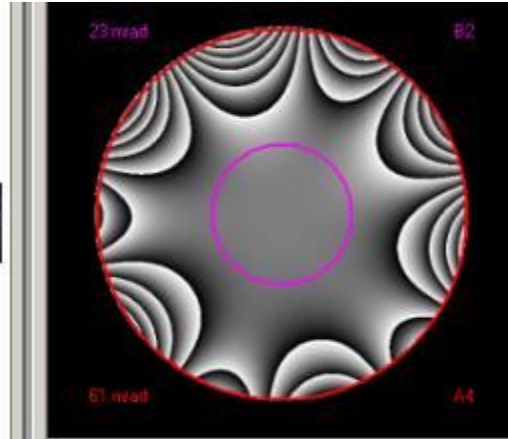
Temporal envelope

Negative-spherical-aberration technique

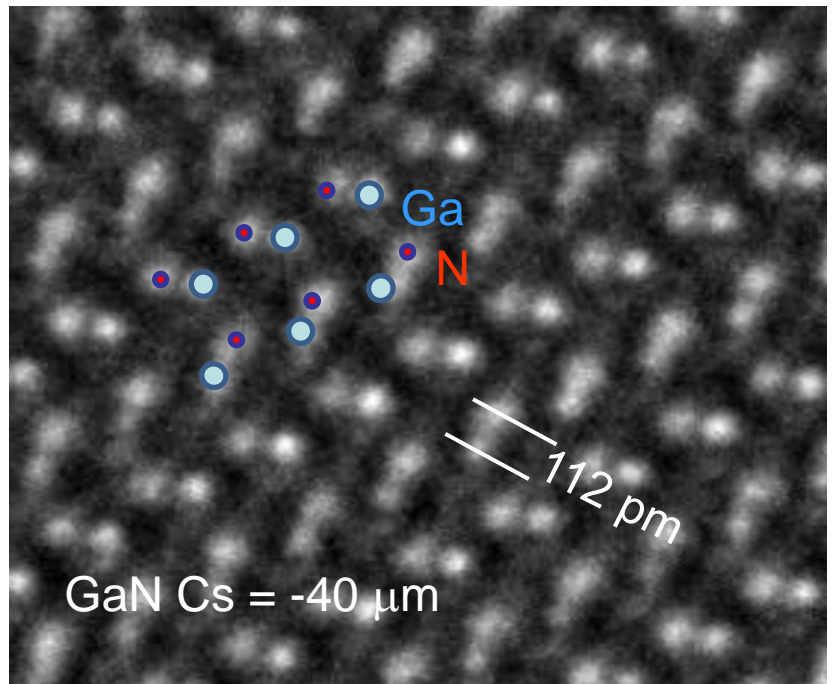
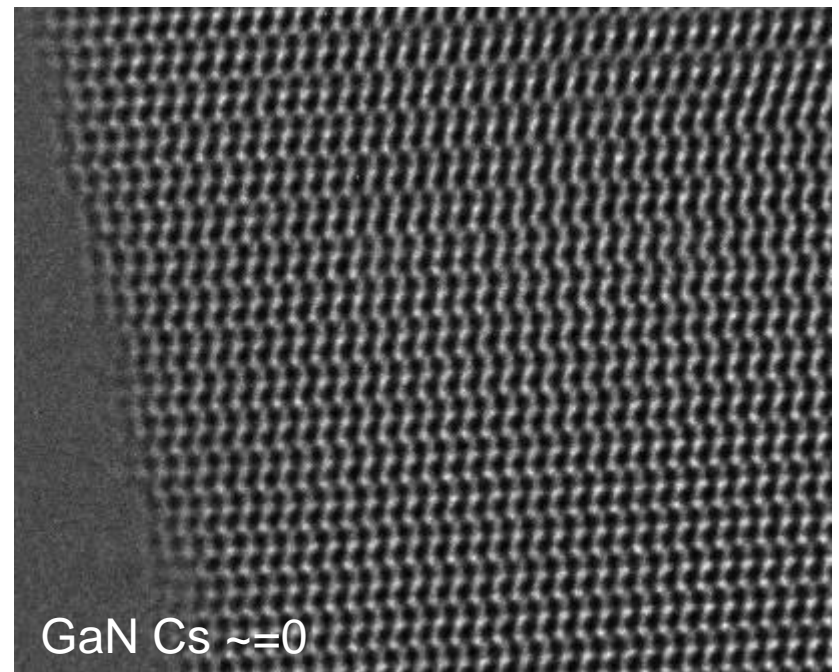
- whit atoms
- Better contrast of light atoms



Zemlin 'Tableaus'



'phase plate'



24 mrad beam tilt

Local strain measurement is a simple and popular method of QHRTEM

The main assumption :

The positions of the intensity maxima may correspond to the location of the atomic columns or tunnels between lattice sites or neither of them.

But this relation is constant in the whole analysed image .

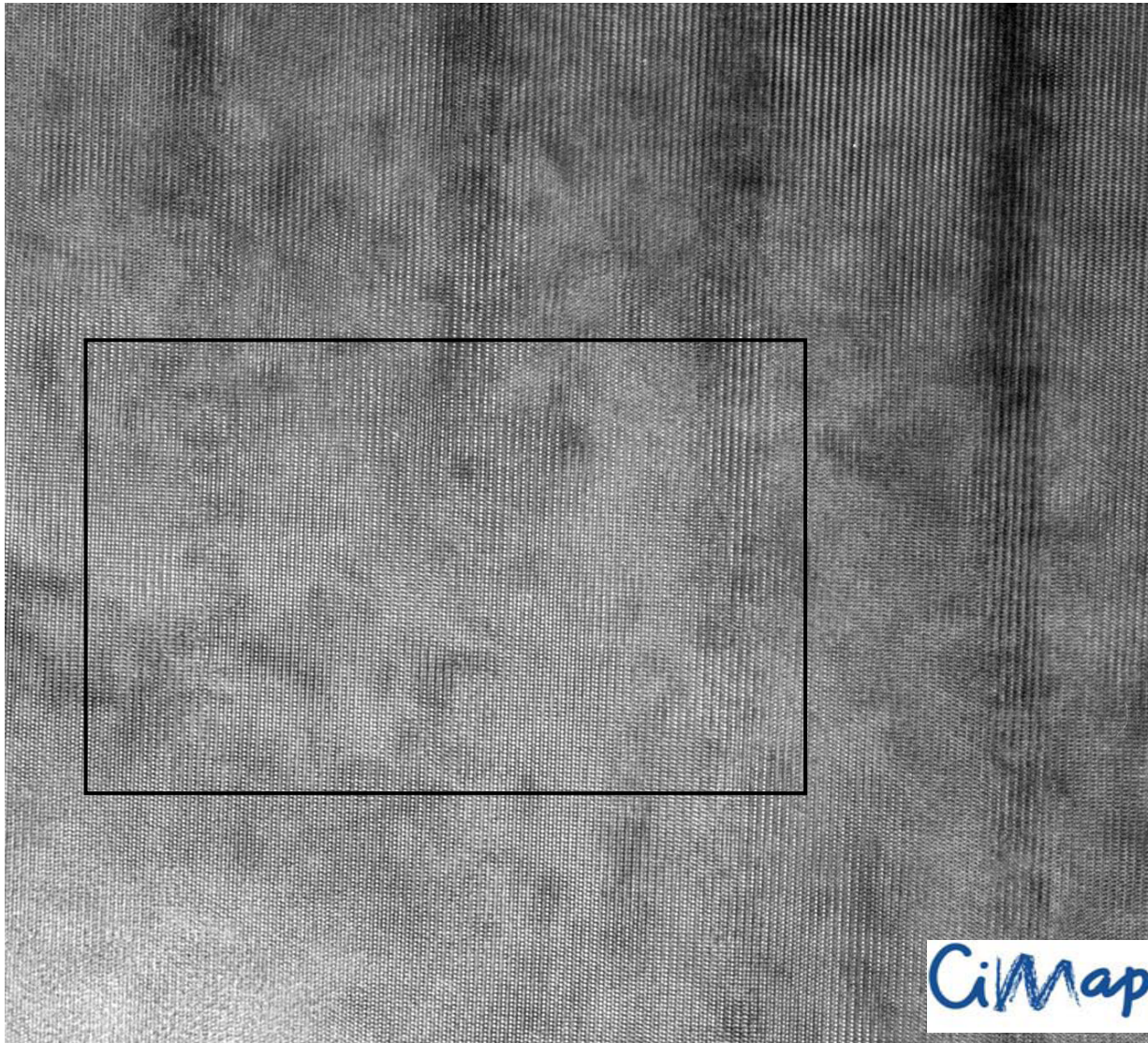
Image simulations for axial HRTEM show that the measured lattice spacing depends locally on the imaging conditions (local foil misalignment and thickness variation) particularly for non-centrosymmetric structures/projection !!

Real word effect :

- surface relaxation
- artefacts due to sample preparation

Errors in processing:

- loss of information
- artifacts due to digitalisation, noise, filtering, interpolation

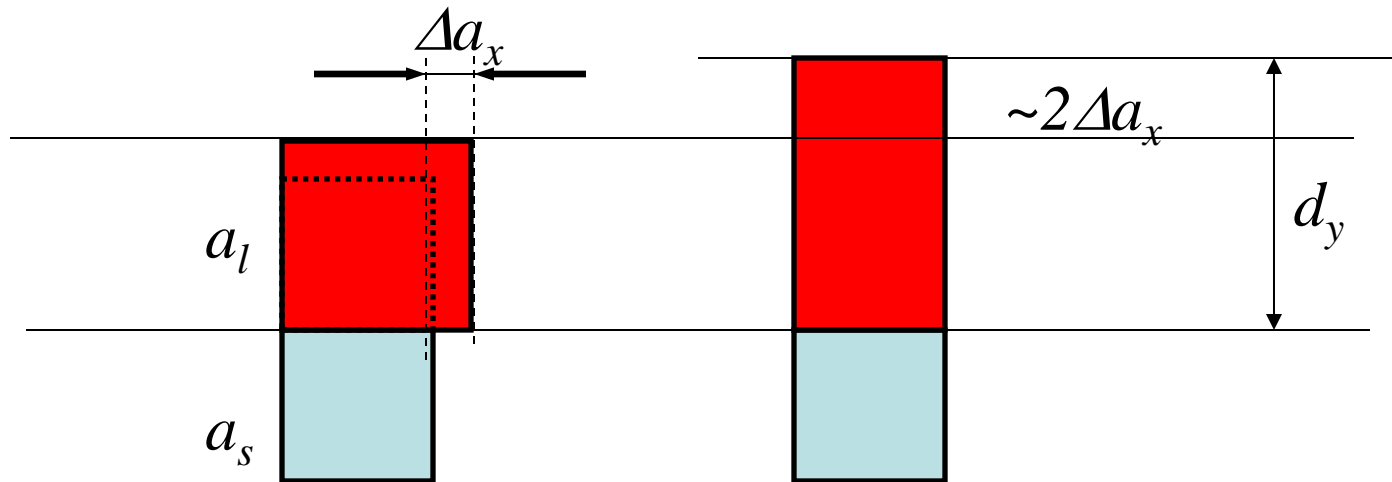


$\text{In}_{0.15}\text{Ga}_{0.8}\text{N}/\text{GaN}$

pseudomorphic

$[\bar{1}1\bar{2}0]$ zone axis HRTEM image of InGaN (MBE) MQWs.

Pseudomorphic growth, tetragonal distortion, biaxial stress



During pseudomorphic growth of a material with lattice parameter a_x on a substrate with lattice parameter a_s the lattice parameter $a_{x||} = a_s$. However the lattice parameter in the y direction is $d_y > a_x$.

$$d_z = \alpha \Delta a_x + a_s$$

Dilatation of lattice in y is $d_y - a_s = \alpha \Delta a_x = \alpha (a_x - a_s)$ where

$$\alpha = \left(1 + 2 \frac{c_{12}}{c_{11}} \right) = \frac{1 + \nu}{1 - \nu} \cong 2$$

Chemical composition from Vegard's Law

InGaN , GaN, InN, (ZnTe, CdTe)

$$a_{In_xGa_{1-x}N} = xa_{InN} + (1-x)a_{GaN}$$

$$a_x = xa_A + (1-x)a_B$$

$$\varepsilon = (d_y - a_s)/a_s = \alpha(a_s - a_x)/a_s$$

$$\varepsilon = \alpha \Delta_{sx}/a_s \rightarrow \Delta_{sx} = \varepsilon a_s / \alpha$$

a_x - relaxed lattice parameter for composition x

a_A - relaxed lattice parameter for component A

a_B - relaxed lattice parameter for component B

a_s - relaxed lattice parameter for substrate

$a_B = a_s$

α - relaxation parameter

Local composition:

$$x(x, y) = \frac{a_s - a_x(x, y)}{a_A - a_s} = \frac{\Delta_{sx}}{\Delta_{AS}} = \frac{\varepsilon(x, y)a_s}{\alpha\Delta_{AS}}$$

Thin foil effect

~Uniaxial stress ?

$$d_y = \alpha \Delta a + a_s$$

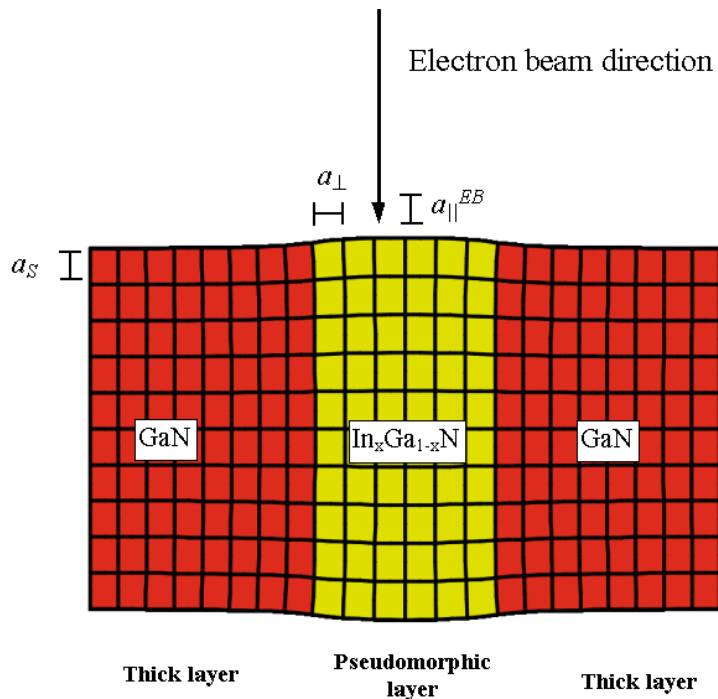
For (110) surface relaxation

$$\alpha = 1 + 4 \frac{C_{44}C_{12}}{C_{11}^2 + 2C_{11}C_{44} + C_{11}C_{12} - C_{12}^2}$$

For CdTe/ZnTe

$$\alpha_{\text{ter}} \approx 2.25 \quad \alpha_{\text{uniax}} \approx 1.6$$

40%



What is α ?

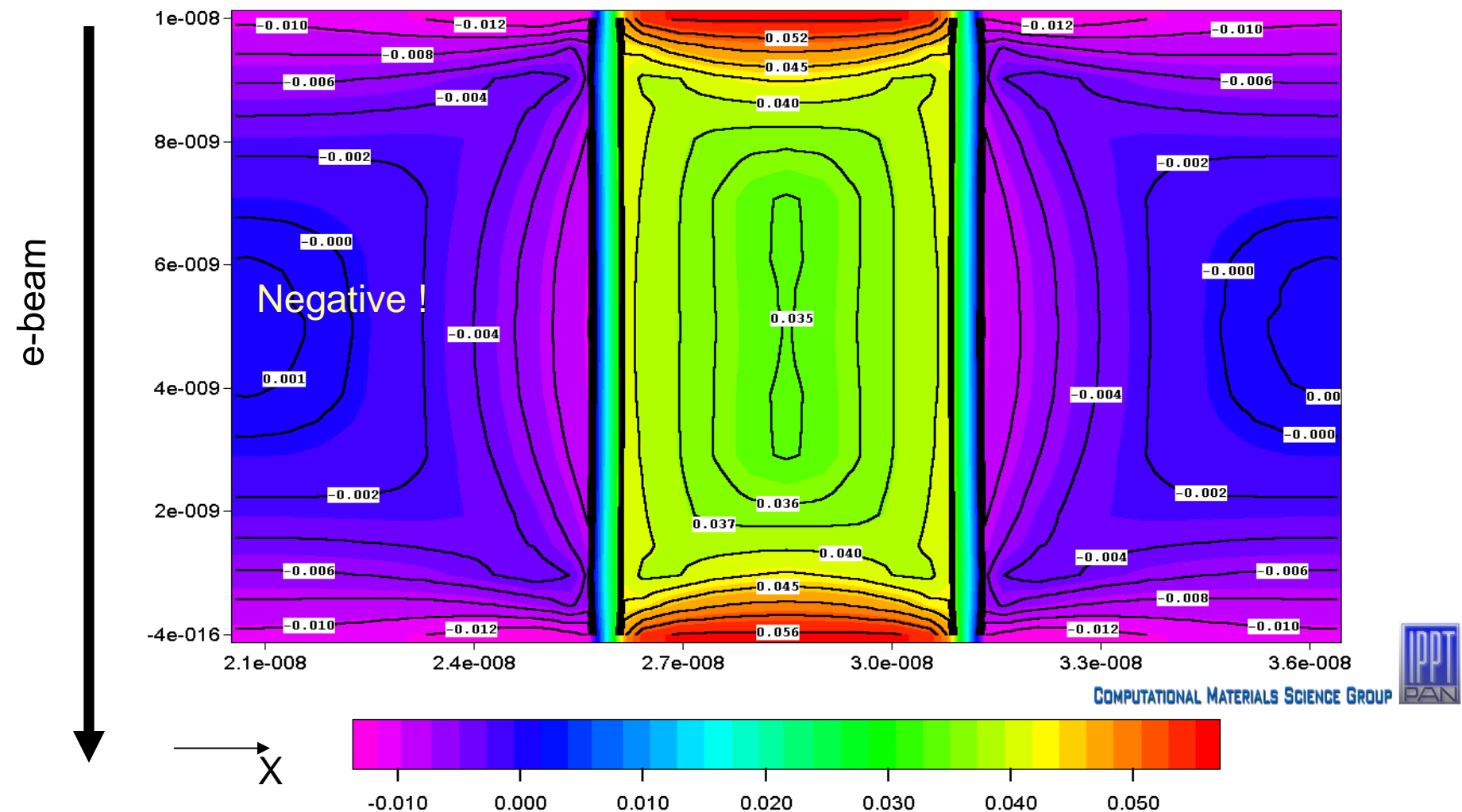
Biaxial or uniaxial ?

2D FE modeling

Geometry and border conditions similar as experimental

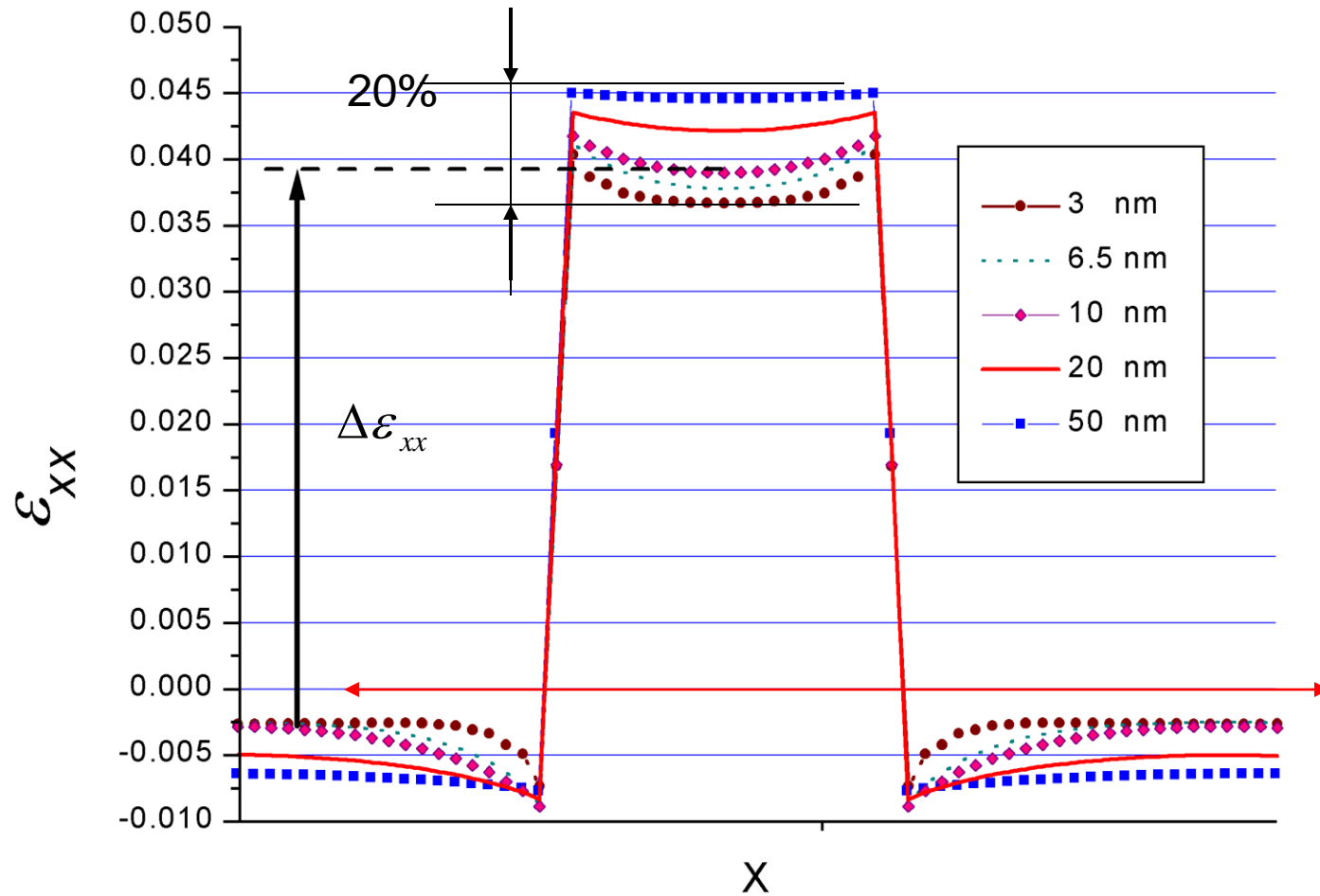
In function of the Indium concentration and t foil thickness

Homogeneous Indium distribution in QW

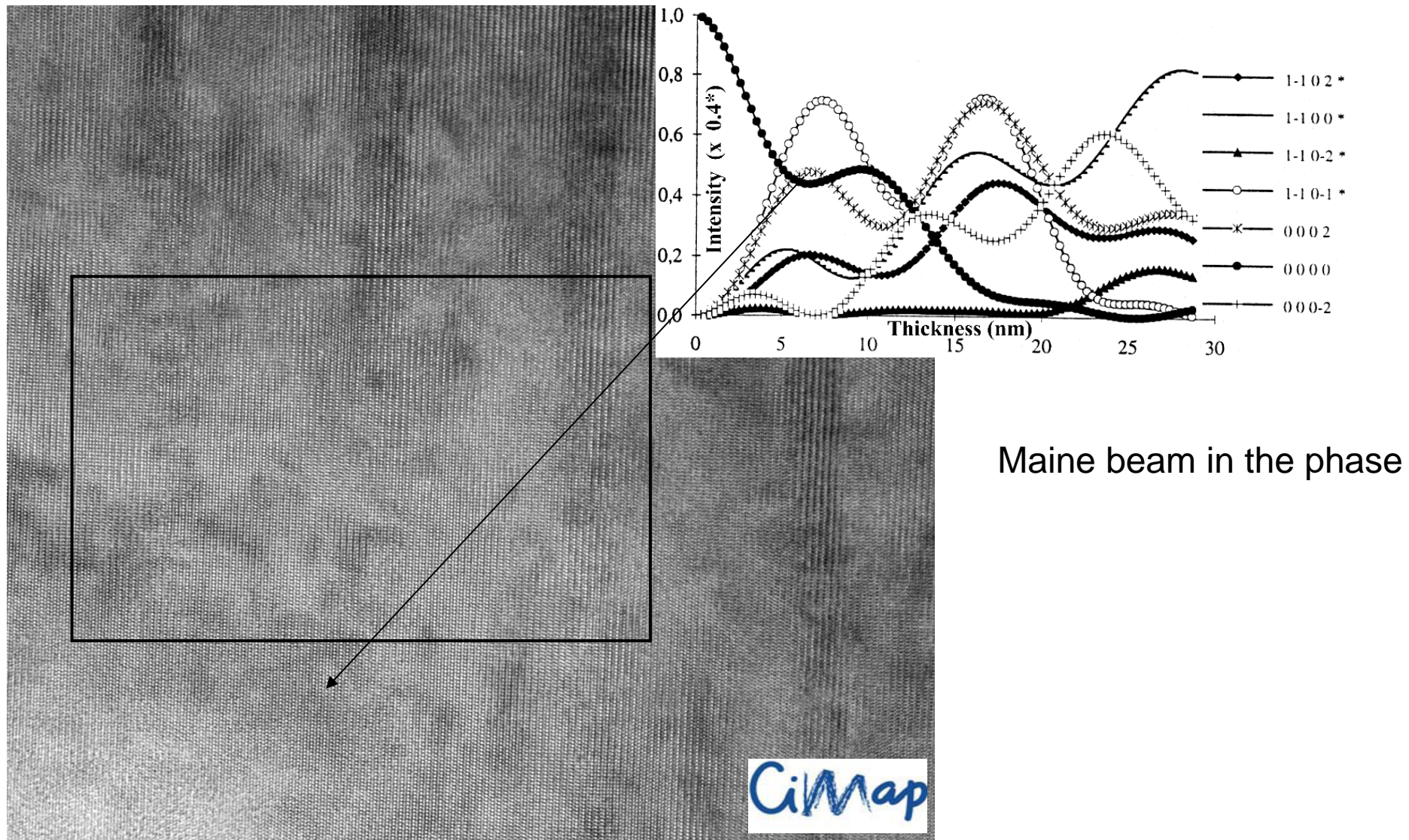


XY Cross-section of the TEM cross-section of MQW

Calculated distribution $\varepsilon_{xx}(x, y)$ after stress relaxation for In concentration %In=30 (QW/barriers geometry, in relation to GaN)

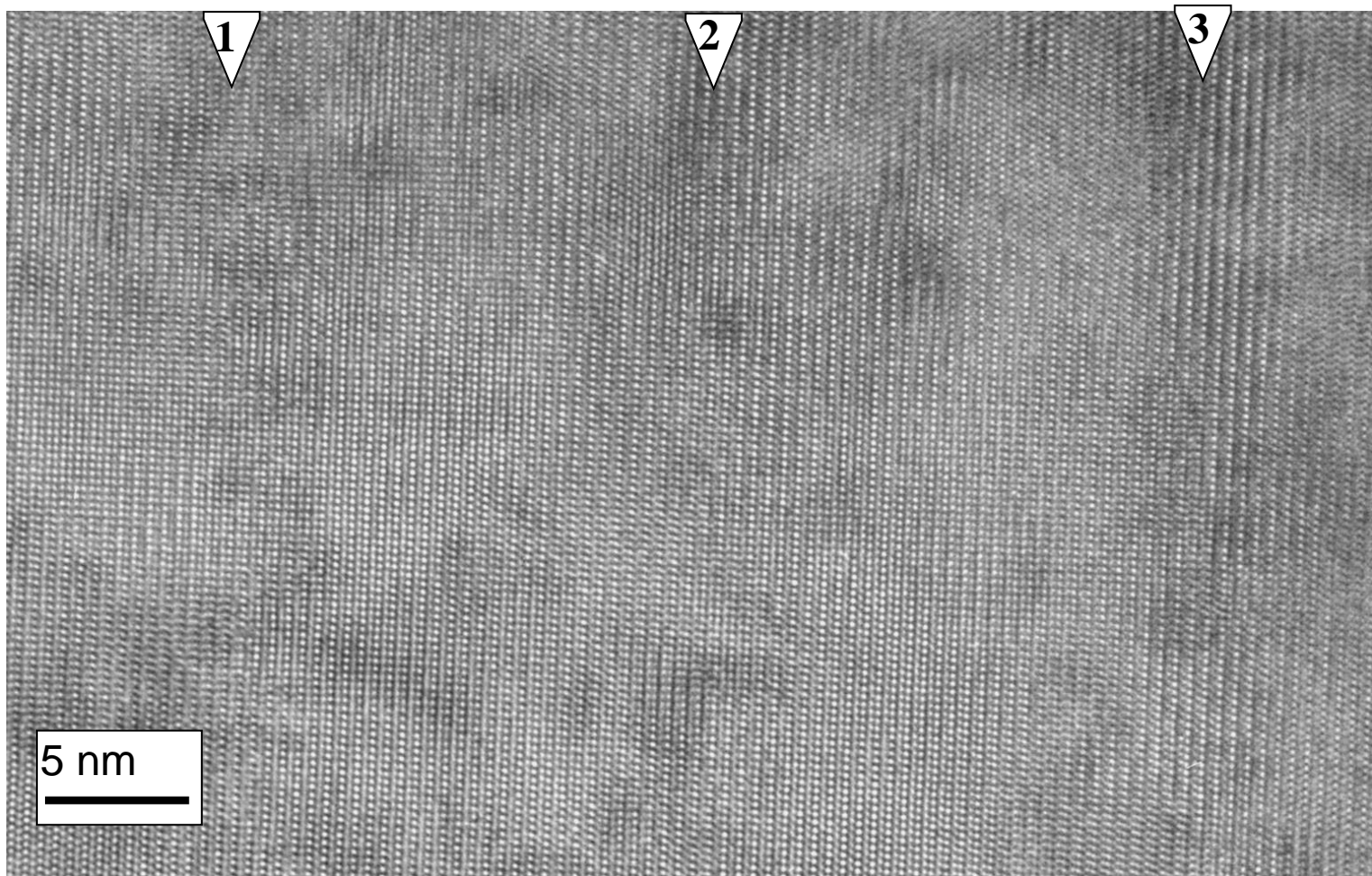


Profiles of $\varepsilon_{xx}(x)$ obtained by averaging $\varepsilon_{xx}(x, y)$ along the y direction for 30% indium concentration and $t=5, 10, 15, 30$ nm.



$[1\bar{1}20]$ zone axis HRTEM image of InGaN (MBE) MQWs .

Thickness 5-10 nm

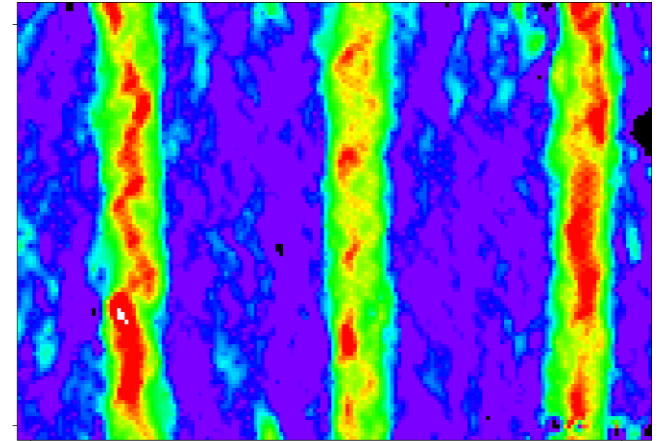
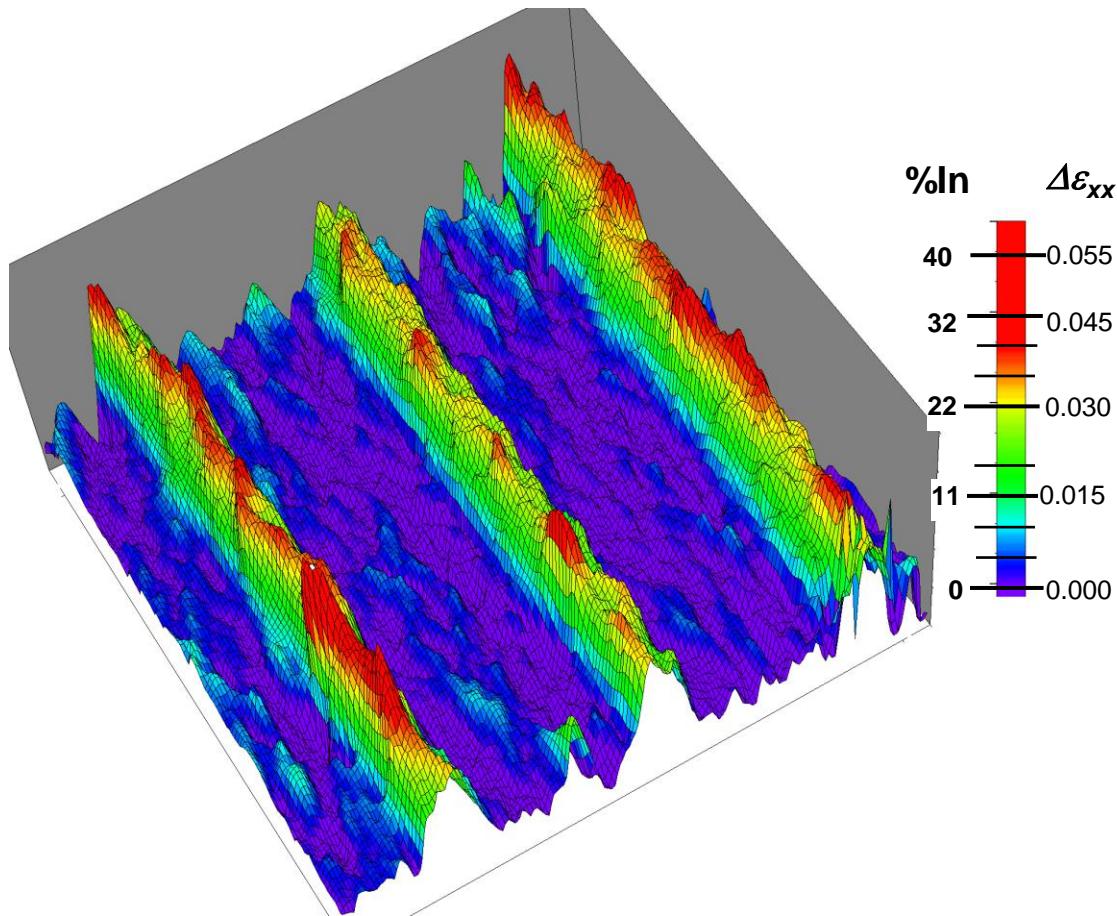


CiMap

Thickness 5-10 nm

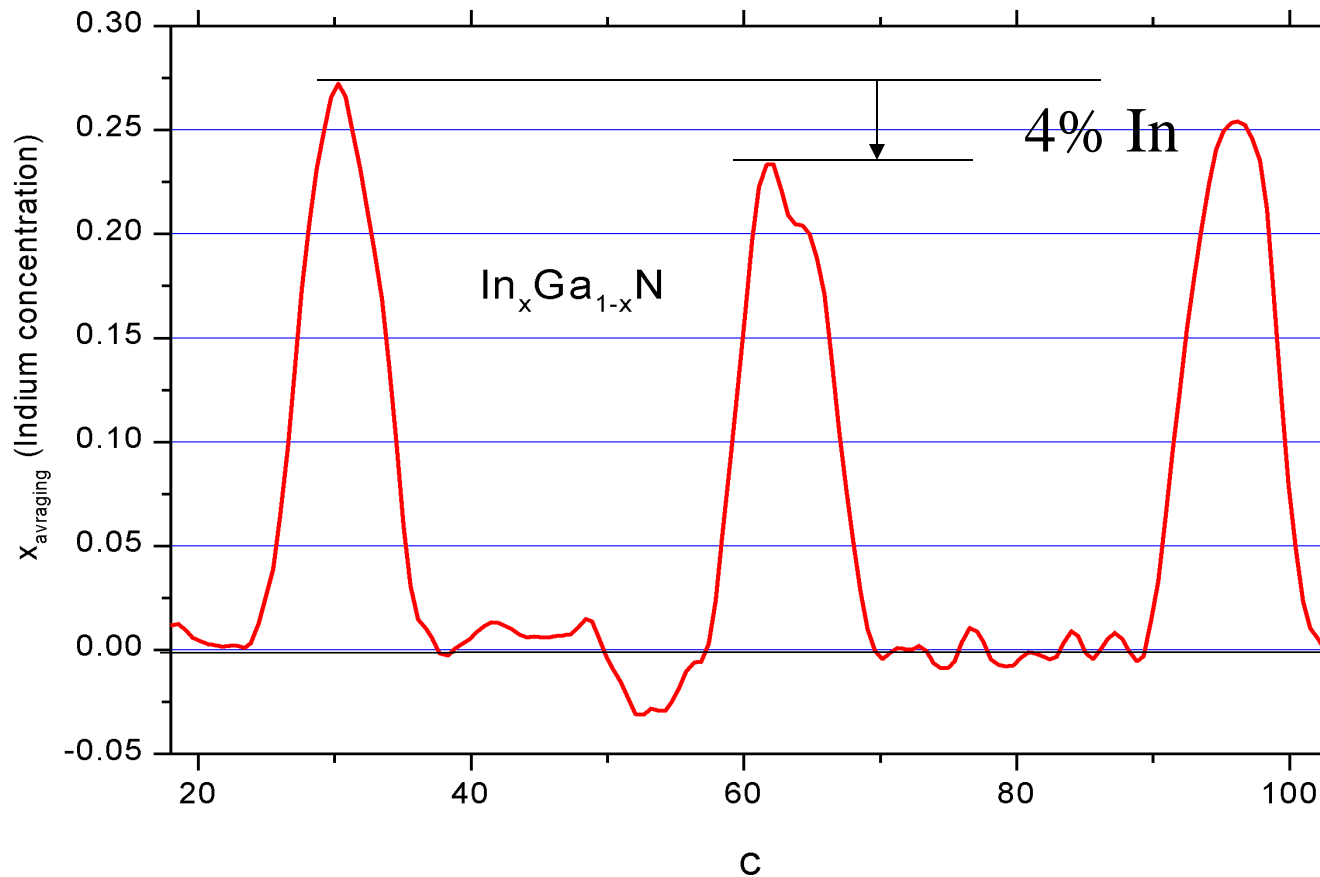
$\epsilon_{\text{MAX}}=0.030-0.038 \rightarrow A=720 \rightarrow \text{In}_{\text{Max}} 22-28\%$

Nominal $\sim 15\%$

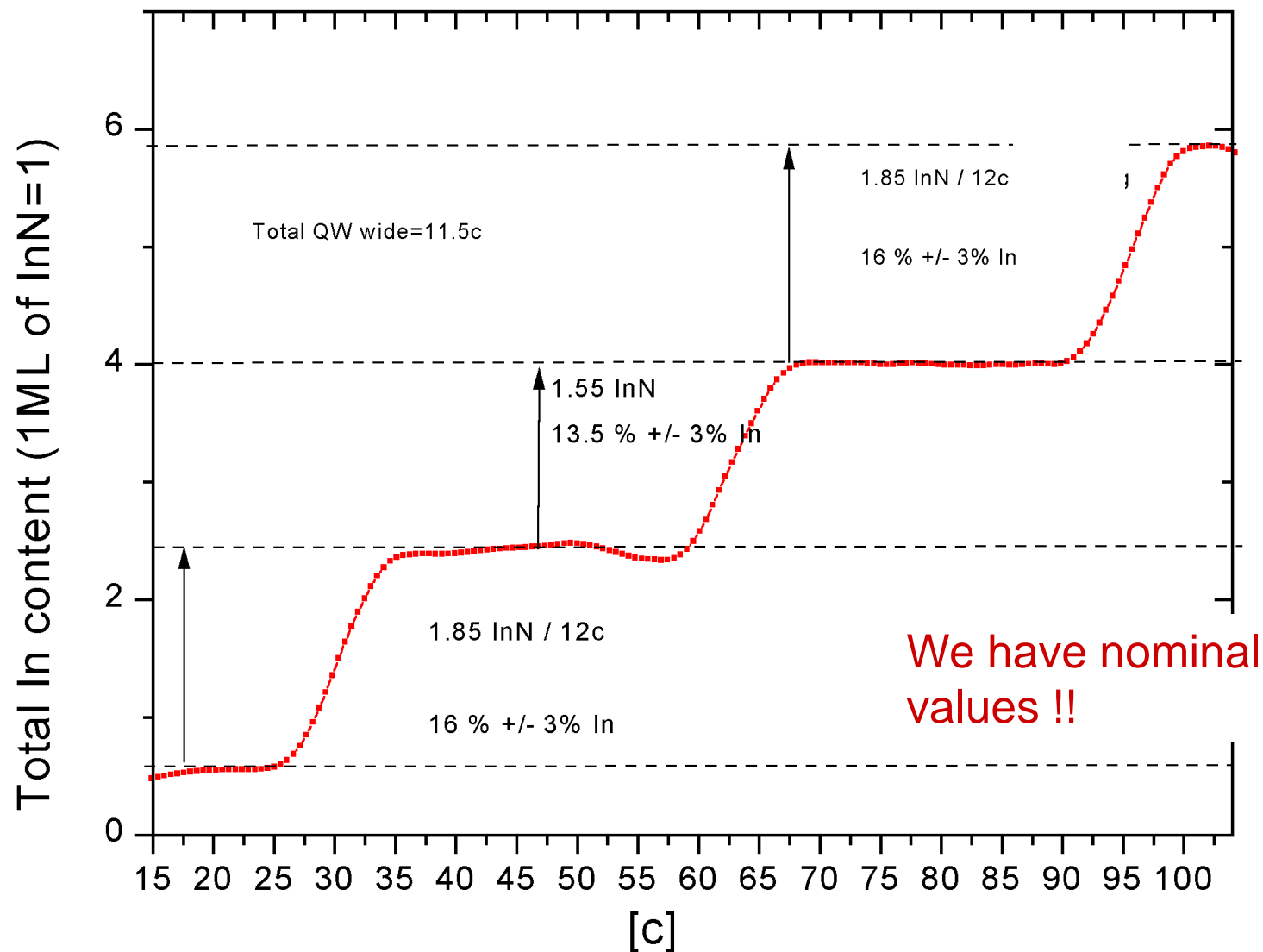


Surface plot of measured indium concentration; colour scales are common for $\Delta\epsilon_{xx}$ and %In

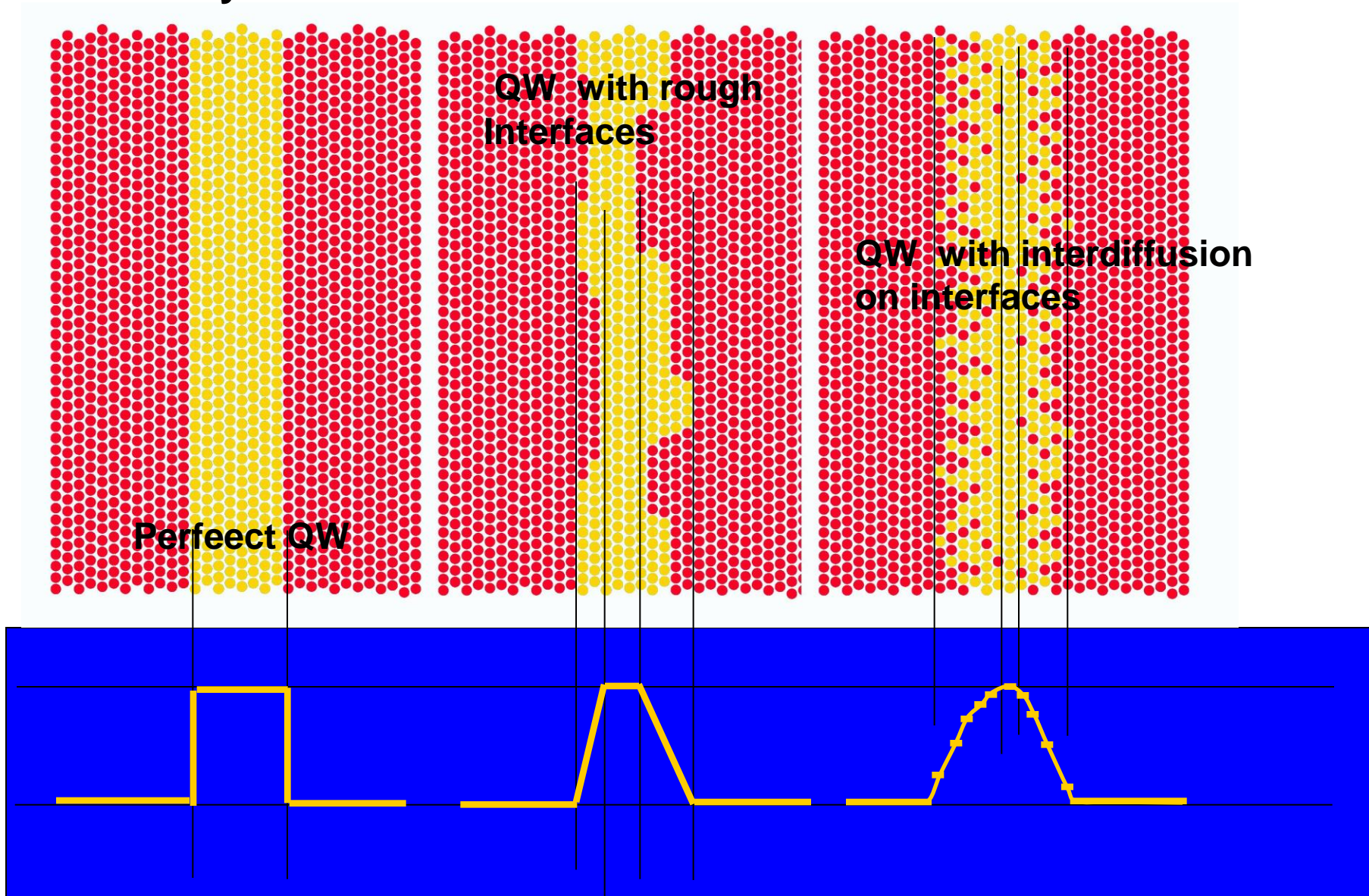
Average profile
→ better S/N ratio



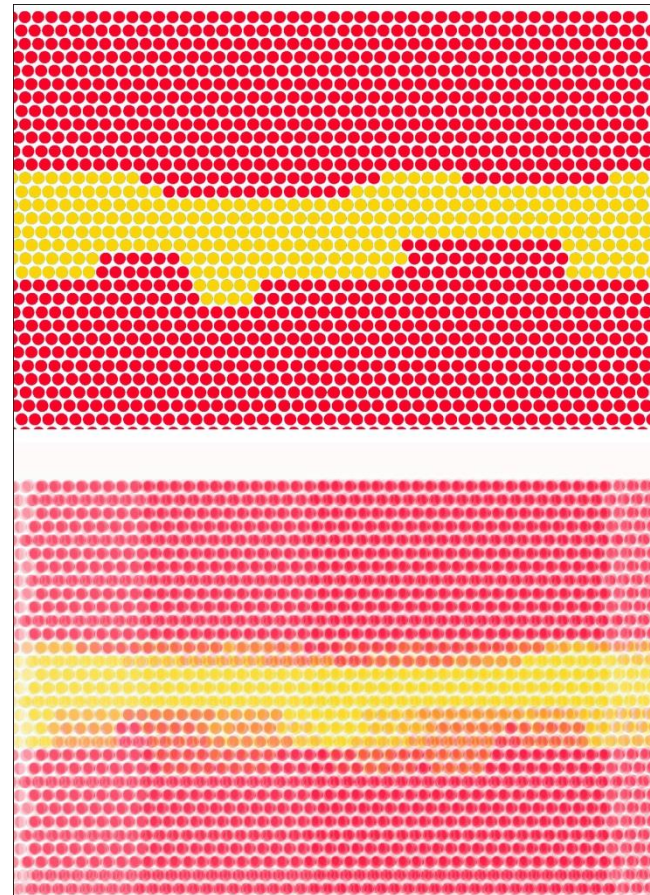
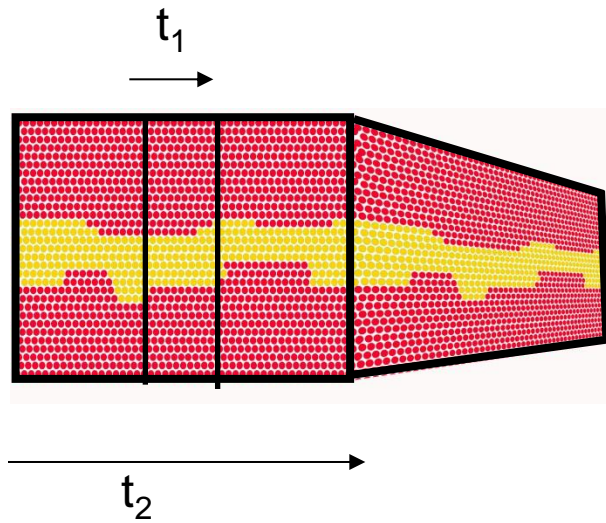
Integration of composition maps → total In content in QW !!



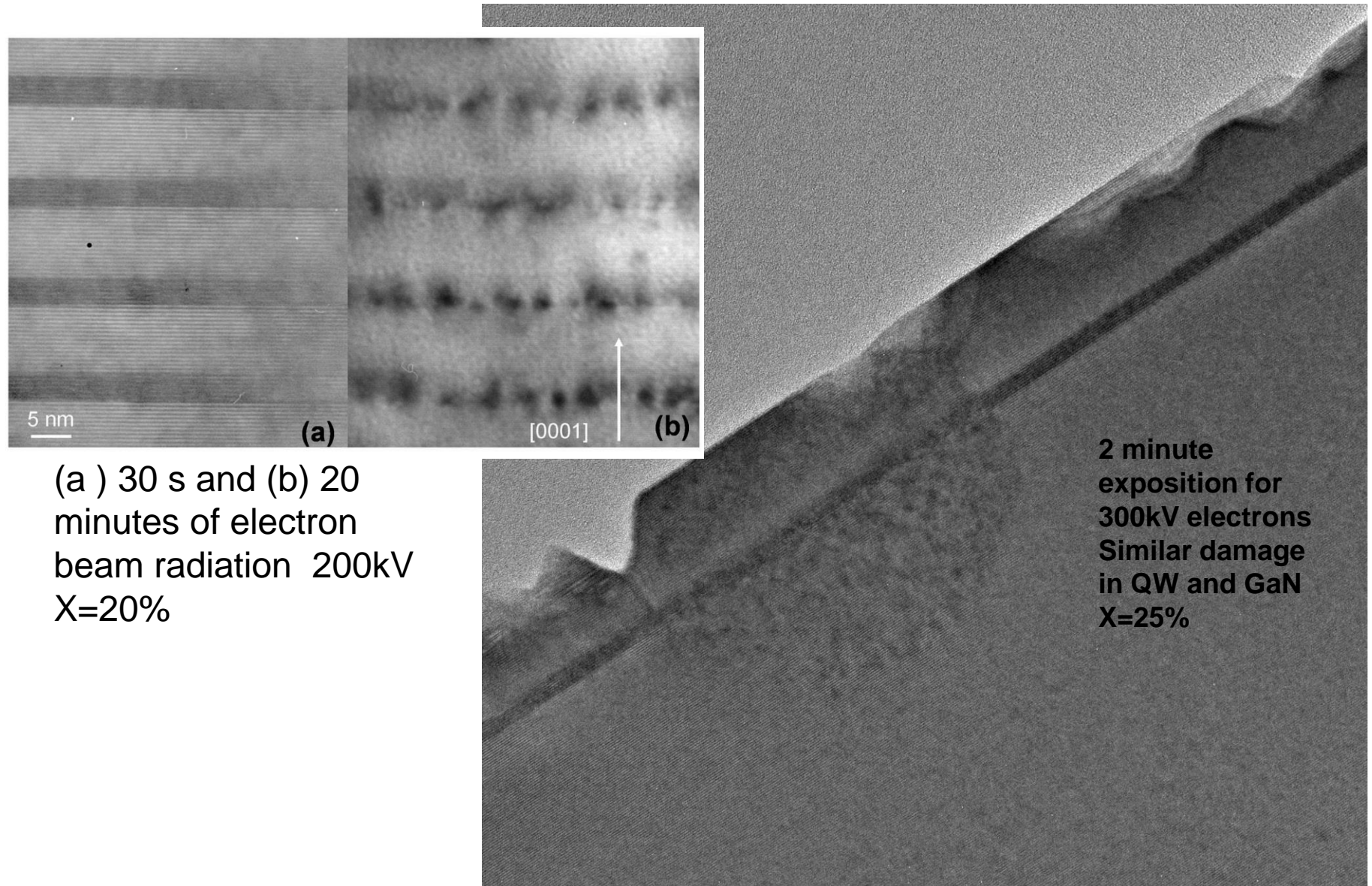
What you want to know about QW



Averaging problem.

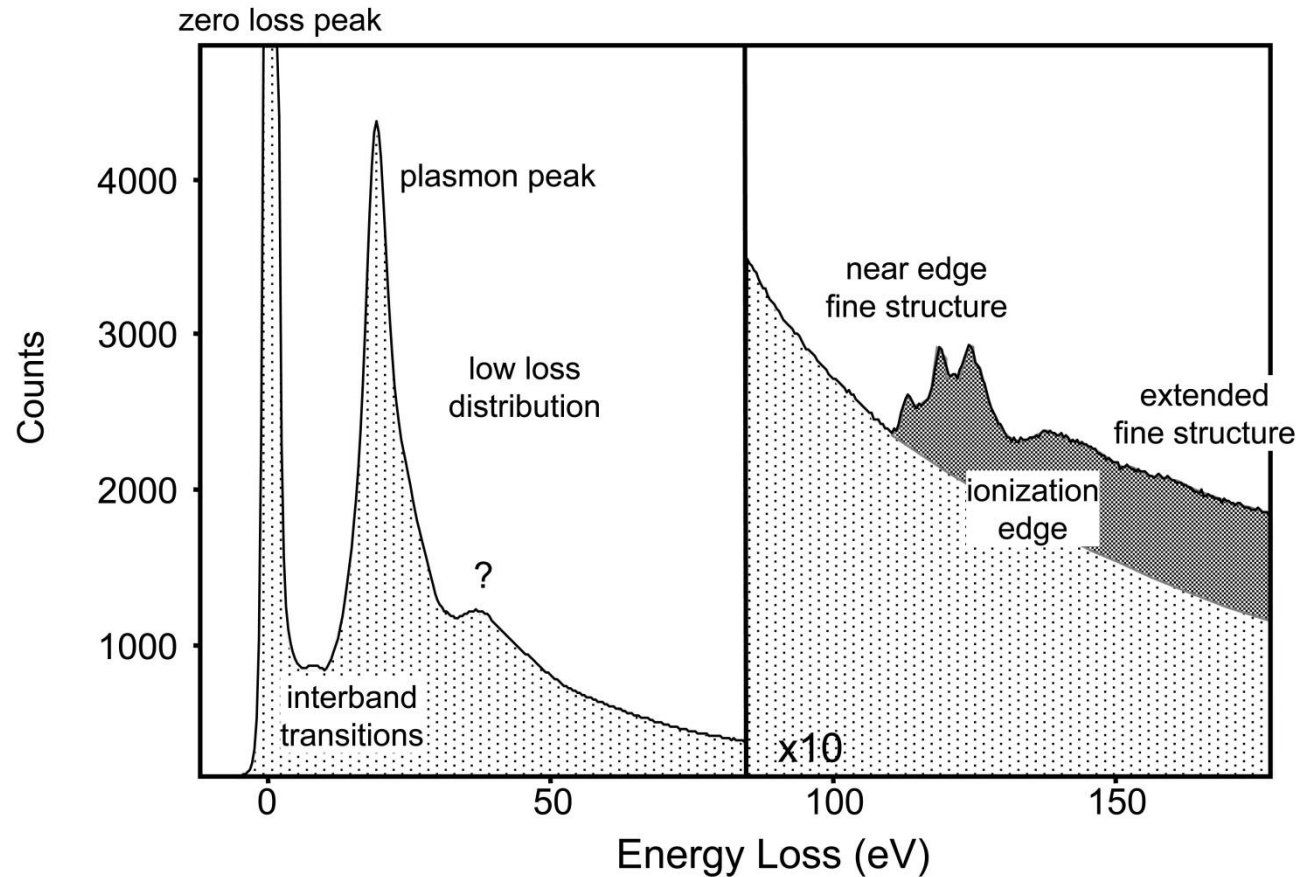


Radiation damage False clusters

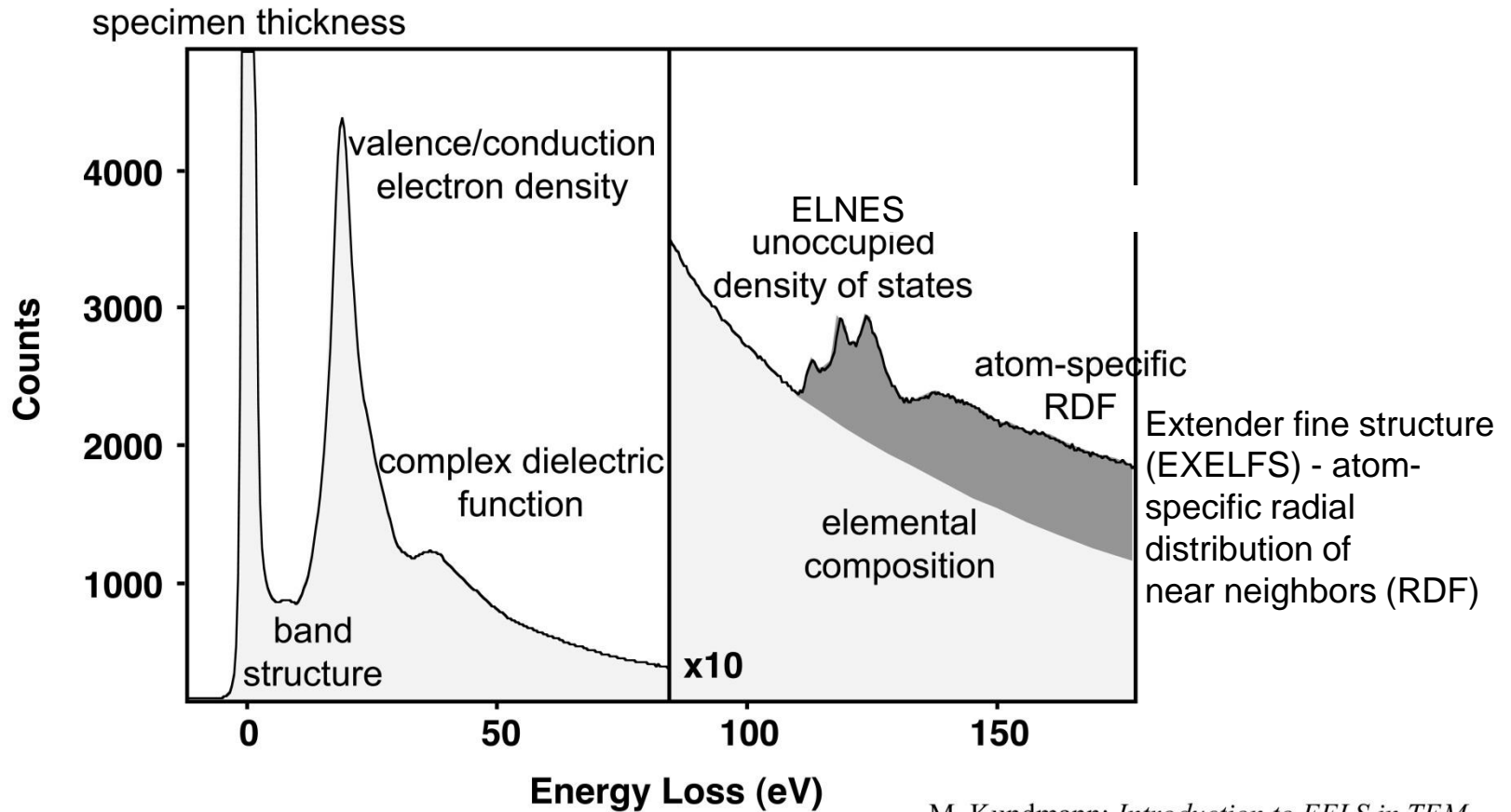


Electron energy loss spectroscopy and mapping the chemical composition

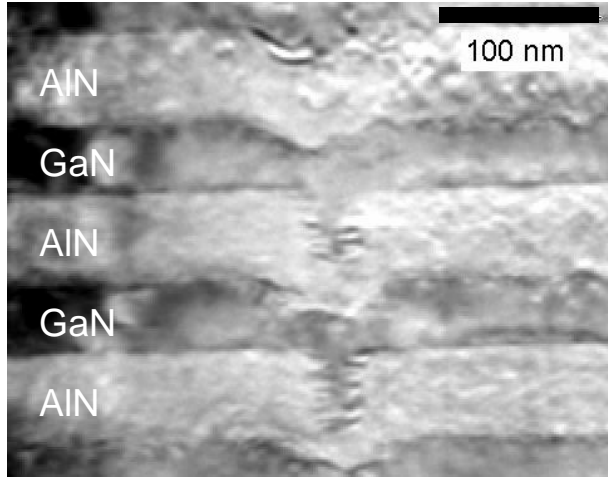
Electrons lose different amounts of energy depending on what they scattered



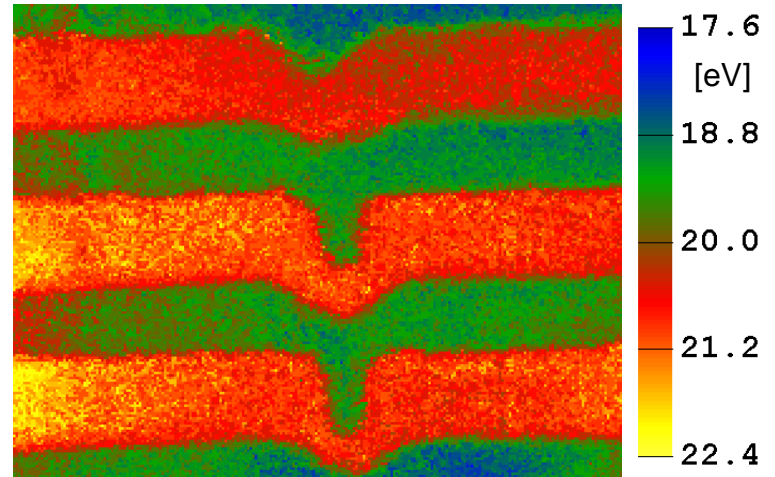
Such information can be obtained on a nanometric scale



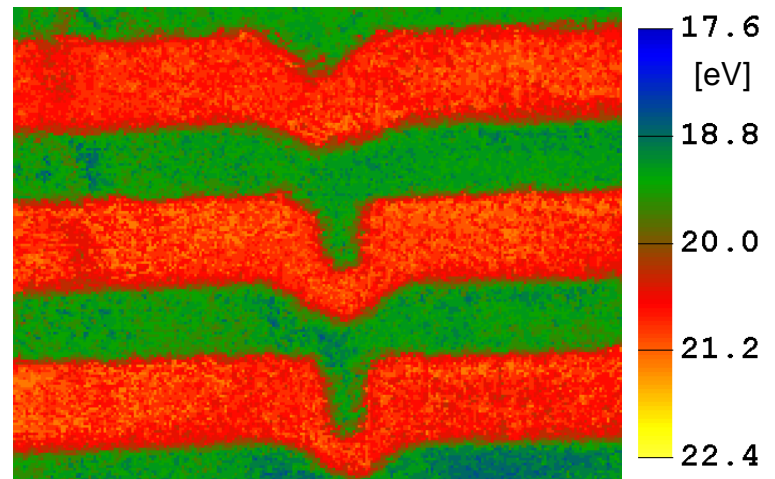
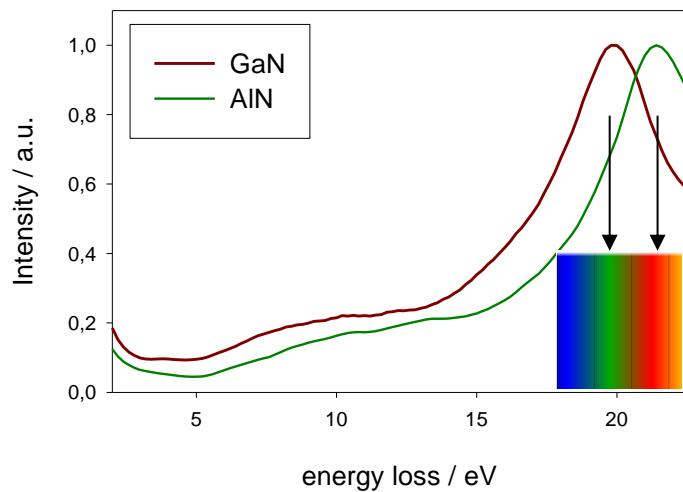
TEM bright field image (diff. area)



Plasmon position maps

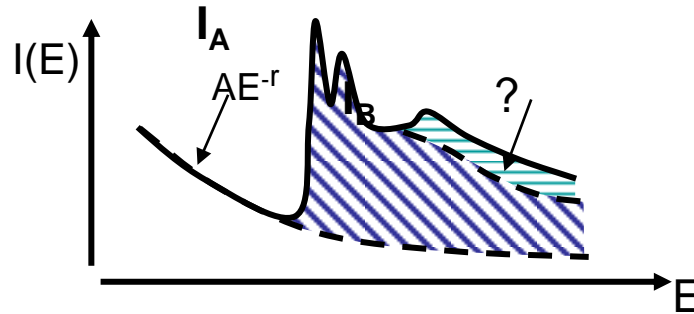


Uncorrected data

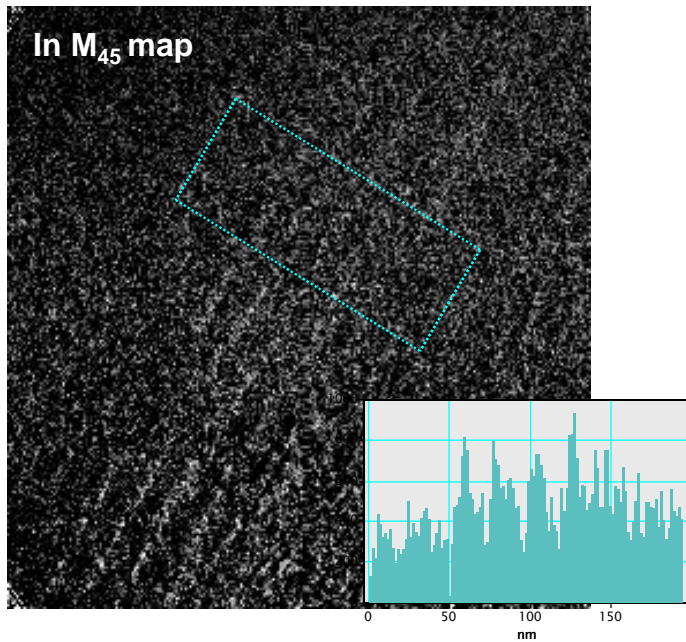


Corrected data

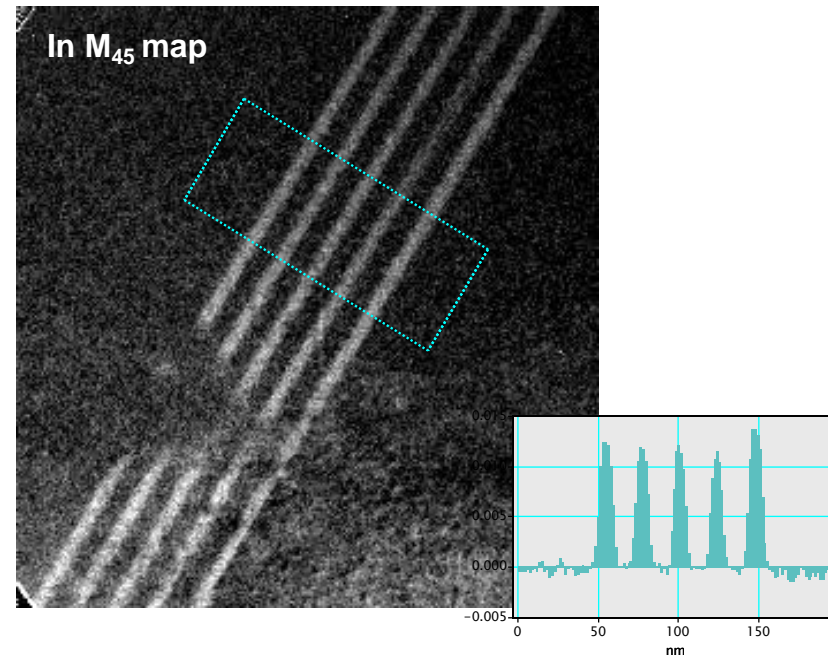
Multiple linear least-squares fitting Mapping of Indium M_{45} Edge

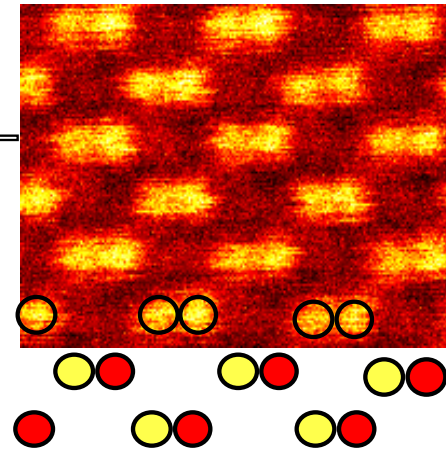


Ray D. Twesten



MLLS fitting
routine



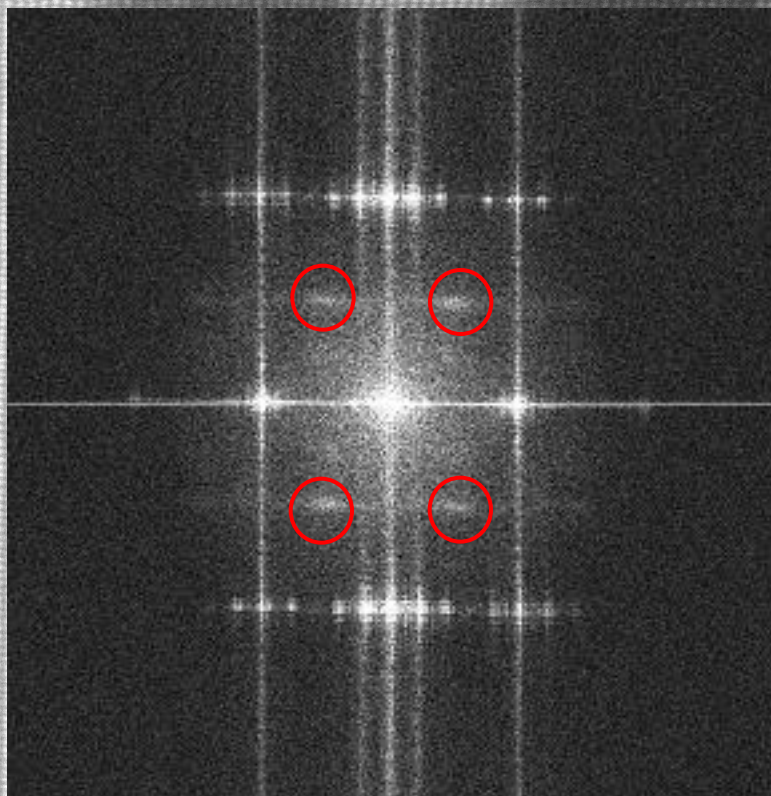


EELS of atomic column

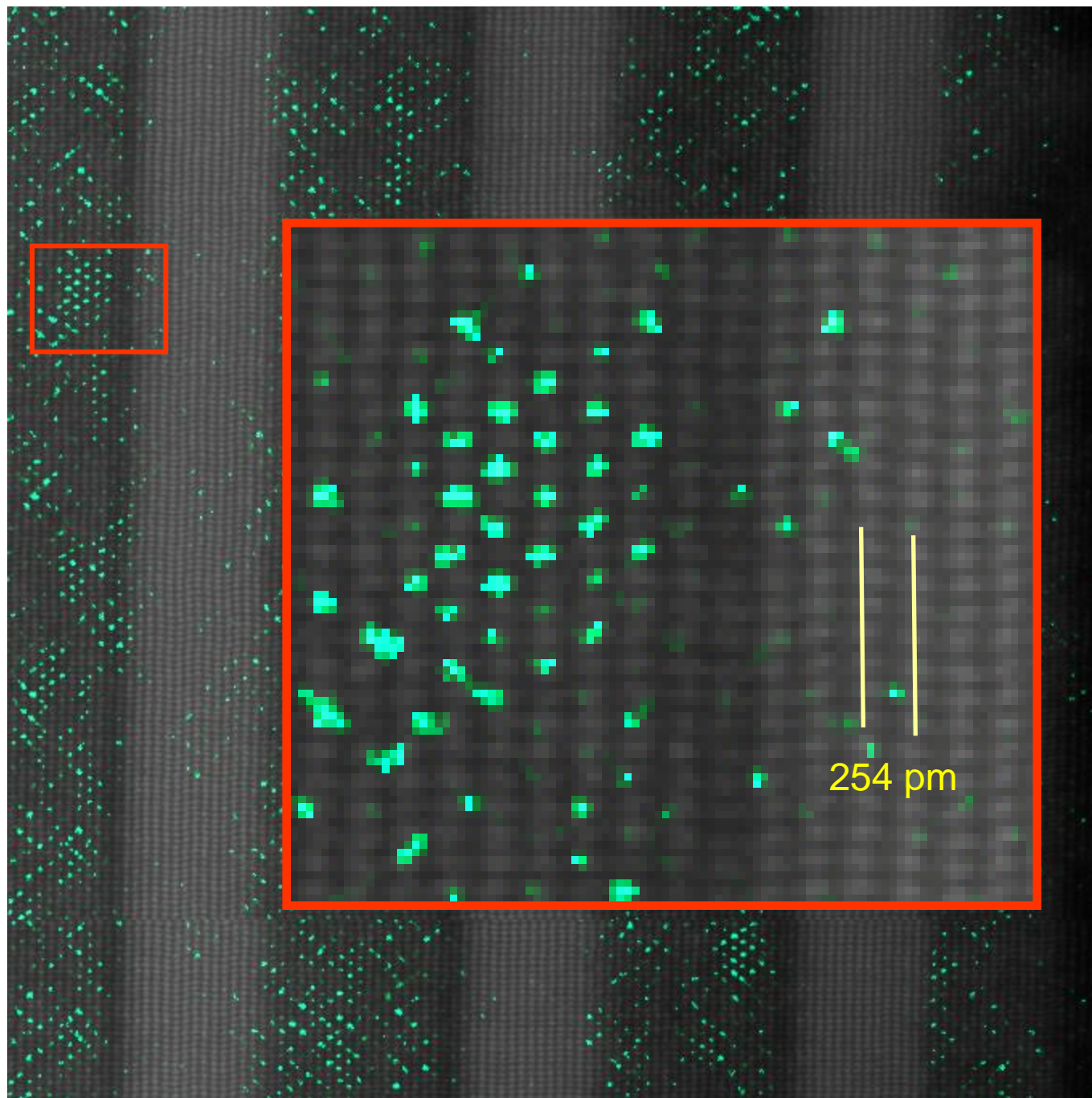
p. 173 in *Advances in Imaging and Electron Physics*, Vol 123, ed. by P. G. Merli, G. Calestani, and M. Vittori-Antisari, 2002

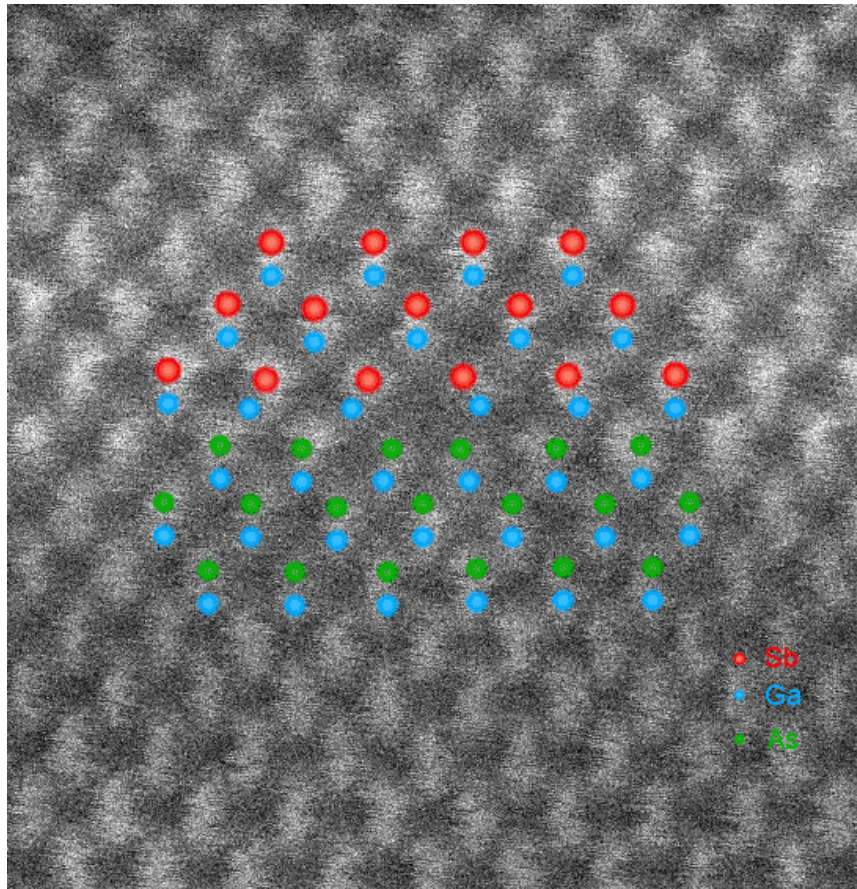
HR-STEM

Sample A (N3075)

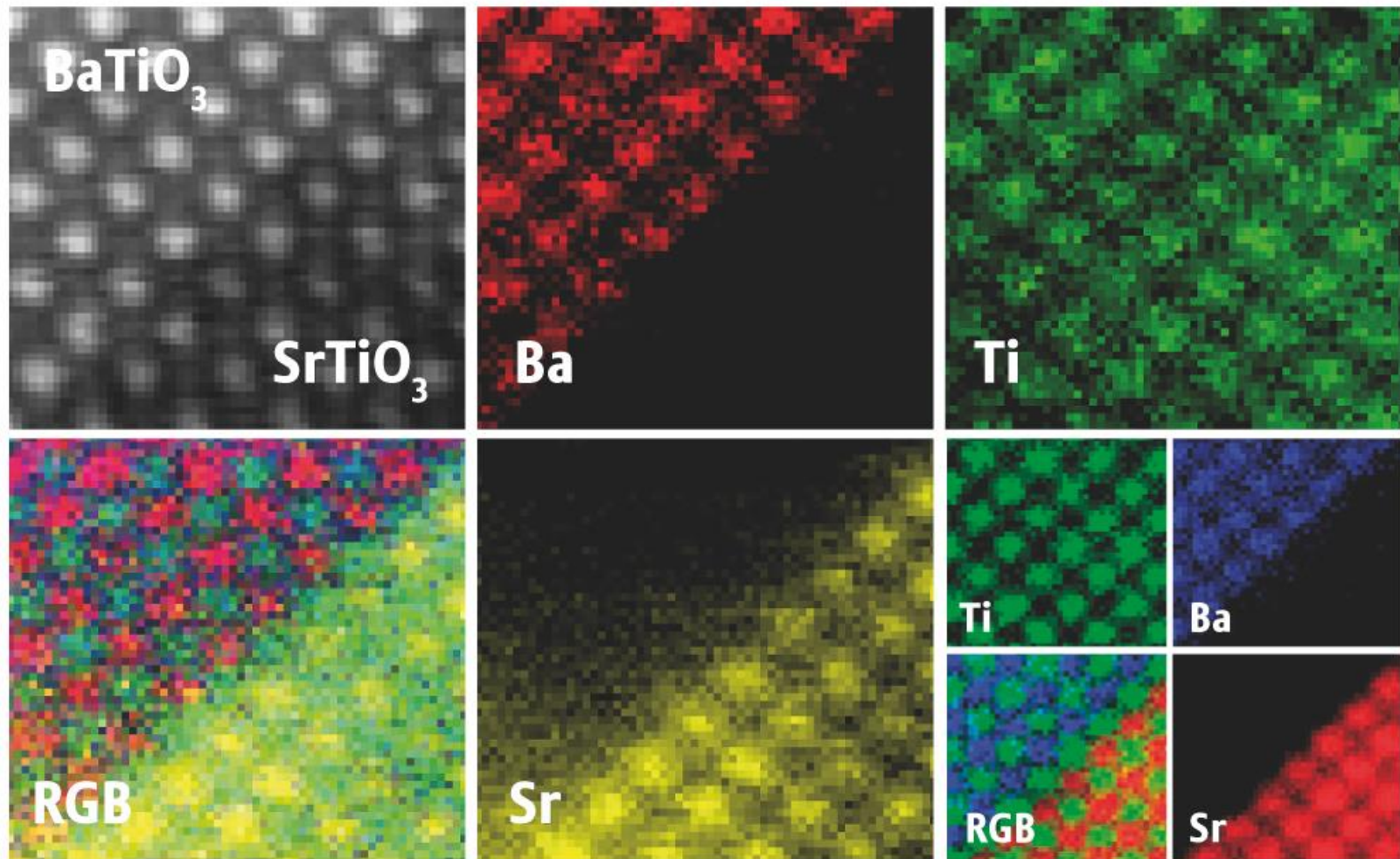


Sample A (N3075)





Wysokorozdzielcze zdjęcie STEM –HAADA otoczenia rdzenia dyslokacji Lomera z doskonałym rdzeniem $5/7$ na granicy GaAs/GaSb .

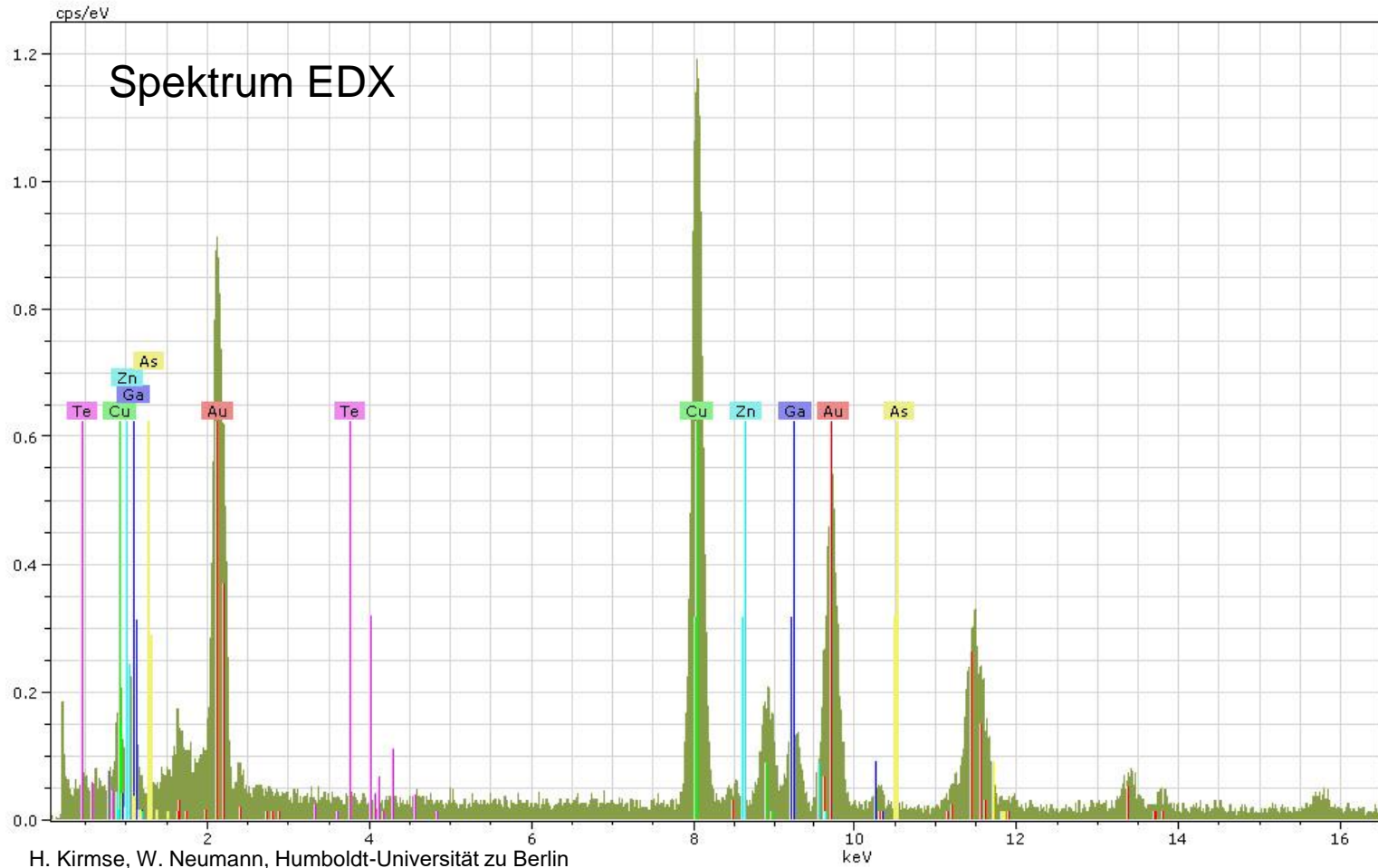


Atomic resolution STEM/EELS map on BaTiO₃/SrTiO₃ interface at 80 and 200 kV acceleration voltage.

Gatan Image filter Fei Titan 80KV

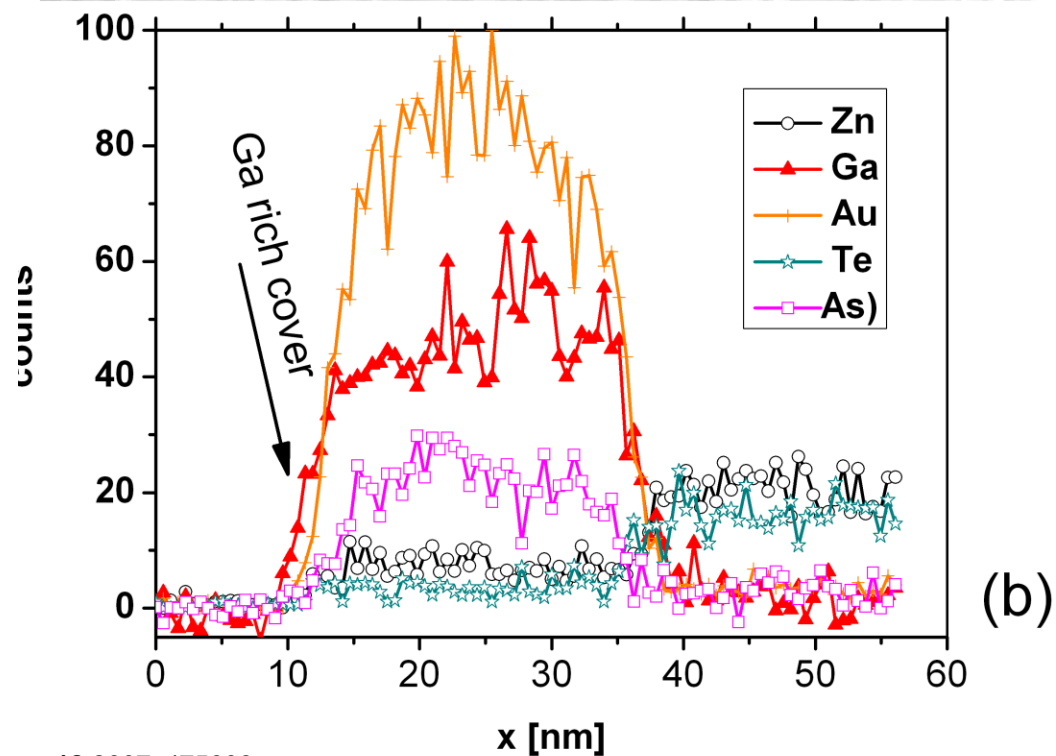
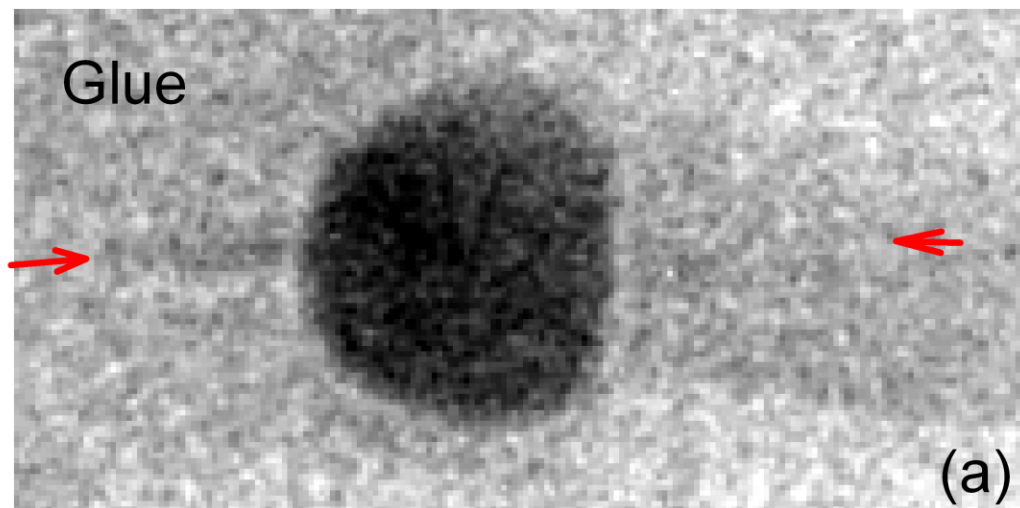
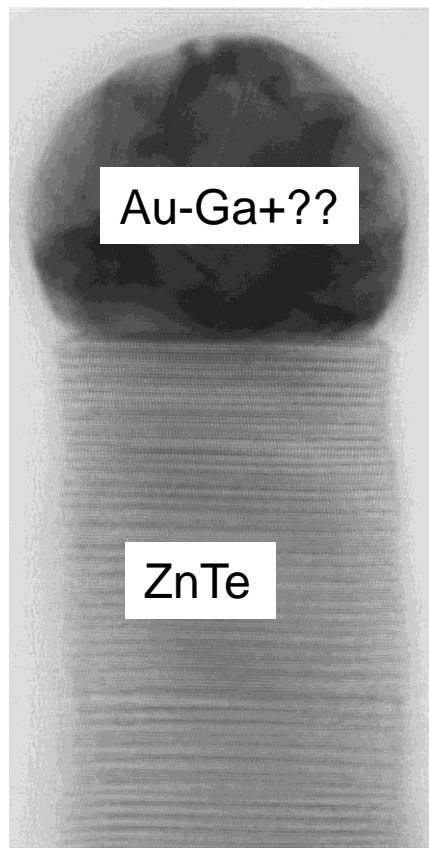
Spectroscopic methods

Characteristic X-ray spectroscopy (EDX)



FEG-EDX

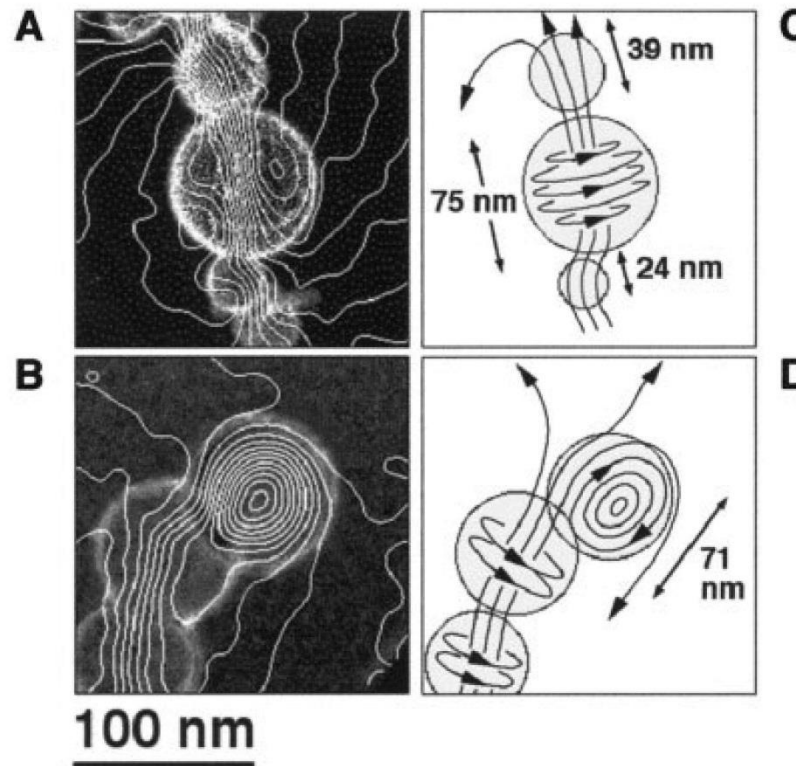
Liniowy profil składu
nanodrut ZnTe/katalizator



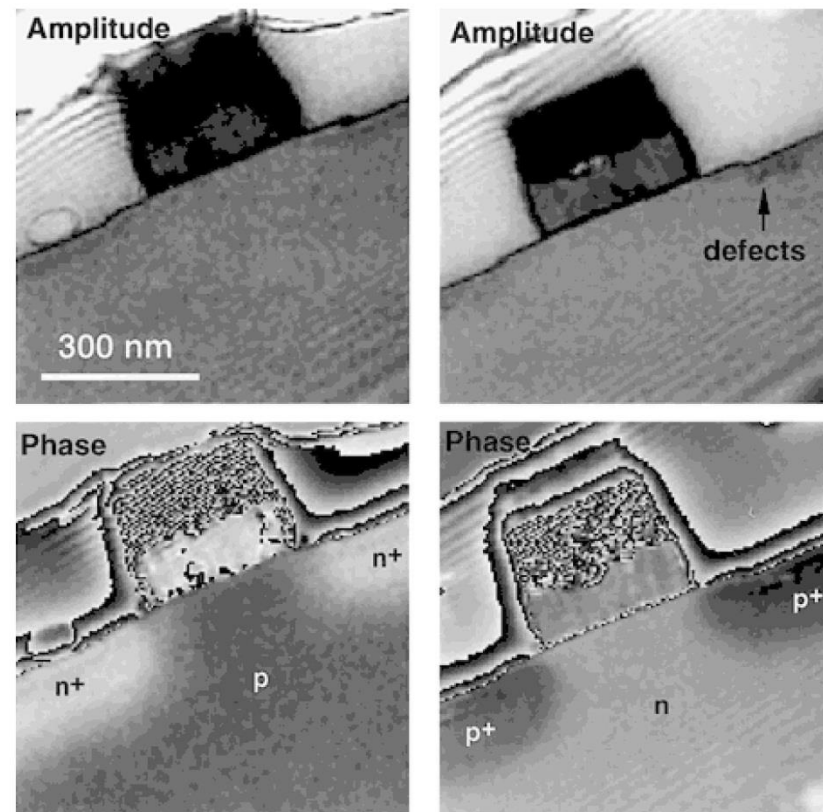
Holografia elektronowa (niskiej rozdzielczości)

→ precyzyjne pomiary zmiany fazy fali elektronowej

→ wizualizacja lokalnych pól magnetycznych i elektrycznych,



Nanocząski FeNi, wiry magnetyczne



Tranzystory 0.3 μm NMOS i PMOS
Amplituda i faza

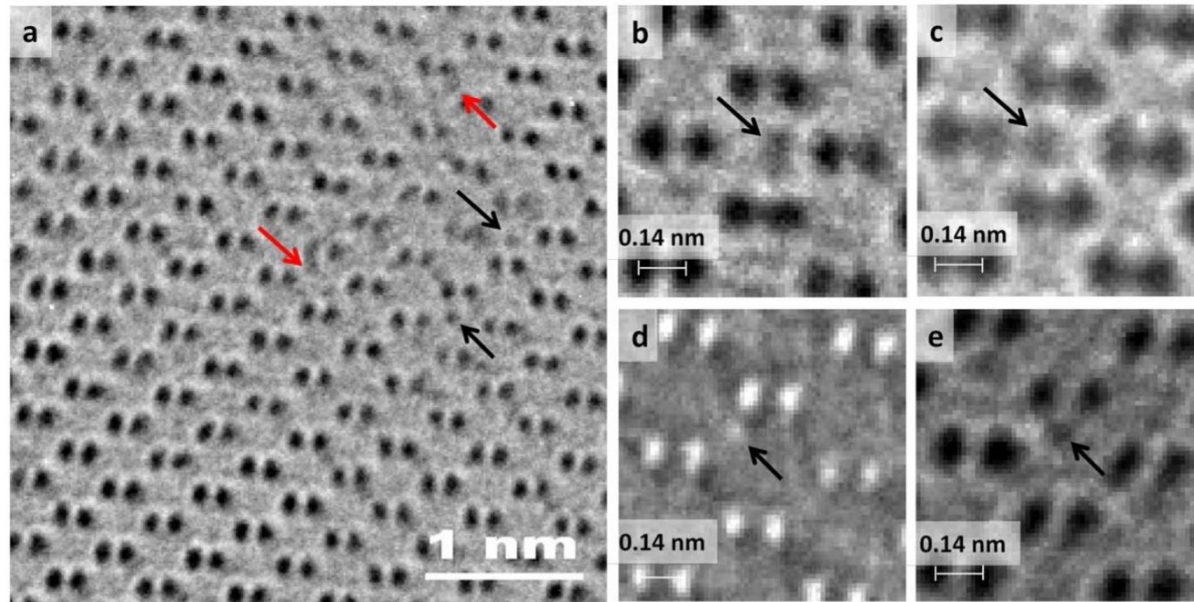
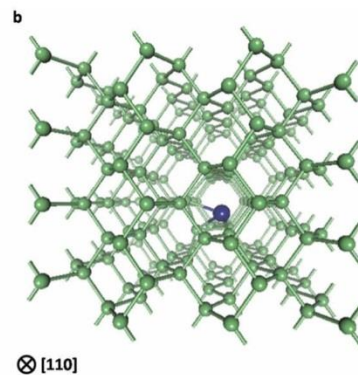
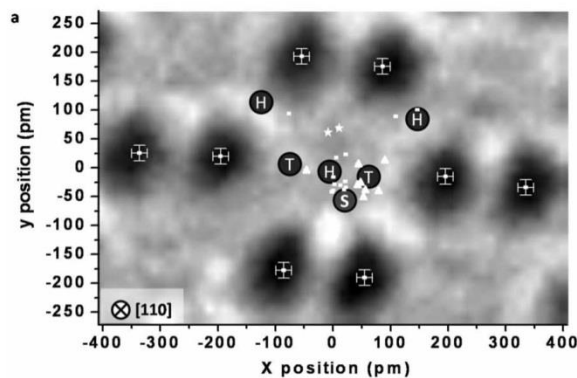


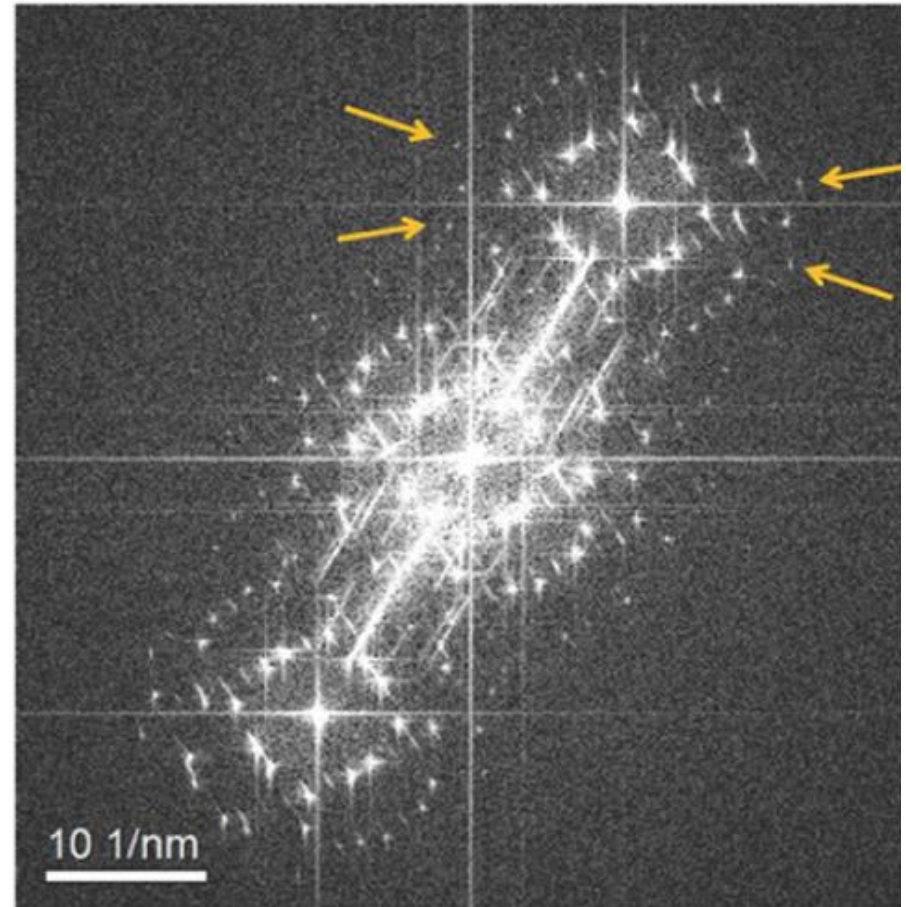
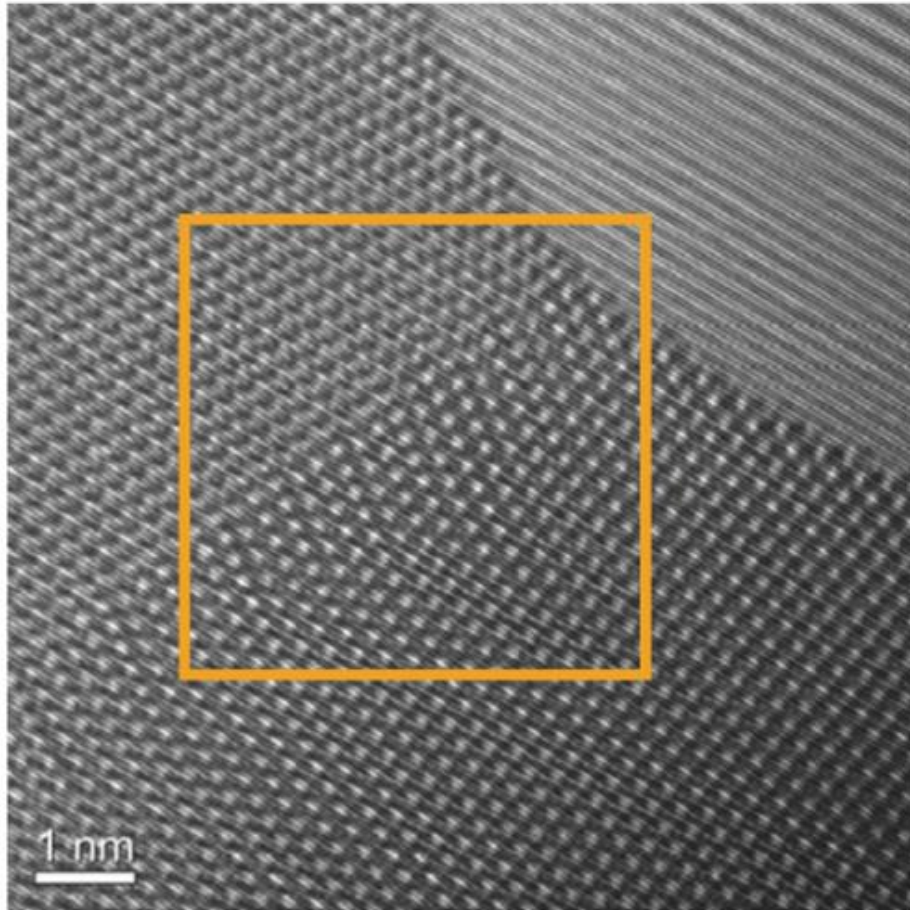
FIG. 1. (Color online) (a) Aberration-corrected images of a thin Ge crystal oriented along the $[110]$ direction [black arrows show occupied interstitial sites, red arrows (dark gray) show column vibrations occurring during the acquisition time]. Magnified areas where an interstitial atom is observed, (b) and (c) In T sites, (d) In an H site that overlaps with a bond-centered site when the crystal is oriented along the $[110]$ zone axis, (e) In an off-center site. Electron dose: 4.0×10^4 electrons/nm². Range of focus from -1 to -8 nm.



Kontrast Fazowy
Międzywęzłowy pojedynczy
Atom Ge zobrażowany i
namierzony !!

Holografia elektronowa (wysokiej rozdzielczości)

Prążki interferencyjne 54 pm 3 prążki na atom



*Prof. M. Lehmann, M. Linck,
Dr T. Niermann of TU Berlin, Germany, Prof. Hannes Lichte of TU Dresden,
Germany, and Dr B. Freitag of FEI Company, The Netherlands*

Problem rzutu i uśredniania

→ Tomografia

H. Stegmann et al. / Microelectronic Engineering 65 (2003) 171–183

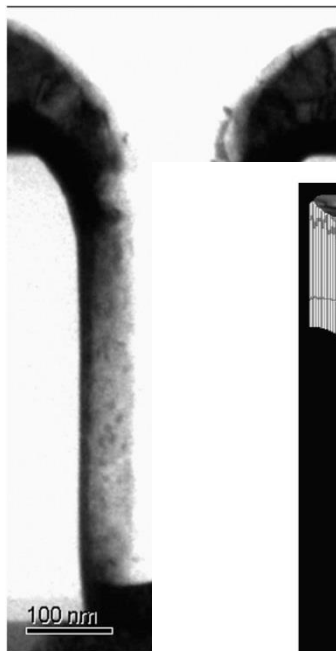


Fig. 5. 0°-projection of

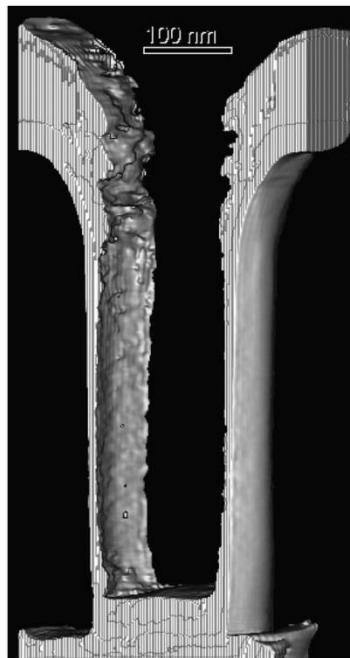
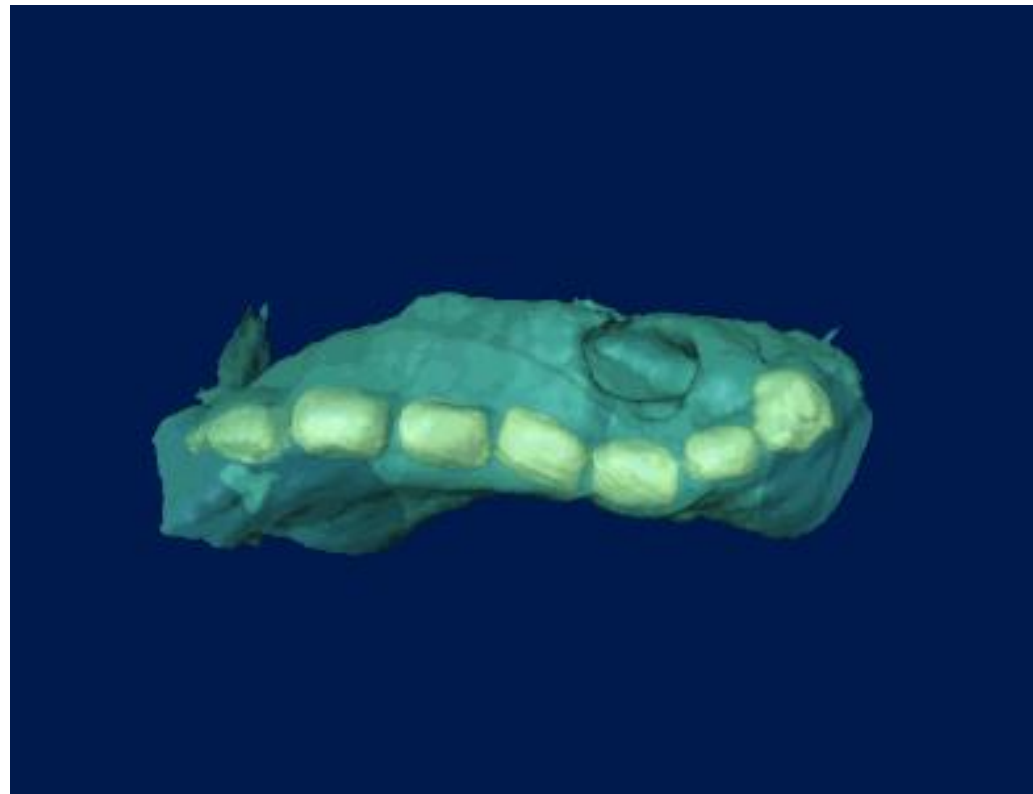


Fig. 3. Surface rendering of the 3D reconstruction of Ta-barrier/Cu-seed sample 1.



Some week points of TEM

- Necessity to perform the preparation
- Destruction of the material
- Poor sampling local information only from electron-transparent regions but up to 0.1-0.5 mm² for the best samples preparation protocols
- Preparation artifacts
- stress relaxation in a thin foil
- amorphization, radiation defects by ions during preparation
- radiation damage with electrons during observation

- the sample is no longer representative due to
- ionization and destruction of chemical bonds heating and diffusion of components in poorly conducting samples, knockout or shifting atoms, spraying

- high costs of equipment,
- time-consuming preparation of thin cross-sections
- complicated "keyboardology" and data interpretation

- imagination and knowledge of a microscopist (still needed)